THESIS

VOLATILE ORGANIC COMPOUNDS AND AIR TOXICS IN NORTHERN COLORADO

Submitted by

Lena Low

Department of Atmospheric Science

In partial fulfillment of the requirements

For the Degree of Master of Science

Colorado State University

Fort Collins, Colorado

Fall 2025

Master's Committee:

Advisor: Emily V. Fischer
Co-Advisor: Jeffrey L. Collett, Jr

Stephanie A. Malin

ABSTRACT

VOLATILE ORGANIC COMPOUNDS AND AIR TOXICS IN NORTHERN COLORADO

The Colorado Northern Front Range (CNFR), stretching from Denver to Fort Collins, has significant air pollution challenges. Regional pollution sources include volatile organic compounds (VOCs) from urban activities, oil and gas (O&G) exploration and production, biogenic emissions, and wildfire smoke. The CNFR has been repeatedly designated as a nonattainment area for ozone, making reductions in VOCs and nitrogen oxides emissions a priority. Hazardous air pollutant (HAP) exposure concerns have also increased with concurrent population growth and expanding O&G production, frequently in close proximity. Sensitive populations and disproportionately impacted communities are at increased risk from air pollution exposure. While prior studies have characterized the composition and sources of air toxics and other VOCs in the southern CNFR, we extend focus to the northern portion of the region.

Leveraging spatially arrayed samples, we present VOC measurements from whole air canister samples collected at eight sites during 2015-2016 and 2022-2025. This analysis includes sites near O&G wells, a large gas station, an urban school, and a suburban site at the base of the Rocky Mountains. We find strong seasonal trends that are driven by meteorological and emission patterns. Laboratory compositional analyses of gasoline and diesel fuel reveal that the ambient gas station samples exhibit a distinct VOC signature indicative of fuel volatilization. Positive matrix factorization analysis shows four source factors best describe sample VOC composition across the region: O&G activity, traffic + urban combustion, fueling station, and biogenic + background. Reflecting the regional distribution of O&G activity, there is a strong eastward increasing gradient in light alkanes and other compounds associated with O&G emissions. Highlighting the influence from traffic and fuel evaporation, the gas station has the largest ambient HAPs concentrations.

Providing a rare opportunity to characterize a large uncontrolled pollution event in a rural town, we collected VOC measurements in rapid response to the largest documented O&G spill in Colorado. Observations indicate that the emission plume from a well accident event near Galeton, CO traveled several miles downwind of the well with high HAPs concentrations, increasing potential acute exposure to residents. Together our measurements add to the growing discussion of potential for chronic and acute air toxics exposure in the CNFR.

ACKNOWLEDGEMENTS

I would like to thank the many collaborators who contributed to this project.

The VOC data from 2015-2016 was collected and analyzed by Derek Weber, Arsineh Hecobian, Yong Zhou, and Amy Sullivan. The City of Fort Collins and Town of Timnath provided the motivation and funding to support this data collection. The Larimer County Resources Department and Pouder School District respectively provided access to the Fossil Creek and Soapstone Prairie natural areas and elementary school campus in Timnath.

Several people helped me collect VOC data from 2022-2025 including Victor Geiser, I-Ting Ku, Yong Zhou, collaborators at University of Northern Colorado, students in ATS 716 during spring 2022 and fall 2023, and the SURE students from summer 2022. I-Ting Ku, Yong Zhou, Seongjun Kim, and Jihee Ban helped me prepare and analyze canister samples. Thank you to the everyone who supported our monitoring network by identifying sampling locations and hosted monitor equipment on their properties. I-Ting Ku and Jared Stickney joined me on mobile survey drives. Matthew Davis and Kevin Cossel collected data in Galeton, CO during the well non-containment event for our CSU + NIST team's second drive. Thank you also to Da Pan for teaching me how to operate the plume tracker. The Thompson School District provided access to multiple school campuses in Loveland and Berthoud.

This work was primarily supported by the EPA through the ARP/IRA Enhanced Air Monitoring for Communities under award number 00I09701. The assumptions, findings, conclusions, judgments, and views presented herein should not be interpreted as necessarily representing the EPA. The City of Fort Collins provided additional funding to maintain monitoring at a site in downtown Fort Collins. This EPA project has many other collaborators including Milena Guajardo from the Department of Atmospheric Science at CSU, Mindy Hill from the Center for Environmental Justice at CSU, Cassie Archuleta and DeAngelo Bowden from the City of Fort Collins, Lea Schneider from Larimer County Department of Heath & Environment, and Josie Plaut from the Institute for

the Built Environment at CSU. Additionally, thank you to the Air Quality-Monitoring Advancement Committee (AQ-MAC) members for supporting our science communication goals.

Finally, a special thank you to my advisors, Emily Fischer and Jeff Collett for your invaluable guidance and mentorship; to Stephanie Malin for providing your environmental justice expertise and serving on my committee; to all of the students, postdocs, research scientists, and project coordinators in the Collett and Fischer groups who have overlapped with me at CSU; and to my friends and family for your endless support.

TABLE OF CONTENTS

LIST OF TABLES

LIST OF FIGURES

Chapter 1

Introduction

1.1 Air Pollution Challenges in Northern Colorado

The Colorado Northern Front Range (CNFR) metropolitan area, stretching from Denver to Fort Collins (Figure 1.1), has unique air pollution challenges due to its diverse combination of pollution sources. Regional sources include emissions from oil and gas (O&G) exploration and production, urban activities (i.e., transportation, industry, manufacturing, and utilities), biogenic emissions, residential activities (e.g., wood burning and solvent emissions), agriculture, and biomass burning (Flocke et al., 2019 and references therein). This complex mixture of emissions presents pollution issues such as temperature inversions trapping fine particulate and gaseous air pollutants near the surface in a phenomenon called the "brown cloud" (Brown et al., 2013 and references therein), and episodic high ozone (O_3) events driven by large emissions of precursor gases, intense sunlight, and local atmospheric circulation patterns (Evans and Helmig et al., 2017; Flocke et al., 2019; Helmig et al., 2020). Local and transported wildfire smoke emissions also frequently impact the region (Lindaas et al., 2017), contributing to both O_3 and fine particle pollution. Associated with adverse effects on human and ecological health, O_3 (Cohen et al., 2017; Monks et al., 2015; Kohut et al., 2007) and fine particulate matter (Cohen et al., 2017; Dockery et al., 2001; Pope et al., 2000) are classified as criteria pollutants by the U.S. Environmental Protection Agency (EPA). For over two decades, the U.S. EPA has designated CNFR as a nonattainment area for O_3 under the U.S. National Ambient Air Quality Standard, making reductions in volatile organic compounds (VOC) and nitrogen oxides emissions a priority. Numerous studies point to VOCs from O&G operation as significant contributors to regional O_3 production (e.g., Albeleira et al., 2017; Benedict et al., 2019; Cheadle et al., 2017; Evans and Helmig et al., 2017; Lindaas et al., 2019; McDuffie et al., 2016; Oltmans et al., 2019; Pfister et al., 2017; Rodriguez et al., 2009; Sullivan et al., 2016).

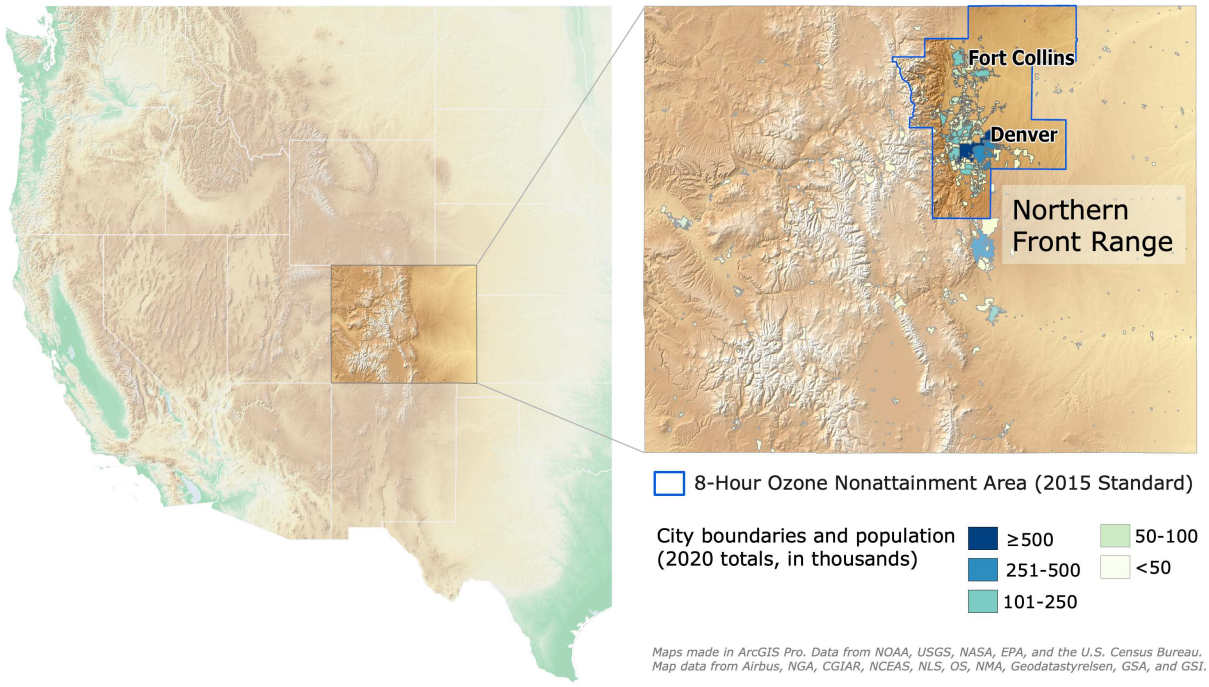

Figure 1.1: Map of the Colorado Northern Front Range metropolitan area. The city boundaries classified by population size and the O_3 nonattainment area are indicated on the map.

In addition to O_3 and fine particle air pollution challenges, there is increasing attention regarding exposure to air toxics in the CNFR. Air toxics are hazardous air pollutants (HAPs) classified by the U.S. EPA that are known to cause cancer or other serious health impacts; they include various VOCs such as *n*-hexane, benzene, toluene, xylenes, and ethylbenzene, which are emitted from urban and traffic emissions and O&G (e.g., Gilman et al., 2013; Pollack et al., 2021; Ku et al., 2024). The region is a hotspot for large stationary air toxics emissions (Figure 1.2.b) that span different emissions sectors including commercial and industrial (e.g., gas stations, fuel wholesalers, and automotive repair shops), manufacturing (e.g., production of cement, glass, ethanol, pharmaceuticals, food, and metal products), utilities (e.g., electric power generation and distribution, gas transmission pipelines, water and wastewater plants, and waste management), O&G (e.g., upstream, midstream, and distribution operations), and other emission sources (Figure 1.2.a; Colorado Department of Public Health and Environment (CDPHE), 2024). Regionally, air toxics are also emitted from mobile (e.g., transportation and vehicles), residential (e.g., wood burning and cleaning, degreasing, and painting products); agricultural, and wild, prescribed, and structural fire

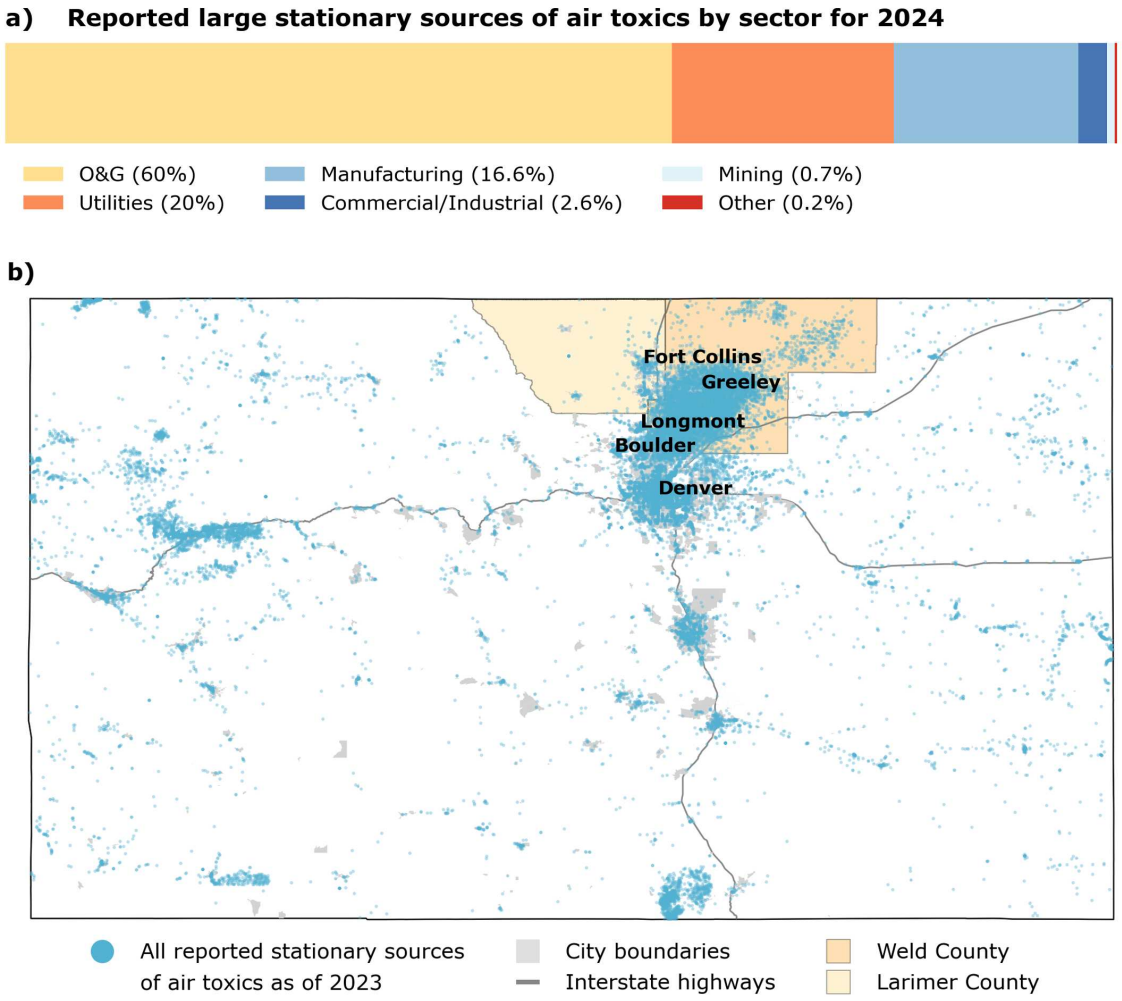

Figure 1.2: Reported large stationary sources of air toxics in Colorado. **(a)** Reports divided by each emission sector in 2024 with percentage contribution in the legend. **(b)** Map of location of all reported sources as of 2023 (blue circles) with Weld County (orange) and Larimer County (yellow) highlighted. City boundaries (light gray) and interstate highways (dark gray) are also indicated on the map. The reports include nearly 3800 facilities and represent emission estimates greater than 250 lbs/year. Data is from CDPHE's Stationary Source Air Pollution Emissions Notices (APEN) database (https://cdphe.colorado.gov/public-information/air-pollution-control-division-records). Sectors were assigned based on the North American Industry Classification System (NAICS) code.

emissions (U.S. EPA, 2023). In Colorado, O&G activities are an important source, comprising 60% of reported air toxics emissions in 2024 (Figure 1.2.a; CDPHE, 2024). Individual counties within the CNFR are disproportionately impacted by VOC emissions, with Weld County alone accounting for 48% of the point and non-point O&G emissions in Colorado compared to < 1% in adjacent Larimer County (U.S. EPA, 2023). As a result of the growing interest in HAPs, Colorado is one of the first states to implement a state air toxics program to increase reporting, monitoring, and enforcement of health-based standards, including air pollution monitoring of O&G facilities (CDPHE, 2025b). Concerns regarding HAPs are growing among residential communities as population growth increases and O&G exploration and production expand in close proximity (McKenzie et al., 2016; McKenzie et al., 2018).

1.2 Impacts of Oil and Gas in Northern Colorado

The CNFR is home to growing population centers and rapidly expanding O&G development. Driven by advances in hydraulic fracturing and directional drilling techniques, there have been substantial O&G production increases in the region since the early 2000s, including in heavily populated areas of the Denver-Julesburg (DJ) Basin. Population influx and urban sprawl are expanding the convergence of residential housing and O&G extraction, which is increasingly occurring via enlarged, high-volume, multiwell facilities (McKenzie et al., 2016; Sansone-Poe et al., 2025). The higher density of wells may strengthen the accumulative exposure to HAPs for individuals living near intense operations (Weisner et al., 2025). As a result of the concurrent development, 19% of the population in the DJ Basin lived within 1.6 km (1 mile) of an active O&G well in 2012, with a higher portion of lower value housing construction near existing O&G wells compared to higher value homes (McKenzie et al., 2016). The CNFR is anticipated to grow by 2% each year, reaching 6.4 million people by 2025 (Weisner et al., 2025 and reference therein). Recently, population increases in Larimer and Weld counties are among the largest in the state; between 2010 and 2020, the population of Weld County grew over 30% (U.S. Census Bureau, 2020). By 2025, the populations of Larimer and Weld counties are expected to increase by 92% (Community Foundation

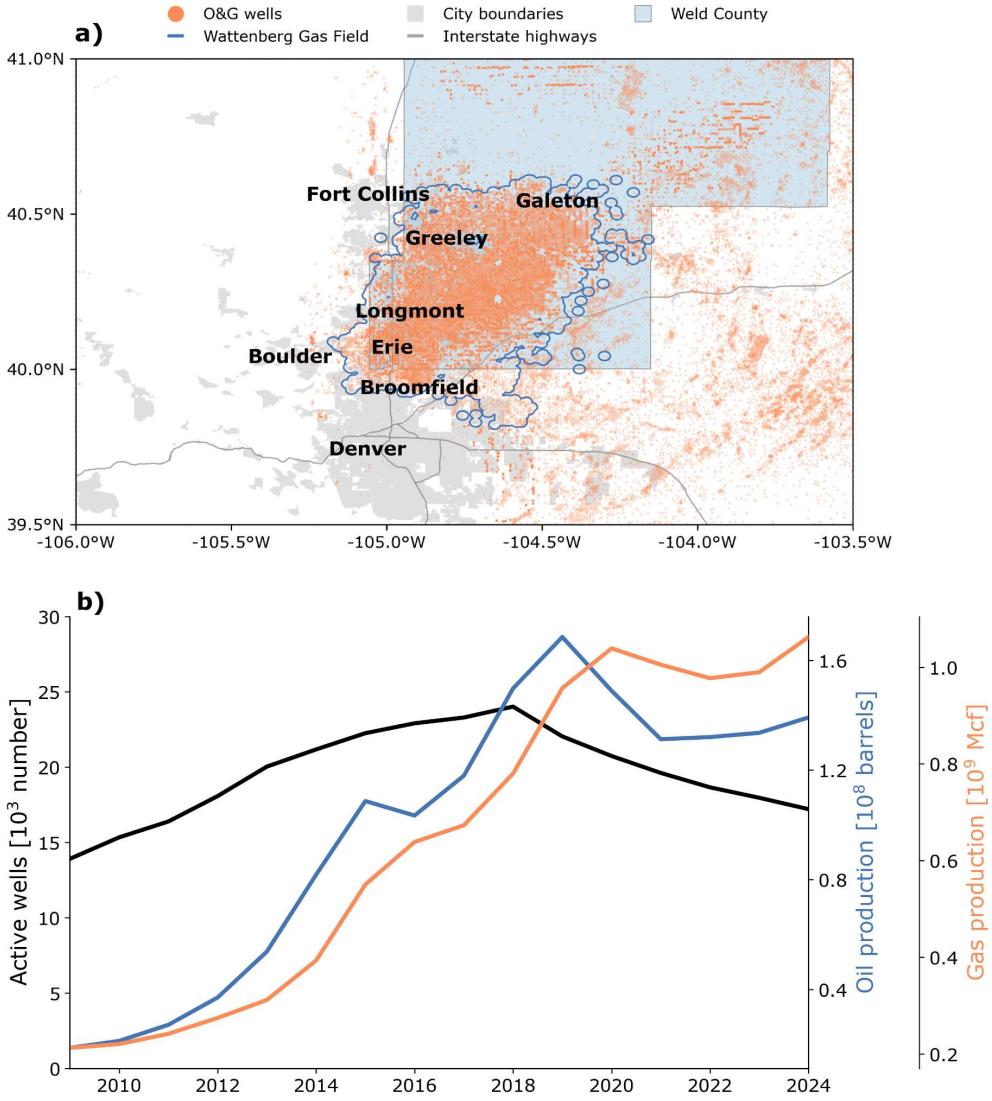

Figure 1.3: Oil and gas development and production along the CNFR. **(a)** Map of the locations of past and present O&G wells (orange circles), with the Wattenberg Gas Field (dark blue line) and Weld County (light blue shading) boundaries drawn. City boundaries (light gray) and interstate highways (dark gray) are also indicated on the map. **(b)** Annual active well count [number] (black line) and annual oil [barrels/year] (blue line) and gas [Mcf (i.e., one million cubic feet)/year] (orange line) production rates from 2009 to 2024. The well surface location, number of active wells, and O&G production data is from the Colorado Energy and Carbon Management Commission (ECMC) databases (ECMC, 2025c,a,d).

of Northern Colorado, 2024), further promoting the widening intersection with O&G production. While more attention is given to active wells, plugged, abandoned, or orphaned wells may still have high air pollutant emissions (Adgate et al., 2014) despite their temporary or permanent inactive status. Overlaid with the locations of past and present O&G wells, Figure 1.3.a shows city boundaries, the DJ Basin, and Weld County in the CNFR. Weld County has the highest density of wells in the DJ Basin (Figure 1.3.a). The number of active O&G wells peaked in 2018, with over 24,000 sites within Weld County, and annual O&G production rates have generally continued to accelerate from 2009 to 2024 (Figure 1.3.b; Colorado Energy and Carbon Management Commission (ECMC), 2025). Motivated by air toxic concerns and rising O&G production, recent community-level studies have explored the influence of O&G emissions in residential areas (e.g., Ku et al., 2024; Lachenmayer et al., 2024; Thompson et al., 2014), finding higher ambient concentration of VOCs and HAPs associated with O&G activities in communities living near O&G wells compared to the regional background and urban industrialized areas.

Acute and chronic exposure to air toxics is a major potential physical and mental health risk for individuals living near sources in the CNFR. Recent research in this area has focused largely on O&G development. Emitting a complex array of VOCs, including air toxics such as benzene, toluene, ethylbenzene, and xylenes (BTEX) (Brantley et al., 2015; Garcia-Gonzales et al., 2019), O&G facilities have been the focus of a growing number of human health risk studies evaluating both chronic exposure and acute pollution events from O&G activities in Colorado (e.g., Adgate et al., 2014; Allshouse et al., 2017; Erickson et al., 2022; Holder et al., 2019; McKenzie et al., 2012, 2014, 2016, 2017, 2018, 2019; 2024; 2025; McMullin et al., 2018; Weisner et al., 2023, 2025). Collectively, these studies indicate potential health concerns spanning respiratory, cardiovascular, neurological, hematological, gastrointestinal, immunological, and developmental effects as well as elevated estimated lifetime excess cancer risk increase with proximity to and density of O&G development. Although the impacts of exposure to O&G emissions can affect people of all ages, sensitive populations including young children, birthing people, older individuals and those with

preexisting health conditions have been shown to have an elevated risk of adverse health impacts in the region.

Many studies aiming to quantify the impact of O&G on health are based on measured or modeled ambient VOC levels from samples collected across the CNFR from the past decade. They use reference concentrations for compounds based on their most sensitive endpoint or symptom (U.S. EPA, 1994) to calculate hazard quotients, hazard indices, and excess lifetime cancer risks. However, recent observations demonstrate that O&G emissions have significantly changed in the CNFR in the past decade (Ku et al., 2024), and health assessment analyses indicate that coexposure of VOCs with multiple pollutants such as O_3 intensify health impacts (Weisner et al., 2025). Illustrating a more comprehensive picture of risk associated with O&G, the recent work demonstrates that considering a combination of pollutants drives health risk further beyond acceptable health thresholds in the region (Weisner et al., 2025). Furthermore, acute high exposure pollution episodes, frequently associated with O&G development activities (Ku et al., 2024), have higher HAP levels than chronic measurements that may underestimate the full range of recurring acute exposure due to dilution (Garcia-Gonzales et al., 2019; Weisner et al., 2025). These brief peak exposures may have a higher potential risk for residents living near O&G development (Garcia-Gonzales et al., 2019; McKenzie et al., 2012; Weisner et al., 2025). Analogously, amplified by institutionalized uncertainties and perceived powerlessness in decision-making about O&G production near their homes, schools, workplaces, and community spaces, O&G development also generates chronic stress and negative mental health outcomes such as depression (Malin, 2020; Mayer et al., 2021). Due to procedural and institutional barriers coupled with inequitable processes and policies, these physiological and physical impacts unequally burden community members across the CNFR. Consequently, VOC source apportionment analysis may be leveraged to inform reduction exposure strategies.

1.3 Characterization of VOCs in Northern Colorado

The expanding footprint of O&G along the CNFR and corresponding air quality concerns have motivated numerous prior studies to investigate the composition and sources of VOCs and HAPs (e.g., Abeleira et al., 2017; Benedict, et al., 2019; Brown et al., 2013; Flocke et al., 2020; Frischmon and Hannigan, 2024; Gilman et al., 2013; Halliday et al., 2016; Helmig et al., 2020; Ku et al., 2024; Lachenmayer et al., 2024; Lyu et al., 2021; McDuffie et al., 2016; Pétron et al., 2012, 2014; Pollack et al., 2021; Swarthout et al., 2013; Thompson et al., 2014). Most of these measurement intensives concentrated in the southern region of the CNFR, south of Longmont, and were conducted on short time scales of several weeks (e.g., Gilman et al., 2013; McDuffie et al., 2016; Swarthout et al., 2013) to months (e.g., Abeleira et al., 2017; Halliday et al., 2016), or they focused on characterizing VOCs at a single location (e.g., Helmig et al., 2020; Pollack et al., 2021) or within a neighborhood (e.g., Ku et al., 2024; Lachenmayer et al., 2024) for multiple years. Largely driven by emissions from O&G activities, the prior work collectively shows the CNFR is characterized by significant abundance of light and heavy alkanes compared to other regions in the country. The measurements additionally display distinct influence from urban sources such as traffic combustion.

To evaluate the relative contribution from different emission sources, prior studies have leveraged characteristic VOC ratios and statistical correlation analyses including simple linear regression, multiple linear regression (MLR), and positive matrix factorization (PMF). Applying MLR for measurements collected at the Boulder Atmospheric Observatory (BAO) in Erie, CO in winter 2011, Gilman et al. (2013) attributed > 70% of light and heavy alkanes and > 60% of cycloalkanes to O&G emissions. Previous aircraft studies in the region (FRAPPÉ in summer 2014) have observed broad northeastward gradients in benzene concentrations measured $\leq$ 2 km above sea level and used VOC ratios and source tracer compounds to indicate O&G activity source origins (Halliday et al., 2016). However, they were not able to capture the full span of VOC spatial complexity added by smaller scale point sources. More recent work from BAO in spring and summer 2015 (Abeleira et al., 2017) and Boulder Reservoir in Boulder, CO from 2017-2019 (Pollack et

al., 2021) employed PMF analysis on high temporal resolution data to increase the number of emission source regimes and showed that the magnitude of source contributions varies by HAPs species and season. Broadening the utility of PMF analysis to capture spatial trends, Lachenmayer et al. (2024) used PMF to apportion emission sources for a sampling network of weekly-integrated whole air canisters collected in Broomfield, CO near O&G well pads from 2018-2020. Using a similar dataset, Ku et al. (2024) showed that short episodic pollution events corresponded with the highest emissions from O&G activities. In this way, prior composition and source apportionment analyses have demonstrated the widespread and variable influence of VOC sources in the southern section of the CNFR that we extend here to the northern portion of the CNFR.

In this work, we use different stationary and mobile measurement techniques to analyze VOCs and HAPs north of Longmont, CO. Employing spatially arrayed samples from Loveland and Greeley to Fort Collins and north toward the Wyoming border, we characterize a large suite of VOCs, including HAPs such as benzene, toluene, *n*-hexane, *2*,*2*,*4*-trimethylpentane, *n*-nonane, and xylenes. To capture the spatial heterogeneity of VOCs at regional and smaller scales as well as their seasonality, we uses weekly measurements from sites near O&G wells adjacent to school grounds and neighborhoods, a large gas station, an urban school adjacent to an automobile repair shop, in suburban areas, in remote grasslands, and site at the base of the Rocky Mountains collected over time scales of months to years. Since VOCs have high spatial heterogeneity, even within the neighborhood scale, air quality issues may more strongly challenge sensitive populations and disproportionately impacted communities. Leveraging this unique dataset, we employ VOC ratios and positive matrix factorization (PMF) to characterize and quantify contributions from various emission source types across the northern portion of the CNFR. Since the impact of fueling stations is underexplored in the literature, we incorporate laboratory compositional analyses of gasoline and diesel fuels to identify a fuel evaporative emissions fingerprint and explore the range of HAPs abundance from fueling stations in the urban and suburban environments. From prior field measurement in the CNFR, we expect that emissions of VOCs and HAPs from O&G activities and urban sources will have large regional impacts on regional air quality, with their relative abundance

and influence reflecting source distributions and emission patterns. Lastly, providing a rare opportunity to characterize a large uncontrolled pollution event in a rural town, we collected air quality measurements in rapid response to the largest documented O&G spill in Colorado. Together these measurements add to the growing discussion of potential for chronic and acute air toxics exposure in the region.

Chapter 2

Methods

2.1 Monitoring Sites

We measured CH_4 and VOCs in whole air canister samples collected at eight sites during 2015-2016 and 2022-2025 across the CNFR. Figure 2.1 displays the sampling schedules and locations. Monitoring sites include those near O&G operations, schools, and interstate highways, as well as, in suburban areas, a remote grassland, and at a large gas station. We provide detailed descriptions of the sampling locations in Section A.1. The descriptions for the 2015-2016 sample locations are adapted from Weber (2018).

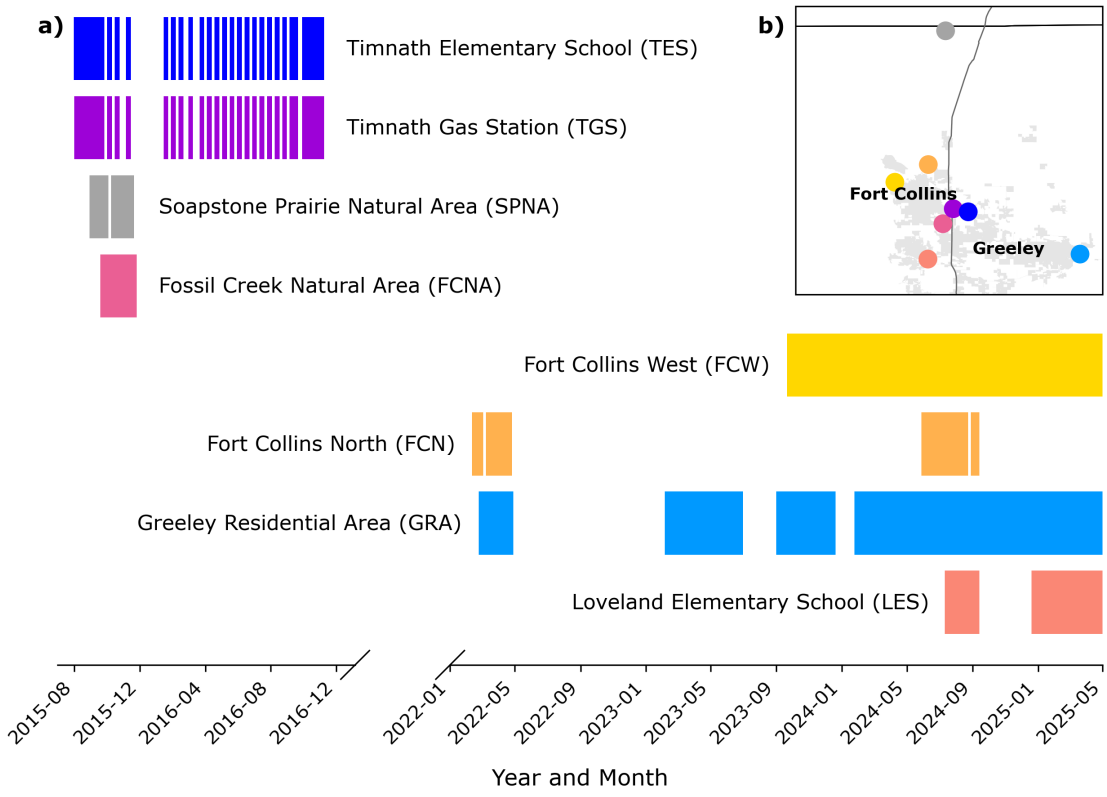

Figure 2.1: **(a)** Sampling time periods for each site from 2015-2016 and 2022-2025 **(b)** and a map of the study region. The seven sampling locations are colored by longitude. The background site (SPNA) is shown with a gray circle. City boundaries (light gray) and interstate highways (dark gray) are indicated on the map.

Located in Fort Collins, CO, Fossil Creek Reservoir Natural Area (FCNA; n = 9) and Fort Collins West (FCW; n = 83) represent remote suburban environments. The FCNA site, in southeast Fort Collins, is about 2 km from I-25 and less than 0.5 km from a busy roadway. FCW is located at Christman Field, on the CSU Foothills campus near the base of the Rocky Mountains.

The Fort Collins North (FCN; n = 24) and Greeley Residential Area (GRA; n = 97) measurements were made in close proximity to producing O&G wells in suburban environments. The samples from FCN were collected at two different locations within 1 km of each other, approximately 4 km from I-25 and near the same active O&G wells. The GRA site is located near a school and roughly 0.5 km from active O&G wells and about 2 km from a busy roadway. The school, Bella Romero Academy, is part of a high profile environmental justice case. After wealthier and predominantly white communities successfully resisted new O&G development near a public charter school, O&G operators built a multiwell pad near more vulnerable populations just a few miles away (Kroepsch et al., 2019; Malin, 2020; Sakas, 2020). Bella Romero Academy has an 89% Latinx enrollment, compared to the 36% Latinx population of Greeley, and 92% of students from low income families (Malin, 2020). Despite state monitoring detecting a short episode of benzene concentrations that exceeded acute health guideline values (i.e., 9 parts-per-billion by volume (ppbv)) in fall 2019 (Sakas, 2020), there are over 20 active O&G wells just hundreds of feet from the school athletic field (Malin, 2020). In response, we installed long-term and on-going air quality monitoring near the school starting in spring 2022.

The samples from an elementary school in Timnath ("Timnath Elementary School" or TES; n = 32) were collected in a suburban environment influenced by regional O&G activity to the East and approximately 3.5 km east of I-25. The site at the gas station in Timnath ("Timnath Gas Station" or TGS; n = 32) is located adjacent to a busy roadway, approximately 20 m away from numerous gasoline and diesel pumps and 0.25 km from I-25. This location is near a large shopping center and another gas station across the street.

The samples from an elementary school in Loveland ("Loveland Elementary School" or LES; n = 28) were collected along a fence on the school property adjacent to an automobile repair shop.

The site was about 5 km away from I-25 and roughly 2 km from a busy roadway. Similar to Bella Romero Academy, the students attending the schhool in Loveland are predominantly non-white and come from low income families (Colorado EnviroScreen 2.0; CDPHE, 2025d).

Last, the background measurements were collected at Soapstone Prairie Natural Area (SPNA; n = 11), a mostly open and undeveloped prairie land. SPNA is located in northern Larimer County, CO, and is about 1.5 km south of the Wyoming border. The site has little vehicle traffic or O&G activity and is about 8-km from the interstate highway (I-25).

Throughout this work, we mainly focus the results and discussion on three sites. FCW and GRA are selected to represent the longitudinal extent of the sampling sites, while TGS provides information near I-25 and we can also utilize the data to identify the influence of evaporated gasoline on ambient air concentrations.

2.2 VOC Sampling and Chemical Analysis

We collected weekly-averaged measurements of CH_4 and VOCs using whole air canisters. At each sampling location, we deployed evacuated 6.0-L Silonite®-coated stainless steel canisters coupled with CS1200E flow regulation systems (Entech Instruments). The flow control systems allow the canisters to collect ambient air at a constant rate over the seven day sampling period. Prior to field deployment, we cleaned and evacuated the canisters (Ku et al., 2024) and we cleaned and calibrated the flow control systems. For quality control, we monitored the flow rates at each sampling location and replaced the flow control systems when necessary. Within a week of collection, we analyzed the samples by gas chromatography (GC) at the Colorado State University (CSU) Department of Atmospheric Science as described in previous studies (Ku et al., 2024; Benedict et al., 2019; Sive et al., 2005; Zhou et al., 2005).

Briefly, we analyzed the canister samples for CH_4 using a Shimadzu GC-8A gas chromatograph (GC) equipped with a digital temperature programmer and flame ionization detector (FID), and we used a custom-built, multi-channel GC to analyze 51 non-methane VOCs (NMVOCs). The NMVOC system consists of three GCs and five detectors (three FIDs, one electron capture

detector (ECD), and one mass spectrometer (MS)). The NMVOCs measured include C_2-C_{10} linear, branched, and cyclic alkanes, alkenes, alkynes, and aromatic, and C_2 halocarbons. Note, the 2015-2016 canister samples do not include measurements of CH_4, halocarbons, or acetonitrile. A complete list of analyzed compounds and their method detection limits (MDL) can be found in Table A.1-A.4. We calibrated both GC systems using certified standards. The accuracies for the CH_4 standard (SCOTT-MARRIN Inc., CA, USA) and NMVOC standard (HC Mix56, Airgas, PA, USA) were $\pm$ 1% and $\pm$ 5%, respectively. To monitor system drift, we analyzed multiple working standards with each sample batch. The measurement precision (1 relative standard deviation, RSD) was 4% for CH_4, and ranged from 2% to 20% for individual NMVOCs. We report canister sample concentrations below the detection limit as 1/2 their MDL value.

To examine spatial and seasonal trends, this work primarily focuses on CH_4, light (C_2-C_7) and heavy (C_8-C_{10}) alkanes, and HAPs species (i.e., *n*-hexane, *2*,*2*,*4*-trimethylpentane, benzene, toluene, ethylbenzene, *m*+*p*-xylene, *o*-xylene, styrene, tetrachloroethylene, trichloroethylene, and acetonitrile). In this work, we include n-nonane in our list of HAPs as it is an air toxic commonly associated with O&G activity despite the EPA not classifying it as one in their list of 188 species.

2.3 Fuel Composition Headspace Analysis

Since the impact of fueling stations is underexplored in previous source apportionment analyses, we conducted laboratory fuel compositional analyses to identify a fuel evaporative emissions fingerprint and explore the range of HAPs abundance from fueling stations in the urban and suburban environments. We employ a headspace analysis technique to examine the chemical composition of volatiles evolved from pure gasoline (winter and summer formulations) and diesel. In this method, we analyze the gaseous "headspace" above the liquid fuel. Here, we focus on the winter blend gasoline as it is presumably more representative of gasoline sold when the gas station samples were collected. Detailed descriptions of the fuel sample collection and analysis procedures can be found in Section A.3, with more information regarding the diesel and summer blend gasoline samples.

Briefly, we filled two clean and dry 20-mL amber glass vials with 85 octane gasoline (winter blend, taken before the summer 2025 switchover to reformulated gasoline) and stored them in the refrigerator. Approximately two hours prior to GC analysis, we transferred 10 mL portions of the fuel sample into two new clean and dry 20-mL amber glass vials, and let them sit at room temperature. To dilute headspace samples, we mixed 1 mL of the headspace air taken from a vial with zero air inside an evacuated 1.4-L Silonite®-coated stainless steel canister (Entech Instruments). We analyzed the diluted headspace samples for 51 NMVOC concentrations using the same method described in Section 2.2. For quality assurance, we also analyzed zero air as blank samples during each sample batch.

We analyzed two gasoline headspace samples within 24 hours of collection and stored two additional vials in the refrigerator to monitor fuel composition stability (Section A.3; Figure A.1). Note that while we obtained the liquid fuel samples from the same gas station as the TGS canister samples, we performed the headspace analysis in 2025. Therefore, it is possible that the composition of fuels supplied at the station changed in the approximately ten years since sample collection at TGS.

2.4 PMF Analysis and Data Treatment

PMF is widely used as a source apportionment technique for VOCs (e.g., Abeleira et al., 2017; Bon et al., 2011, Brown et al., 2007, Frischmon and Hannigan, 2024; Guuha et al., 2015; Lachenmayer et al., 2024; Lyu et al., 2021; Orak et al., 2020, Pan et al., 2023; Pollack et al., 2021; Yuan et al., 2012). The EPA PMF v5.0 (Norris et al., 2014) we use in this work is a multivariate factor analysis model that decomposes the speciated VOC data matrix (**X**) into factor profiles (**F**), factor contributions (**G**), and residual (**E**) matrices (Equation 2.1).

$$\mathbf{X} = \mathbf{G} \cdot \mathbf{F} + \mathbf{E}, \tag{2.1}$$

The sample concentration data matrix (**X**) has dimensions $m \times n$, where m is the number of VOC species and n is the number of samples. The factor profile matrix (**F**), which is interpreted

as fingerprints of VOC sources, has $p \times m$ elements, where p is the number of profiles. The factor contribution matrix (**G**) has dimensions $n \times p$. The residual matrix (**E**), with dimensions $m \times n$, represents residuals between the data points and the model fit. The model minimizes the residuals and has the constraint that no samples have significantly negative source contributions.

The number of factor profiles p is chosen by the user to represent realistic sources that contribute to the species concentration in data matrix **X**. The best solution to the PMF receptor model is typically identified as the minimum value of Q, the quality of fit parameter (Equation 2.2). This objective function is the squared difference between the fit of the summed predicted speciated factors and the original matrix normalized by the uncertainties (**U**), which has the dimensions $m \times n$. Considerations for selecting p for the PMF solution are discussed in Section A.4.1.

$$Q = \sum^{n} \sum^{m} \left(\frac{\mathbf{E}}{\mathbf{U}} \right)^2 \tag{2.2}$$

In this work, we ran base PMF model 100 times with a random seed to evaluate the stability of the solutions with a range of two to eight factors. We determined the appropriate number of factors p by examining the rate Q decreases with increasing p, indicating the amount of information gained by the addition of each factor (Section A.4.1). To evaluate the robustness and rotational ambiguity of the PMF solution for each factor number, we conducted additional error testing through bootstrapping and displacement techniques. We estimated the solution uncertainty using 100 bootstraps of the most convergent base model PMF solution (i.e., the lowest Q value). Figures in this work show factor profiles and factor contributions from the base model PMF solution, and uncertainties represent the mean and the 25th and 75th percentiles.

We performed PMF analysis on a subset of the speciated concentration data from our background location (SPNA) plus the five sites with the longest sampling periods: FCW, GRA, TES, TGS, and LES. We excluded samples with missing speciated concentration data from the data matrix **X** we used in PMF analysis. We prepared the uncertainty matrix **U** according to Hopke (2016) and Polissar et al. (1998). Weighting data points in this manner allows for the level of confidence in the VOC measurement to be accounted for in the PMF model solution. Details about the uncer-

tainty calculations we used in this study can be found in Section A.4.2. Following Hopke (2016), we considered the signal-to-noise ratio (*S/N*) and coefficient of determination (r^2) to determine which VOC species to exclude before running the PMF model. Note we took additional considerations into account when finalizing the NMVOC compound list as described in Section A.4.3. In total, we included 40 species and 283 weekly-integrated canister samples in the PMF analysis.

2.5 PID Continuous Air Monitoring

In addition to weekly-integrated whole air canisters, we deployed real-time, medium-cost air monitoring systems that combine air pollutant concentration and wind field measurements to detect emission plumes and help locate their sources. At three sampling locations (i.e., FCN, LES, and GRA), we installed SPOD sensor systems (SENSIT Technologies Corp.) coupled with an automatic canister trigger system. The SPOD system contains a photoionization detector (PID) sensor that produces a non-speciated, uncalibrated concentration of a subset of VOCs that can be ionized with a 10.6 eV PID, a sonic anemometer for measuring temperature, relative humidity, pressure, and wind speed and direction, a solar panel to power the system, and a cellular connection for data upload and system monitoring. To ensure adequate response in the field, we conducted pump tests on the PIDs using 1 ppmv ($\pm$ 5%) isobutylene gas. Since the response of the detector varies by compound, we interpret the output as a semi-quantitative measurement of the integrated mix of total VOCs photoionized at 10.6 eV. Response factors are available from the manufacturer (https://gasleaksensors.com/products/sensit-spod/). The sensor measurement range is 10-3000 ppbv $\pm$ 20% with a 30-60 second response time. The SPOD reports one minute integrated readings for total VOC and meteorological parameters.

To provide a more comprehensive compositional analysis of emission plumes, we used a coupled trigger system to collect whole air canister samples. With solenoid valves attached to a canister valve controller (SENSIT Technologies Corp.), the system fills evacuated 1.4-L Silonite®-coated stainless steel canisters (Entech Instruments) for two minutes during high-VOC pollution events. Using a dynamic trigger configuration, we programmed the SPOD system to collect canis-

ter samples following two criteria: a trigger threshold and a static limit. As configured, the SPOD system calculated a baseline as the ten-minute mean ppbv value. It then collected a sample when either the instantaneous enhancement of the PID reading (i.e., instantaneous value minus baseline value) was higher than 100 ppb or the reading exceeded a static threshold of 200 ppb. To increase the number of plumes captured, we installed two to four values and canisters at each site. We analyze the trigger canister samples for CH_4 and 51 NMVOC using the methods described in Section 2.2.

The SPOD air monitoring system worked well overall for detecting and characterizing plumes with elevated VOC concentrations and compositions indicative of O&G and urban combustion emissions at all times of the day. While we do not investigate the SPOD-derived total VOC data or trigger samples in this work, examples of speciated trigger canister measurements can be found in Figure A.5.

2.6 Mobile Sampling Platform

To survey CH_4 and NMVOCs concentration around Northern Colorado and identify and locate emission plumes, we used an instrumented hybrid SUV "plume tracker" (Hecobian et al., 2019) equipped with real-time gas analyzers. We measured one-second averaged CH_4 concentrations with a LI-7810 $CH_4/CO_2/H_2O$ Trace Gas Analyzer (LI-COR Environmental).

Additionally, we utilized an AROMA-VOC (Entanglement Technologies Inc) to identify increases in BTEX (i.e., benzene, toluene, ethylbenzene, and xylenes) and other VOC family concentrations. The AROMA-VOC was operated in RapidScan mode to provide semi-quantitative real-time plume detection and used primarily to locate possible sources for additional characterization using VOC canister grab sample collection.

Using an Airmar 220WX WeatherStation mounted on the vehicle roof, we record one-second averaged meteorological data including wind direction, wind speed, and temperature. We corrected wind direction and wind speed for the influence of the movement of the vehicle. A bump test with a calibration gas (1 ppb isobutylene) is used to assure the system properly detects VOC plumes

and to determine the inlet delay for GPS synchronization. The AROMA-VOC and meteorological sensors both report longitude and latitude coordinates during the drive.

We deployed the plume tracker for multiple survey drives along roads with expected VOC emissions from commercial, industrial, manufacturing, and utility sources, in disproportionately impacted communities including around several mobile home communities, and in response to individual concerns. However, we focus our results on a drive in Galeton, CO where we intercepted the pollution plume during an uncontrolled O&G well accident event in Chapter 4.

Chapter 3

Source Trends of VOCs and Air Toxics

3.1 Seasonality of VOCs in Northern Colorado

CH_4 and NMVOCs with the highest weekly-averaged ambient concentrations have strong seasonal patterns in the NCFR that are driven by meteorological and emission patterns. Figure 3.1 displays the distribution of weekly-averaged concentrations by month for total measured NMVOC and four individual VOCs at three sampling locations: FCW, GRA, and TGS. We provide the average concentrations for all measured compounds, divided by season and sampling location in Figures B.1-B.5 (also see Table B.1).

The average concentrations of total NMVOCs tend to increase in the wintertime relative to other seasons across all sampling sites (Figure 3.1.a-c). The robust seasonal cycle reflects weaker dilution of NMVOC emissions near the surface by atmospheric mixing dynamics in a shallower winter boundary layer and reduced irradiance for photochemical loss in colder months compared to warmer months. Previous studies in the CNFR have observed similar trends (e.g., Pétron et al., 2012, Pollack et al., 2021, Ku et al., 2024, Helmig et al., 2025; Thompson et al., 2014). Ethane, which generally dominates the total NMVOC concentration in the samples, likewise has a winter maximum at all sampling locations (Figure 3.1.d-f). As a compound commonly associated with emissions from O&G activity in the region (e.g., Gilman et al., 2013), the pattern is strongest in the samples from GRA (Figure 3.1.e) which sits in the heart of the DJ Basin (Figure 1.3). Benzene and *n*-hexane similarly have higher average concentrations during the winter at FCW and GRA (Figure 3.1.g,h and 3.1.j,k).

Isoprene and acetonitrile deviate from the winter maximum trend for at all sampling locations (Figure 3.1.j-l and Figure B.6). Since biogenic sources largely dominate isoprene emissions (Bryant et al., 2023; Guenther et al., 1995) and acetonitrile is a tracer for biomass burning emissions (Huangfu et al., 2021), we expect them to both have higher weekly-average concentrations

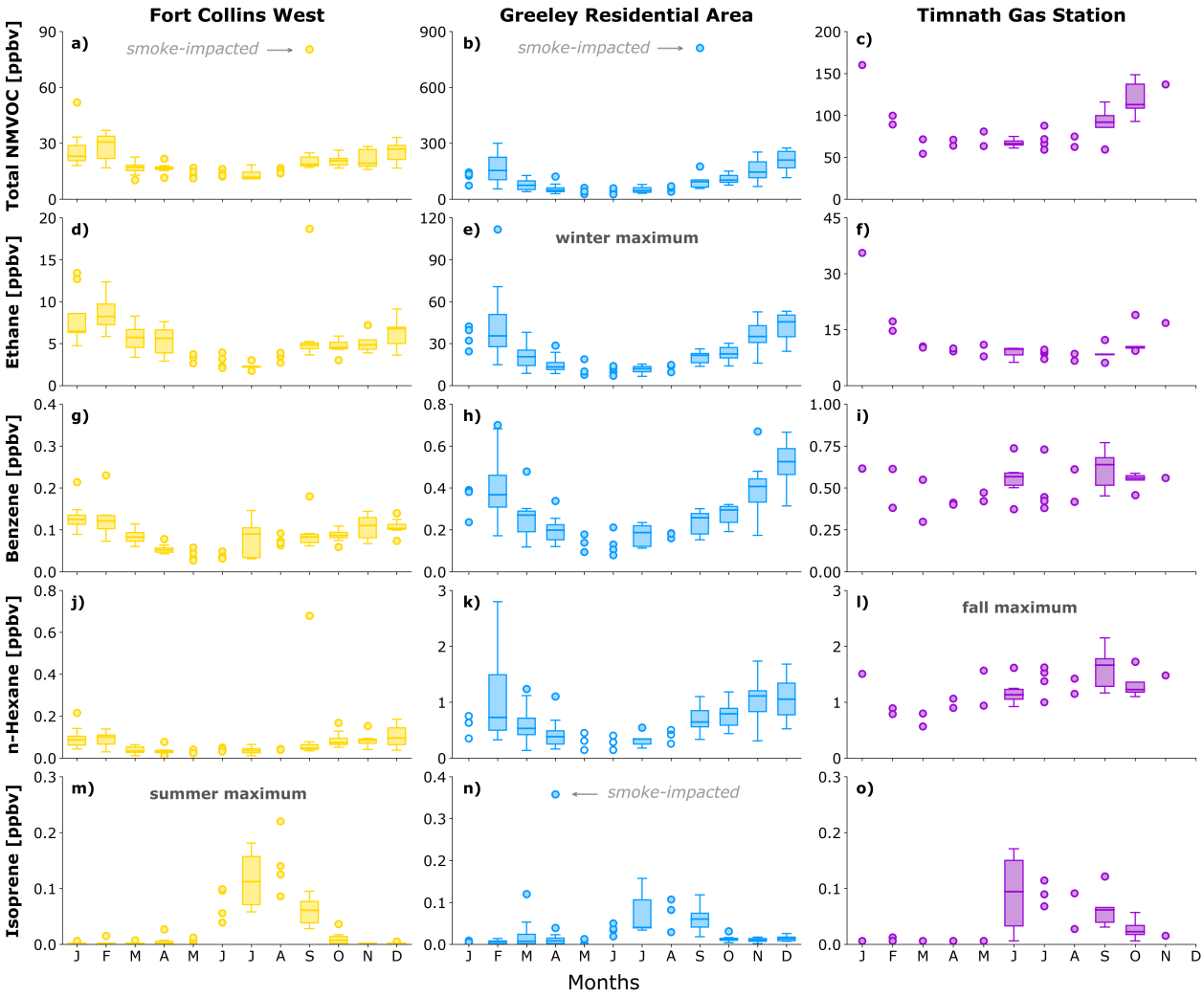

Figure 3.1: Distribution of weekly-averaged concentrations [ppbv] of total NMVOC **(a-c)**, ethane **(d-f)**, benzene **(g-i)**, *n*-hexane **(j-l)**, and isoprene **(m-o)** at three sites in Northern Colorado. Box and whisker plots show the median value (box middle), first quartile (box bottom), third quartile (box top), and range (whiskers for data within 1.5 times the interquartile range) including outliers (scatter points for data beyond 1.5 times the interquartile range) for months with n = 5 or greater samples. Individual data points are plotted for months with less than n = 5 samples. Measurements below species detection limits are replaced with 1/2 of their MDL value. The seasonal maxima are highlighted for panels e, l, and m. Smoke-impacted measurements are annotated in light gray.

during the warmer summer months. Previous studies investigating NMVOCs in the Boulder Reservoir in Boulder found that isoprene concentrations remain below 0.1 ppbv most of the year, except for during the summer (Pollack et al., 2021, Helmig et al., 2025). We note that the anomalously high values of total NMVOCs and various individual NMVOCs (e.g., ethane, benzene, *n*-hexane, and isoprene) from FCW in September and from GRA in April might be partially explained by smoke impact from biomass burning that we discuss further in Section B.2.

The samples from near the gas station have seasonal patterns that are distinct from the other sites suggesting that the TGS ambient concentrations are partially dependent on emission source seasonality. At TGS, the benzene has a weak seasonal cycle (Figure 3.1.i) and *n*-hexane concentration displays a slight increase in the summer and fall months (Figure 3.1.l). Since we observe similar summer and fall maxima for other VOC species abundant in gasoline (i.e., *n*-nonane, *n*-decane, *2*,*2*,*4*-trimethylpentane, toluene, ethylbenzene and xylene isomers), we presume the flipped seasonal trend is influenced by higher gasoline evaporation rates associated with warmer temperatures in the summer and fall months. In Section 3.2, we investigate compositional differences between measurements from TGS compared to other sampling locations.

3.2 Spatial Gradients of VOCs in Northern Colorado

Two dominant spatial patterns emerge from investigating weekly-averaged ambient concentrations across Northern Colorado. Figure 3.2 shows the spatial gradient for CH_4, light and heavy alkanes, and HAPs species concentrations at all sampling locations in the winter. Here, we highlight winter measurements when concentrations of many VOCs are highest compared to other seasons (Section 3.1); however, these spatial gradients are broadly consistent across all seasons (Figures B.1-B.5; Table B.1).

First, the average concentrations of CH_4 and light alkanes generally increase moving from Fort Collins in the west to Greeley in the east (Figure 3.2.a), reflecting the regional distribution of O&G activity. Figure 3.2.c illustrates the gradient in average ethane concentrations overlaid with the locations of past and present oil wells. For example, ethane is about five times higher at GRA (37

ppbv) than FCW (7 ppbv) in the winter. Several other light and heavy alkanes that are commonly associated with O&G activity (e.g., propane, *n*-heptane, *n*-octane, *n*-nonane, and *n*-decane) likewise have a strong eastward gradient, even when considering the measurements from TGS (Figure 3.2.a). In general, FCW has the lowest average concentration of CH_4 and many light and heavy alkanes with approximately an order of magnitude increase in alkane concentrations at GRA in the spring, summer, and winter (Figures B.1-B.5; Table B.1). In the fall, we have measurements from our background site SPNA, which are typically the lowest observed concentrations (Figures B.1-B.5; Table B.1).

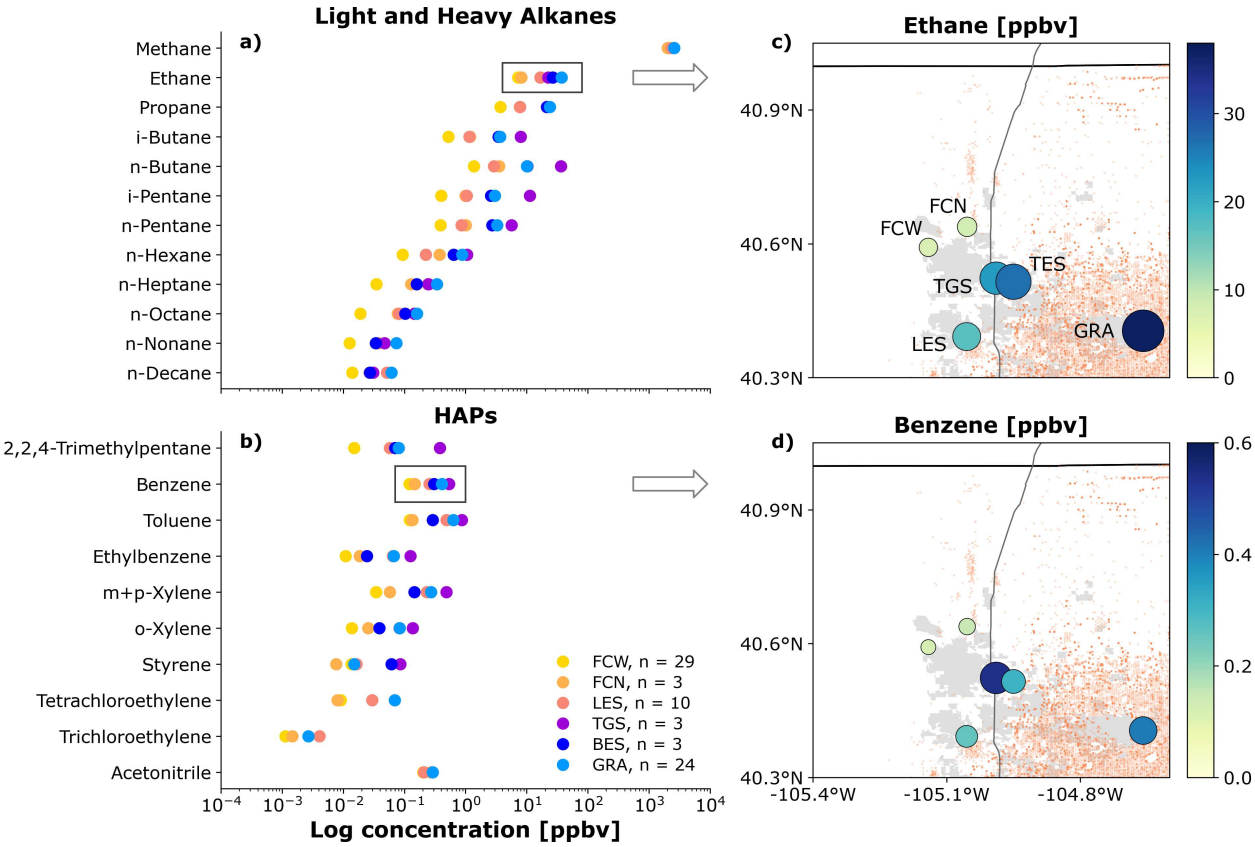

Figure 3.2: Average log scale winter concentration [ppbv] of **(a)** light and heavy alkanes and **(b)** HAPs in Northern Colorado. Maps with average winter concentrations [ppbv] of **(c)** ethane and **(d)** benzene. The concentrations are indicated with the size and color of the points. Species concentrations below the detection limit are replaced with 1/2 of their MDL value. The site colors and name abbreviations correspond to the map in Figure 2.1. The samples collected in 2015-2016 were not analyzed for methane, tetrachloroethylene, trichloroethylene, or acetonitrile. Note, over 60% of the samples from FCW are below the detection limit for *n*-nonane, *n*-decane, *2,2,4*-trimethylpentene, styrene, *o*-xylene, and acetonitrile. Similarly, over 60% of the samples from FCN are below the detection limit for *n*-decane and styrene, and the same for styrene measured at GRA.

Second, we find that most of the HAP compounds have a more complex spatial distribution, highlighting the influence from traffic and point emission sources. Breaking up the eastward gradient discussed above, the average concentration for HAPs (Figure 3.2.b) and some of the light alkanes (i.e., the butane and pentane isomers, and *n*-hexane; Figure 3.2.a) are highest at the TGS. The map in Figure 3.2.d illustrates the spatial distribution of average wintertime benzene concentrations at all of the sampling sites, with the TGS site standing out with the highest levels. Benzene is over four times higher at TGS (0.54 ppbv) than FCW (0.12 ppbv) and about three times higher at GRA (0.41 ppbv) than FCW in the winter. As shown in Figure 3.2.b, *2*,*2*,*4*-trimethylpentane—which we largely attribute to gasoline evaporation in Sections 3.3 and 3.4—has the largest difference in average concentrations between GRA (0.08 ppbv) and TGS (0.38 pbv) for the HAPs species. Note that *2*,*2*,*4*-trimethylpentane is also associated with O&G activities (Garcia-Gonzales et al., 2019). While gasoline evaporation appears to strongly influence the ambient NMVOC concentrations at the gas station, urban combustion emissions likely also influence the measurements since the site is near the interstate, a busy commuter road, and a large shopping center parking lot (Section 2.1).

Briefly, to contextualize these measurements from the northern portion of the CNFR, we compare them to samples from the southern part of the region. Table 3.1 summarizes annual-average concentrations of several NMVOCs from FCW, GRA, and TGS and juxtaposes them with samples collected at an urban site in Denver, CO [39.751207°N, -104.987648°W] (CDPHE, 2025c) and the measurements from nine neighborhoods near O&G activity in Broomfield, CO (Ku et al., 2024). The data from CDPHE's Denver-CAMP site consists of 3-hour samples (6:00-9:00 a.m. MST) 2020-2023, while the Broomfield measurements include weekly-integrated whole air canister samples from before O&G pre-production, during pre-production stages, and into O&G production. The morning-only sampling schedule at Denver-CAMP likely increases measured concentrations from vehicular emissions due to larger traffic volume during the morning commute and reduced dispersion inside a lower morning mixed layer. The average light alkane (i.e., ethane, propane, *i*-butane, *n*-butane, *i*-pentane, *n*-pentane, and *n*-hexane) and HAP aromatics (i.e., benzene and toluene) concentrations measured in Broomfield fall between FWC and GRA (Table 3.1). A

similar trend is observed for the light alkanes at the Denver site; however, the benzene and toluene concentrations are comparable to and two times higher than that from GRA, respectively, but still lower than measured at TGS (Table 3.1). In Section 3.3, we further explore the differences in the TGS samples.

Table 3.1: Annual average and standard deviation of ambient NMVOC concentrations [ppbv] from various locations in Northern Colorado.

Species	FCW	GRA	TGS	Denver[1]	Broomfield[2]
Year	*2023-2025*	*2022-2025*	*2015-2016*	*2021-2023*	*2018-2022*
Ethane	5.5 ± 2.7	24.6 ± 16.2	10.9 ± 5.4	14.7 ± 14.7	11.3 ± 7.2
Propane	2.5 ± 1.7	15.7 ± 10.3	12.3 ± 4.5	4.6 ± 3.8	5.6 ± 3.8
i-Butane	0.3 ± 0.3	2.5 ± 1.6	5.2 ± 2.9	1.1 ± 4.9	1.0 ± 0.7
n-Butane	0.9 ± 0.7	6.7 ± 4.4	22.6 ± 15.6	2.4 ± 2.2	2.6 ± 1.8
i-Pentane	0.3 ± 0.2	2.1 ± 1.3	15.7 ± 4.7	1.2 ± 0.9	0.9 ± 0.5
n-Pentane	0.3 ± 0.2	2.3 ± 1.4	6.7 ± 2.1	1.0 ± 0.9	0.9 ± 0.6
n-Hexane	0.07 ± 0.08	0.66 ± 0.47	1.26 ± 0.34	0.38 ± 0.31	0.36 ± 0.35
Benzene	0.09 ± 0.04	0.28 ± 0.14	0.53 ± 0.12	0.29 ± 0.19	0.16 ± 0.08
Toluene	0.18 ± 0.52	0.44 ± 0.23	1.31 ± 0.42	0.88 ± 1.35	0.29 ± 0.26
Acetylene	0.4 ± 0.2	1.0 ± 0.7	0.6 ± 0.2	1.5 ± 1.5	0.7 ± 0.8

[1] Data collected at the Denver-CAMP site in Denver, CO [39.751207°N, -104.987648°W] as 3-hour samples (6:00–9:00 a.m. MST) from 2020–2023 (CDPHE, 2025c).
[2] Data collected at nine residential sites surrounding O&G well pads in Broomfield, CO as weekly whole air canister samples from October 2018 to December 2022; measurements include samples from before O&G pre-production, during pre-production stages, and into O&G production (Ku et al., 2024).

3.3 Gas Station VOC Signature

The weekly-integrated samples from the gas station exhibit a distinct compositional NMVOC signature partly resembling a gasoline emission fingerprint. Figure 3.3 displays the average percentage contributions of light and heavy alkanes and HAPs in the ambient measurements from FCW, GRA, and TGS juxtaposed against that in gasoline headspace samples. Here, we use FCW and GRA to represent a range of ambient NMVOC concentrations at suburban sites in Northern Colorado to contrast with the TGS measurements that are strongly influenced by fresh vehicular

combustion and evaporated gasoline emissions. Evaluating the percent contributions of NMVOCs in the annual-average ambient TGS measurements against those in the pure gasoline headspace samples is not an equivalent comparison, because the ambient samples at the gas station also reflect contributions from local vehicle exhaust and other regionally transported NMVOCs. However, it can provide insights into some of the key impacts of gasoline evaporation on the TGS samples. We discuss a more quantitative source apportionment approach in Section 3.4.

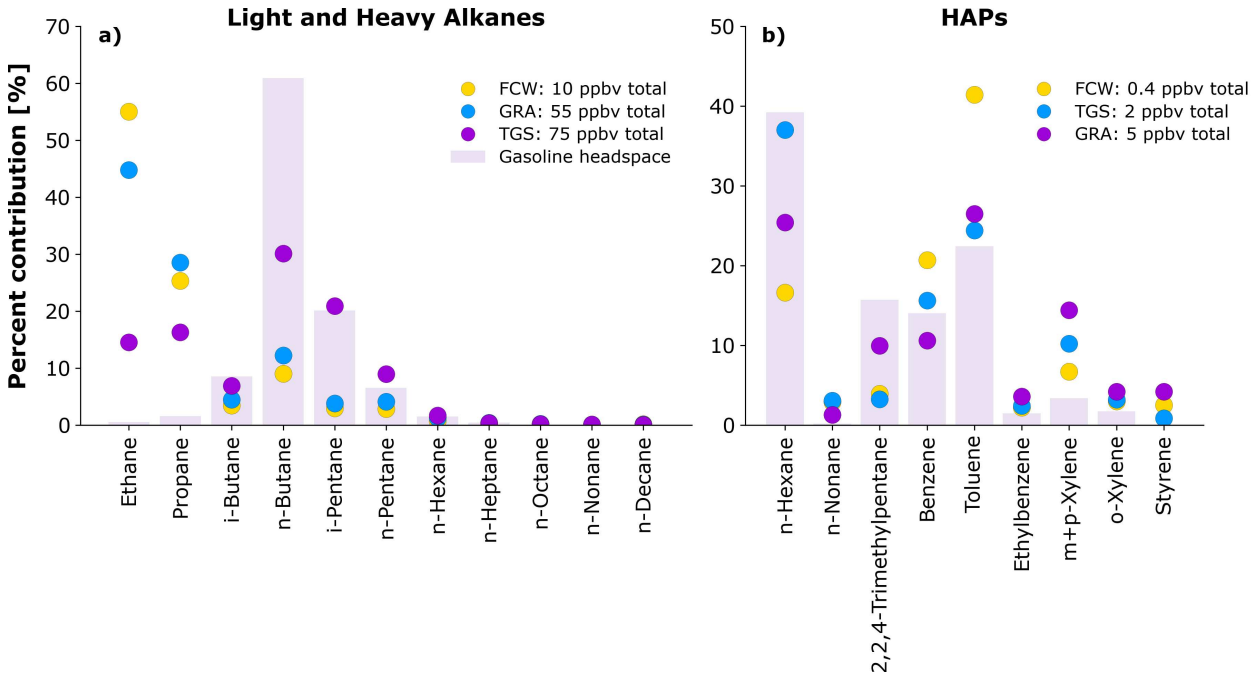

Figure 3.3: Percent contributions [%] of average **(a)** light and heavy alkanes and **(b)** HAP compounds at three sites in CNFR and in gasoline headspace samples. The colored circles represent the annual-average contributions for ambient concentrations from Fort Collins West (FCW; yellow) and Greeley Residential Area (GRA; blue), and Timnath Gas Station (TGS; purple). The bar plot (light purple) shows the average contributions of two gasoline headspace samples. The total average concentrations of light and heavy alkanes and HAPs compounds are included in the legends. We do not include tetrachloroethylene, trichloroethylene, and acetonitrile in the HAPs analysis as we did not measure them in the TGS samples.

The annual-average percentage contribution of light alkanes are higher at TGS than the other ambient measurement sites, except for two noteworthy O&G tracers, ethane and propane. Figure 3.3.a shows that the relative contributions of *i*-butane, *i*-pentane, *n*-pentane, and *n*-hexane to the total measured light and heavy alkanes in ppbv are higher in the TGS measurements (7%, 20%,

9%, and 2%) than the fairly similar FCW (3%, 3%, 3%, and 0.7%) and GRA (4%, 4%, 4%, and 1%) samples. Their percentage contributions in the TGS samples more closely track those in the gasoline headspace samples (9%, 20%, 7%, and 2%; Figure 3.3.a). Likewise, the relative contribution of *n*-butane to the total measured alkanes in the ambient TGS measurements (30%) is significantly more than that in the FCW (9%) and GRA samples (12%), but still lower than the gasoline samples (61%; Figure 3.3.a). Since *n*-hexane and butane and pentane isomers are associated with both the evaporation (Chin and Batterman, 2015; Connor et al., 2012; Gentner et al., 2009, 2013; Harley et al., 2000; Na et al., 2004; Rubin et al., 2006; Sun et al., 2025) and combustion of gasoline and other fossil fuels (Connor et al., 2012; Gentner et al., 2009, 2013; McLaren et al., 1996; Rubin et al., 2006), we expect their relative abundance to be highest at TGS compared to the other sites. In contrast, the relative contributions of ethane and propane—which are primarily emitted by O&G activities—are much higher in the FCW (55% and 25%) and GRA (45% and 29%) samples than in the TGS samples (15% and 16%; Figure 3.3.a). Their abundances are even lower in the gasoline headspace samples (0.5% and 2%), consistent with influence on the TGS samples from other regional emission sources. We characterize and quantify the emission sources that impact the gas station samples further in Section 3.4.

Benzene, toluene, and *n*-hexane are among the HAPs we analyzed with the largest average percent contributions in the ambient measurements and gasoline headspace samples. They are emitted from a variety of sources including gasoline evaporation (Chin and Batterman, 2015; Connor et al., 2012; Gentner et al., 2009, 2013; Harley et al., 2000; Na et al., 2004; Rubin et al., 2006; Sun et al., 2025), vehicular combustion (Connor et al., 2012; Gentner et al., 2009, 2013; McLaren et al., 1996; Rubin et al., 2006), and O&G activity (e.g., Pollack et al., 2021; Ku et al., 2024). Benzene and toluene are among the most abundant aromatic NMVOCs measured in gasoline vapor and liquid fuel (e.g., Chin and Batterman, 2015; Harley et al., 2000; Sun et al., 2025). Multiple factors impact the composition results for both liquid fuels and vapor samples, including the gasoline brand, fuel grade, season, location, formulation, year, and the laboratory conditions and variables (e.g., temperature and measured compounds). Figure 3.3.b shows that benzene is the only measured HAP

species that has a lower relative contribution at TGS than FCW or GRA. Comprising about 27% and 26% of the measured HAPs in the TGS samples (Figure 3.3.b), toluene and *n*-hexane dominate the concentration of air toxics. However, benzene, *n*-nonane, and the xylene isomers have higher potentials for health hazards when considering the estimated chronic exposure hazard quotient for the TGS measurements (i.e., the annual-average weekly concentration of each HAP divided by the appropriate non-carcinogenic chronic health guideline value; Figure B.7). This hazard quotient does not consider health concerns arising from any additive or synergistic effects associated with simultaneous exposure to the complex mixture of gasoline-related compounds.

The HAPs composition in TGS samples shows important influence from vehicular combustion and gasoline evaporation. Figure 3.3.b illustrates that the relative contribution of *2*,*2*,*4*-trimethylpentane, ethylbenzene, the xylene isomers, and styrene are higher in the TGS samples (10%, 4%, 15%, and 4%) than the FCW (4%, 2%, 7%, and 3%) and GRA (3%, 3%, 11%, and 3%) measurements. Previous studies have found that *2*,*2*,*4*-trimethylpentane, *m*+*p*-xylene, and *o*-xylene are among the most abundant NMVOCs measured in liquid gasoline and gasoline vapors (e.g., Chin and Batterman, 2015; Gentner et al., 2009); these compounds are also found in vehicle emissions (e.g., Connor et al., 2012; Gentner et al., 2009, 2013). Alternatively, styrene—which is mainly emitted from automobile exhaust (Na et al., 2004, Montells et al., 2000) and found in relatively small concentrations in gasoline fuel itself (Na et al., 2004)—is not found in the gasoline headspace sample we analyzed with 24 hr of collection (Figure 3.3.b; Figure A.1). Hence, we attribute the styrene in the TGS samples (4% of included HAPs) primarily to influence from vehicular combustion emissions. As discussed in Section 2.2, the TGS sampling location is near a major roadway, interstate highway, parking lot, and shopping center. Styrene has higher ambient concentrations in the 2015-2016 samples (i.e., TGS, TES, SPNA, and FCNA) than those from 2022-2025 (i.e., FCW, FCN, LES, and GRA; Figure 3.2.b and Figure B.4), following long-term downward trends in gasoline-related styrene exposures in California (Sultana and Hoover, 2024). In Section 3.4, we further utilize the gasoline headspace sample fingerprint for source apportionment interpretation.

3.4 Source Apportionment of VOCs in Northern Colorado

3.4.1 *i*/*n*-Pentane Ratios

To characterize emission source regimes, we first use the ratio of pentane isomers (*i*/*n*-pentane) as a robust indicator of the relative influence of O&G activity and urban combustion emissions on ambient air samples. This ratio is minimally impacted by boundary layer conditions, the proximity to emission sources, or photochemical processing (Gilman et al., 2013) as it is largely independent of air mass mixing and dilution (Parrish et al., 2007) and the isomers have similar reaction rates with the hydroxyl radical (Atkinson et al., 1990). Ratios below one are associated with substantial influence with O&G emissions, while ratios approaching two indicate strong influence from urban combustion sources, including vehicular and gasoline emissions. Samples with ratios between one and two are influenced by a mix of O&G and urban combustion sources. Figure 3.4 displays the average *i*/*n*-pentane ratios distributions for the eight sites in this study overlaid with reference ratio values. The ratios from FCW, TGS, TES, and GRA include measurements from over a year of sampling and can be interpreted as annual-averages. We note that there is not significant seasonal variability in the *i*/*n*-pentane ratios in our samples (Figure B.8).

Pentane isomer ratios reveal O&G and combustion emissions have a large-scale impact on air-quality in the CNFR. Excluding the gas station, which has the highest average *i*/*n*-pentane ratio (2.35), the sites in this study have ratios ranging from 0.93 to 1.36, which are lower than the ratio observed in Denver, CO (1.53; CDPHE's Denver-CAMP canister samples; CDPHE, 2025c) or other large cities such as Los Angeles, CA (1.80; AEROMMA summer 2023 aircraft campaign) and Chicago, IL (1.63; Figure 3.4). The average *i*/*n*-pentane ratios in this study are mostly lower than New York City, NY (1.28; AEROMMA), except at the elementary school in Loveland that is adjacent to an automobile repair shop (1.36; Figure 3.4). TGS is the most impacted by traffic combustion and evaporative gasoline emissions; for comparison, the gasoline headspace samples have an average *i*/*n*-pentane ratio of 3.08 (Figure 3.4). As introduced in Section 3.3, the fact that the samples from TGS have lower *i*/*n*-pentane ratios than pure gasoline emissions suggests that this site is also impacted by transport of emissions from regional O&G activities. GRA is the site

most influenced by O&G activities, with an average ratio of 0.93 (Figure 3.4). It falls between the average ratios from two other regions with strong O&G influence, Broomfield, CO (1.07; Ku et al., 2024) and samples of raw natural gas from the Greater Wattenberg Area near Denver (0.86;Greater Wattenberg Area Baseline Study 2007; LT Environmental, Inc. (LTE), 2007). The canister sample with the lowest ratio we collected from GRA was 0.80 in March 2023. The more quantitative PMF source apportionment analysis results in Section 3.4.b similarly show widespread impact from O&G and urban combustion emissions on ambient NMVOC concentrations in the CNFR.

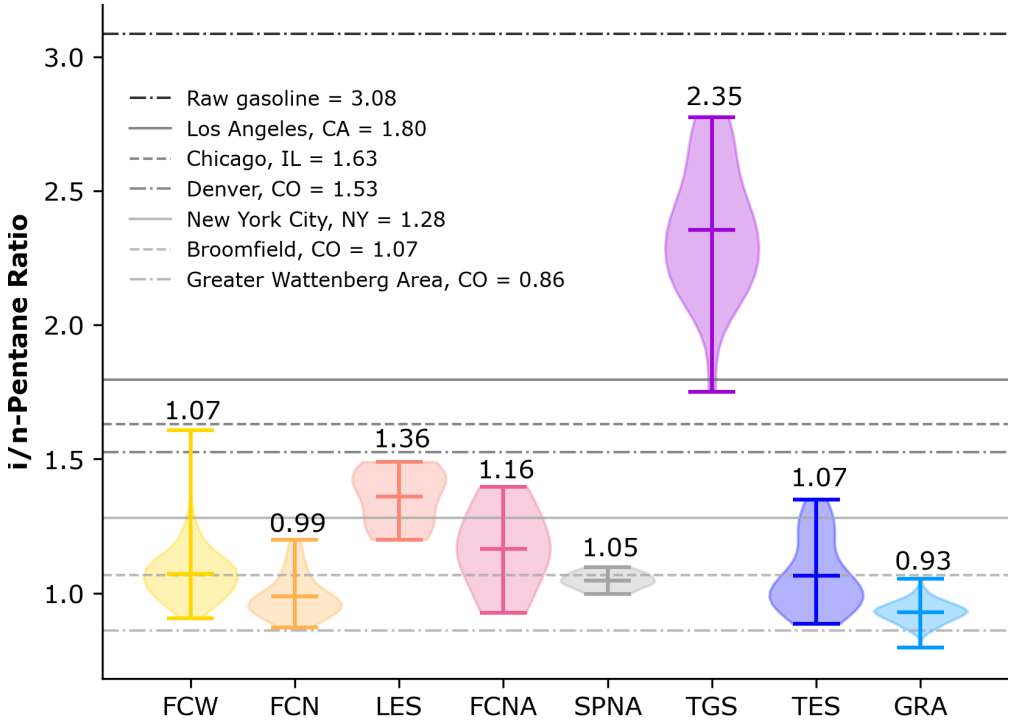

Figure 3.4: Distribution of *i*/*n*-pentane ratios [ppbv/ppbv] in the CNFR. Violin plots show the maximum, mean, and minimum values represented by the three colored lines. The mean ratios are printed above the violin plots. The site colors and name abbreviations correspond to the map in Figure 2.1. The gray lines show the mean pentane isomer ratios from a gasoline headspace sample (Section 3.3), Los Angeles, CA in summer 2023 (AEROMMA summer 2023 aircraft campaign), Chicago, IL in summer 2023 (AEROMMA), Denver, CO from 2020-2023 (CDPHE's Denver-CAMP canister samples), New York City, NY in summer 2023 (AEROMMA), Broomfield, CO from 2018-2023 (Ku et al., 2024), and the Greater Wattenberg Area, CO in 2006 (Greater Wattenberg Area Baseline Study 2007; LTE, 2007).

3.4.2 PMF Analysis

Leveraging the weekly-integrated canister measurements, we employ PMF to characterize and quantify contributions from emission source categories. Previous studies have often applied the receptor modeling tool to high time-resolution (e.g., hourly) and stationary VOC measurements collected over several months in the CNFR (e.g., Abeleira et al., 2017; Pollack et al., 2021), but a few have demonstrated the technique also works for weekly-integrated canister samples collected across multiple locations (e.g., Lachenmayer et al., 2024). Here, we use NMVOC measurements from five long-term sampling locations (FCW, LES, TGS, TES, GRA) and the background site (SPNA) to explore spatial trends in emission source contributions to VOC levels in the CNFR. We find that four factors best describe the samples. Based on VOC composition and proximity to particular source locations, we label these as O&G activity, traffic + urban combustion, fueling station, and biogenic + background. Figure 3.5 illustrates the average percent of species sum of 40 NMVOCs for the four PMF factor profiles. Briefly, note that while prior studies have successfully employed MLR analysis on VOC measurement (e.g., Gilman et al., 2013; Pollack et al., 2021), the weekly-integrated canister samples we use here are not well suited for this technique due to the model constraints and underlying assumptions.

The O&G activity factor—comprised of short-chain, longer chain, branched, and cyclic alkanes—contributes a significant portion of the ethane (57%), propane (69%), *n*-butane (62%), *i*-butane (60%), *n*-hexane (54%), *2*,*4*-dimethylpetane (57%), and methylcyclohexane (57%) in the samples (Figure 3.5). The factor has an *i*/*n*-pentane ratio of 0.81, indicative of O&G influence as discussed in Section 3.4.a. Additionally, it contains NMVOC species similar to the long-lived, short-lived, and process-specific O&G source factors found in previous studies in regions impacted by emissions from O&G activities (e.g., Abeleira et al., 2017; Pollack et al., 2021; Lachenmayer et al., 2024; Pan et al., 2023). For example, the long-lived O&G include light alkanes. The branched C_7-C_8 alkanes have been closely linked with specific O&G extraction activities such as flashing from oil and condensation tanks (Pan et al., 2023; Warneke et al., 2014). High emissions of C_9-C_{10} alkanes, ethylbenzene, and xylenes have been observed during O&G development processes

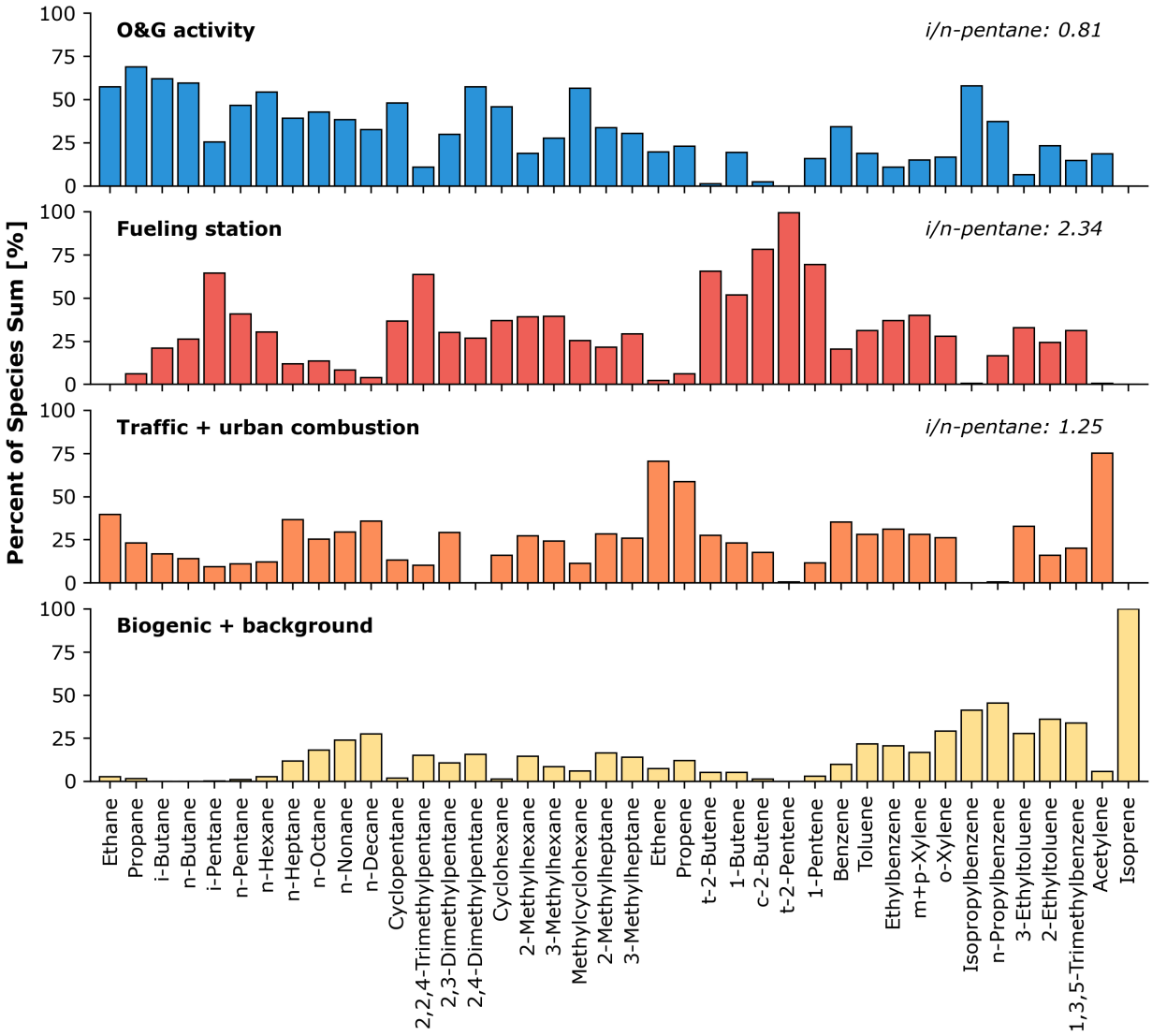

Figure 3.5: The average percent of species sum of 40 NMVOCs for the four factor profiles calculated using PMF with their *i*/*n*-pentane ratios. The factors include OG activity (blue), fueling station (red), traffic + urban combustion (orange), and biogenic + background (yellow) sources. The NMVOC compounds with "weak" classification in the PMF model include *n*-decane, *3*-methylheptane, *1*-pentene, isopropylbenzene, *n*-propolbenzene, and *2*-ethyltoluene.

such as drilling, fracking, and flowback (Pan et al., 2023; Hecobian et al., 2019; Ku et al., 2024; Lachenmayer et al., 2024). A five-factor PMF solution appears to split the long-lived alkanes from the short-lived and process-specific O&G emission, but the *i*/*n*-pentane ratios complicate source attribution by indicating mixed influence from combustion emissions (Section A.4.1). Thus, we focus on the four-factor PMF solution in the work.

The fueling station and traffic + urban combustion factors have identifiable tracer species and NMVOC signatures. Dominated by combustion tracers, the traffic + urban combustion factor accounts for the majority of acetylene (75%), ethene (71%), and propene (59%) in the measurements as also observed in other studies (e.g., Abeleira et al., 2017; Pollack et al., 2021; Lachenmayer et al., 2024; Pan et al., 2023). Emissions of light alkenes have been linked to vehicular emissions (Baker et al., 2008; Swarthout et al., 2013) and industrial activities (Washenfelder et al., 2010), while acetylene is a robust tracer (Fraser et al., 1998; Gentner et al., 2009, 2013). The factor has an *i*/*n*-pentane ratio of 1.25, and displays a seasonal pattern with a winter maximum at all of the sampling sites (Figures A.9-A.11). Alternatively, the fueling station factor is primarily associated with the TGS samples (Figure A.12) and includes NMVOCs associated with the evaporation of gasoline and combustion emissions (Figure 3.5). It represents a significant portion of the *i*-pentane (65%) and *2*,*2*,*4*-trimethylpentane (64%) in all the samples, which are abundant in gasoline vapor as we discussed in Section 3.3. The fueling station factor has an *i*/*n*-pentane ratio of 2.34 (Figure 3.5), which is similar to the ratio of 2.35 in the TGS canister samples (Figure 3.4). Since the PMF model attributes a small portion of the total NMVOC from GRA and LES to the fueling station factor (Figure 3.6.a), it suggests that the factor primarily represents NMVOCs from fuel evaporation with a smaller fraction from combustion sources. Supporting this notion, we find general agreement between modeled concentration from the fueling station PMF factor and measurements from TGS when contrasting the percentage contribution of light and heavy alkanes (Figure B.16).

The biogenic + background factor accounts for all of the isoprene in the samples. It displays a strong seasonal cycle, with peak contributions in the summer, when vegetation growth and elevated temperatures increase biogenic emissions (Figures B.9-B.11). The heavy branched alkanes

and aromatics also associated with this factor are typically found at low ambient concentrations in the region (Figures B.1, B.2, and B.4), and they indicate influence of emissions from anthropogenic activities (e.g., industrial and chemical processing) found in urban areas. This hypothesis is supported by the fact that LES, which is located in downtown Loveland and impacted by emissions from industrial activities, is the site with the largest contribution to total NMVOCs from this factor (Figure 3.6.a). Similar PMF factor profiles have been found in previous studies in the CNFR (Abeleira et al., 2017; Lachenmayer et al., 2024; Lyu et al., 2021; Pollack et al., 2021).

The relative contributions from these four factors to total NMVOCs reflect the complex spatial patterns of emission sources in the CNFR explored in Section 3.2. Figure 3.6.a maps the annual-average percentage contributions of total NMVOC from O&G activity, traffic + urban combustion, fueling station, and biogenic + background source factors at four long-term sampling locations. Here, the total NMVOC is the sum of the 40 NMVOCs species we use in the PMF model. Similar to the *i*/*n*-pentane ratio source attribution method in Section 3.4.a, the PMF analysis results highlight the large-scale impacts of O&G development and combustion on air-quality in the region. The percent of total NMVOC we attribute to O&G activity using PMF ranges from 13% and 34% in LES and FCW in the west to 67% at GRA in the east (Figure 3.6.a). Conversely, the percent of total NMVOC from traffic + urban combustion is the highest at LES (73%) and FCW (61%), compared to 29% at GRA (Figure 3.6.a), and is the lowest at TGS (11%; Figure 3.6.a). While we would expect the gas station to have a large influence from various combustion sources, as mentioned above, the fueling station PMF factor may group fuel evaporation with local combustion-derived emissions. Thus, we postulate that a portion of total NMVOC concentration from combustion emissions might be represented in the fueling station PMF factor, which dominates at TGS (62%; Figure 3.6.a). The less than 5% of total NMVOCs we attribute to the fueling stations factor at LES and GRA might be explained by this tangled combustion emission influence and fuel evaporation from nearby roads and fueling stations. Last, we note that the TES measurements, which we collected within 0.5 km of Weld County from 2015-2016, have an O&G activity factor contribution of 88% to total NMVOCs (Table B.2), which may indicate that the overall influence of regional

O&G emissions has decreased over the past decade in response to declining O&G emissions, partly due to increased state regulations (Ku et al. 2024; Wells et al., 2017). The relative contributions of O&G to several of the HAPs species indicate a similar temporal trend (Table B.2).

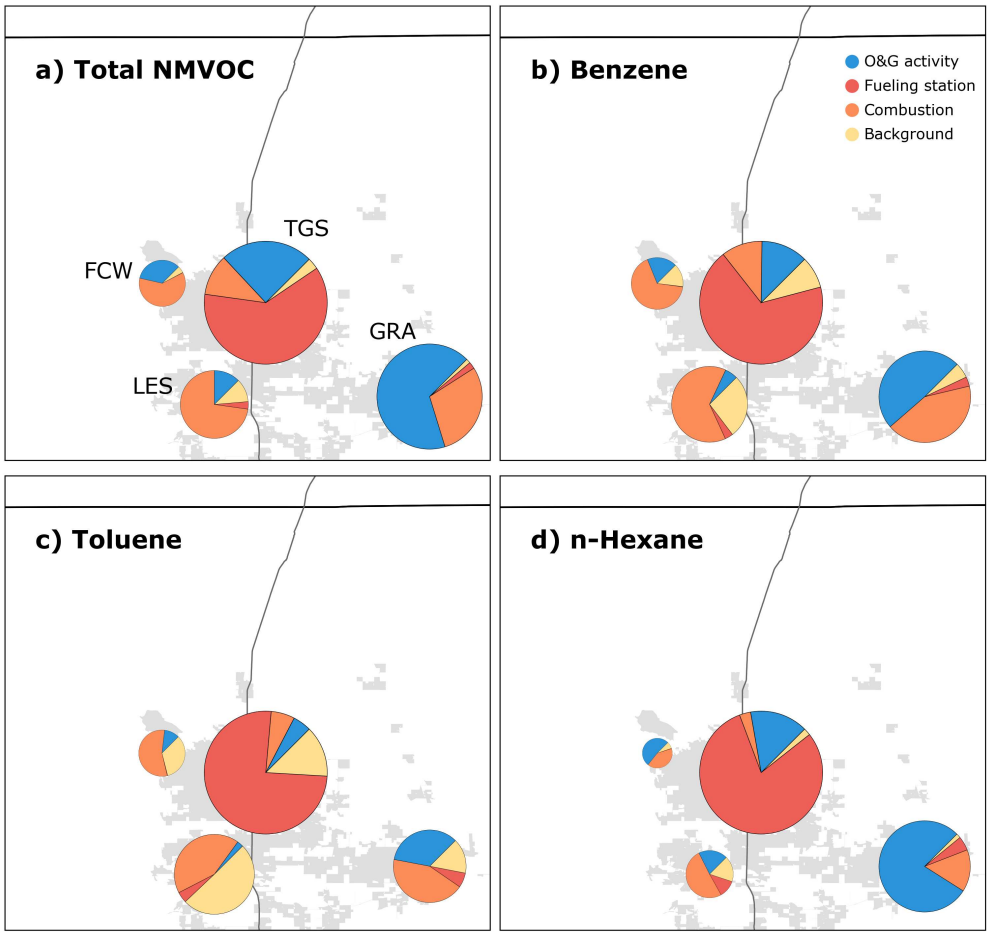

Figure 3.6: Map with annual-average percentage contributions of **(a)** total NMVOC, **(b)** benzene, **(c)** toluene, and **(d)** *n*-hexane from four emission source factors calculated using PMF from Figure 3.5. The area of the pie charts is scaled to annual-average concentrations in the canister measurements. Total NMVOC is the annual-average sum of the 40 NMVOCs used for PMF in the samples. The light gray shading and dark gray lines represent city boundaries and interstate highways, respectively.

Driven by emission source patterns, PMF analysis shows that the relative impact of these emission sources vary by HAP species and location. Figure 3.6.b-d depicts maps of the annual-average percentage contributions of benzene, toluene, and *n*-hexane from the same four PMF source factors. As expected, concentrations of these three important HAPs measured at TGS are dominated

by contributions from the fueling station factor (69%, 76%, 80%, respectively; Figure 3.6.b-d). As these canisters were collected 20 m from the fuel pumps, they demonstrate the range of abundances of HAPs in these locations and may be useful for predicting exposure for individuals living and working near gas stations. Shifting to the other locations, similar to the total NMVOC source attribution, benzene, toluene, and *n*-hexane have the most influence from O&G activity at GRA (49%, 35%, and 79%, respectively), while contributions from urban + traffic combustion emissions are highest at FCW (67%, 56%, and 41%) and LES (64%, 43%, 51%; Figure 3.6.b). The biogenic + background factor comprises half of the toluene from LES samples (50 %; Table B.2). We postulate that the toluene in this factor is explained by urban emissions such as solvent evaporation from the automotive repair shop that are enhanced in the warmer months relative to colder months (Figures B.9 and B.13). We will investigate toluene further in further work using trigger canister samples (Section 2.5; Figure A.5). The urban + traffic combustion factor contributes 42% of benzene, 43% of toluene, and 15% of *n*-hexane at GRA (Figure 3.6.b). On a regional-scale, this PMF analysis indicates that ambient *n*-hexane concentrations are more strongly influenced by emissions from O&G activities compared to benzene and toluene (Figure 3.6.b-d). Alternatively, urban and traffic combustion plus regional background emissions have the largest impact on ambient toluene concentrations regionally. Ambient benzene concentrations appear to have large-scale influence from a mixture of O&G and urban + traffic combustion in the CNFR.

Chapter 4

Episodic Exposure: Air Toxics in a Pollution Plume

4.1 Well blowout in Northern Colorado

On the evening of April 6, 2025, the designed well barriers failed at an O&G well under development near Galeton [40.5223°N, -104.5853°W], a small town in rural Northern Colorado, resulting in the loss of pressure and an uncontrolled flow of liquid and gas for over four days. The Bishop Well [40.5052°N, -104.5853°W], where the incident occurred, is operated by Noble Energy, Inc., a subsidiary of Chevron Corporation. During the blowout–which is an uncontrolled release of waste water, crude oil, and other byproducts of fracking into the environment–an estimated one million gallons of fluid rich with hydrocarbons erupted to the surface (ECMC, 2025b) in the largest spill recorded in Colorado (Chevron, 2025). The chair of the ECMC, Jeff Robin, called the event "significant and unprecedented" (Thakore, 2025). Within the first few hours of the incident, local officials issued a voluntary exclusion zone a half-mile around the well pad and fourteen families evacuated; some of them did not return to their residences until several months after well containment. To protect more sensitive populations, government officials also closed the local elementary school for two weeks. On April 10, 2025, the well contractors contained the liquid flow, and the response team declared the well control incident successfully secured the following day.

With immediate and long-term implications for environmental and human health, the Bishop well blowout provides a rare opportunity to investigate concentrated, uncontrolled O&G emissions. Few prior studies have been able to examine emission events from O&G development of the same high magnitude as the incident in Galeton. This work includes a brief exploration of CH_4 and air toxics measurements we collected during the blowout event and provides groundwork for possible future modeling studies to characterize the potential exposure and health impacts of the blowout.

4.2 Mobile sampling and meteorological conditions

In response to the blowout, we drove two mobile platforms to intercept and characterize the composition and evolution of the blowout plume at different times. During the evening of April 8th, we used the plume tracker described in Section 2.6 to collect real-time CH_4 measurements to sample cross-sections of the plume at locations roughly one and three miles downwind from the well. We also collected 30-second integrated whole air canister samples inside the edge of the plume and upwind at the Galeton Elementary School (for a background measurement) with 1.4-L Silonite®-coated stainless steel canisters that we analyzed for CH_4 and NMVOCs following the methodology outlined in Section 2.2. The next afternoon, we measured four cross-sections of the plume one to three miles downwind from the well and collected three whole air samples in the plume center. On this drive we obtained one-second average concentrations of CH_4 and ethane from a MIRA Laser Diode Source (LDS) analyzer (Aeris Technologies, Inc.) in the National Institute for Standards and Technology (NIST) mobile laboratory. Figures 4.1-4.3 map the location of the well pad, as well as, the driving routes and the approximate locations of canister samples for both days. We report additional information about the individual canister samples on Table 4.1.

Table 4.1: Information for the whole air canister samples collected during the O&G blowout in Galeton, CO on April 8, 2025 and April 9, 2025.[1]

Canister	Date and Time	Location	Distance from well	Notes
1	8 April 7:53 PM	40.4933°N, -104.586°W	1.3 miles, downwind	In plume
2	8 April 8:06 PM	40.5199°N, -104.587°W	1.0 mile, upwind	Background
3	9 April 12:12 PM	40.5198°N, -104.587°W	1.0 mile, upwind	Background
4	9 April 12:30 PM	40.4958°N, -104.546°W	2.2 miles, downwind	In plume
5	9 April 12:50 PM	40.4986°N, -104.564°W	1.2 mile, downwind	In plume
6	9 April 1:56 PM	40.4866°N, -104.546°W	2.5 miles, downwind	In plume

[1] The sample collection locations and distances from the Bishop Well are approximate.

The dynamic meteorological conditions during the blowout event would have impacted the transport and dispersion of the plume in various ways. The wind and gust speeds in the region were moderate during the April 8 evening drive, blowing from the south west to north west during

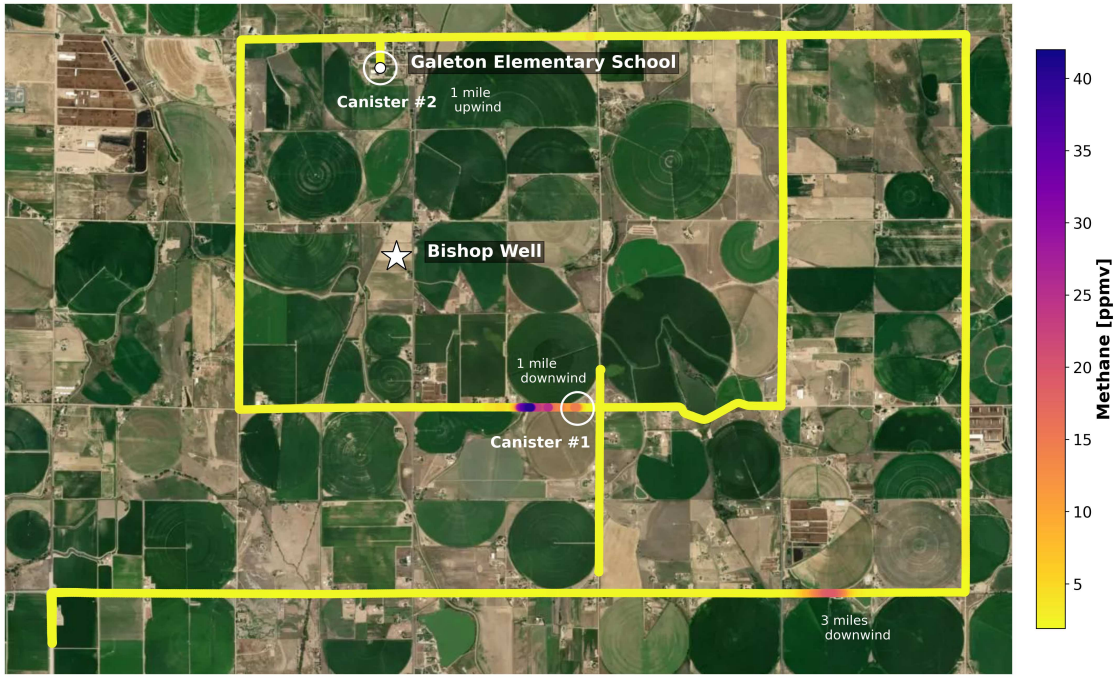

Figure 4.1: CH_4 concentration map from the drive on April 8, 2025 during the blowout at Bishop Well [40.5052°N, -104.5853°W] in Galeton, CO. The locations of the wellpad (white star), Galeton Elementary School (white filled circle), and canister samples (white hollow circles) shown on the map. The canister sample numbers from Table 1 and the distances from the wellpad are also annotated. The methane colorbar ranges from 1.9-41 ppmv.

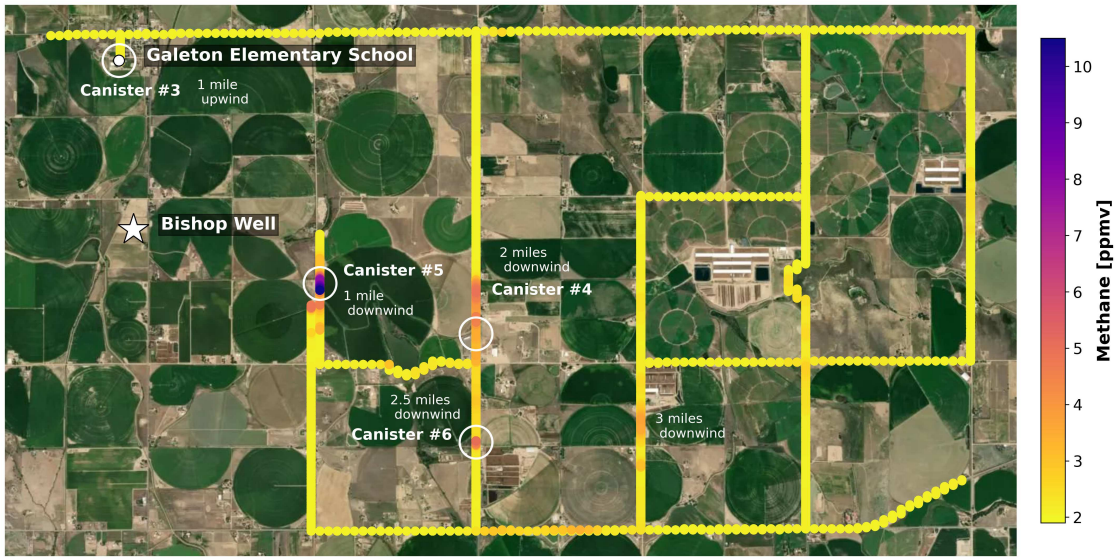

Figure 4.2: CH_4 concentration map from the drive on April 9, 2025 during the blowout at Bishop Well [40.5052°N, -104.5853°W] in Galeton, CO. The locations of the wellpad (white star), Galeton Elementary School (white filled circle), and canister samples (white hollow circles) shown on the map. The canister sample numbers from Table 1 and the distances from the wellpad are also annotated. The methane colorbar ranges from 1.9-11 ppmv.

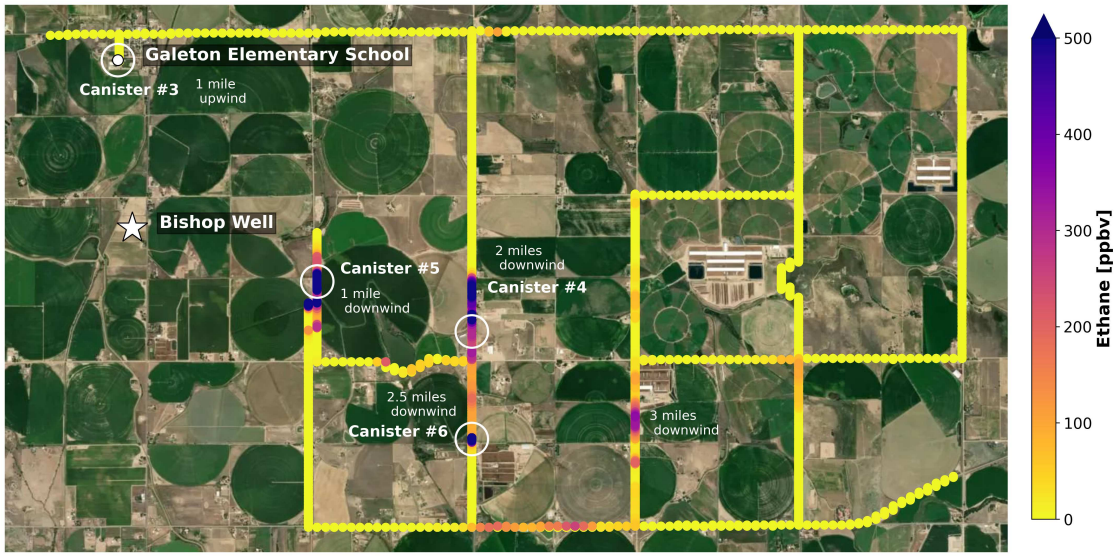

Figure 4.3: Ethane concentration map from the drive on April 9, 2025 during the blowout at Bishop Well [40.5052°N, -104.5853°W] in Galeton, CO. The locations of the wellpad (white star), Galeton Elementary School (white filled circle), and canister samples (white hollow circles) shown on the map. The canister sample numbers from Table 1 and the distances from the wellpad are also annotated. The ethane concentration colorbar is capped at 500 ppbv but there are higher measurement values up to 1925 ppbv.

the two-hour sampling period (Figure 4.4). The map of CH_4 concentrations in Figure 4.1 indicated that the winds were predominately transporting emissions to the south east in Galeton during the drive. In combination with lower air temperatures and the lack of solar irradiance, the modest wind and gust speeds would reduce turbulent dispersion and dilution of material in the plume as it travelled from the well to our mobile sampling locations (e.g., Payne et al., 2017). In contrast, wind gusts reached 30-40 mph and winds shifted to the west during the April 9 afternoon drive (Figure 4.4); the wind measured by the NIST mobile laboratory reached 50 mph (Figure 4.5). The CH_4 and ethane concentrations indicating plume intercept locations on Figures 4.2 and 4.3 suggest that wind directions varied (230 - 350 degrees) over the three-hour sampling period, but were generally carrying the plume to the east southeast (Figure C.1). A higher daytime boundary layer, increased solar radiation, and increased turbulence associated with higher wind speeds and gustiness would have increased rates of turbulent dispersion in the plume during this sampling period relative to the prior evening. The high wind speeds may have also forced rapid plume travel near the surface as opposed to buoyant lofting that might have dominated under calmer

conditions with strong surface heating. This discussion can only be qualitative without explicitly simulating plume dispersion constrained with meteorological observations and CH_4 and ethane measurements; however, examination of the CH_4 and NMVOC concentrations in the following section largely support these hypotheses.

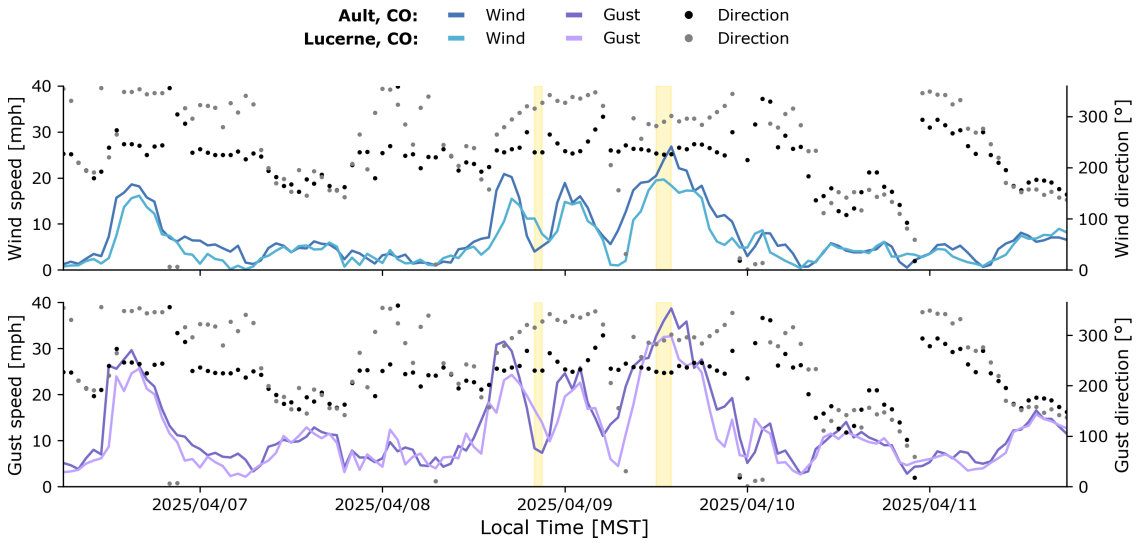

Figure 4.4: Wind and gust speeds (color lines) and directions (circle markers) from towns near Galeton, CO during the blowout. The yellow shading represents periods with mobile sampling. The data spans from 6:00 PM on April 6, 2025 to 6:00 PM April 11, 2025, capturing the entire blowout event. Data for Ault, CO and Lucerne, CO are from CSU Colorado Climate Center CoAGMet (https://coagmet.colostate.edu/). Ault is located approximately 14 km to the northwest and Lucerne is located approximately 11 km to the southwest of Galeton.

We observed the largest CH_4 and NMVOC abundances during the evening of April 8, 2025. Figure 4.6 displays a time series of CH_4 concentrations for a portion of the drive that includes the two plume interceptions. At approximately one and three miles downwind of the well, the peak one-second average CH_4 concentrations were 41 and 19 ppmv, respectively, during the drive (Figure 4.1). The plume canister sample collected inside the edge of the plume had 14 ppmv of CH_4, 2670 ppbv of ethane, 185 ppbv of *n*-hexane, 36 ppbv of benzene, and 91 ppbv of toluene at a one-mile distance from the well (Canister 1; Table 4.2). Table C.1 has concentrations for CH_4 and all 51 measured NMVOC compounds for the in-plume canister sample from April 8, 2025. While we were unable to intercept the plume at distances beyond two-miles downwind during the evening

drive, based on measurements from the next day, we expect there were elevated concentrations of CH_4 and HAPs several miles downwind from the well release.

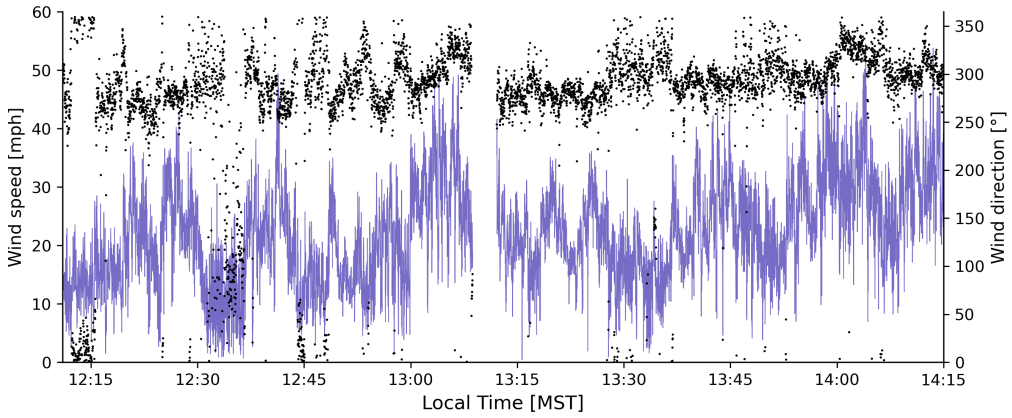

Figure 4.5: Wind speed (purple lines) and direction (black circles) measured by the NIST mobile laboratory during the blowout in Galeton, CO on April 9, 2025.

4.3 Measurements of the blowout emission plume

We observed the largest CH_4 and NMVOC abundances during the evening of April 8, 2025. Figure 4.6 displays a time series of CH_4 concentrations for a portion of the drive that includes the two plume interceptions. At approximately one and three miles downwind of the well, the peak one-second average CH_4 concentrations were 41 and 19 ppmv, respectively, during the drive (Figure 4.1). The plume canister sample collected inside the edge of the plume had 14 ppmv of CH_4, 2670 ppbv of ethane, 185 ppbv of *n*-hexane, 36 ppbv of benzene, and 91 ppbv of toluene at a one-mile distance from the well (Canister 1; Table 4.2). Table C.1 has concentrations for CH_4 and all 51 measured NMVOC compounds for the canister sample from April 8, 2025. While we were unable to intercept the plume at distances beyond two-miles downwind during the evening drive, based on measurements from the next day, we expect there were elevated concentrations of CH_4 and HAPs several miles downwind from the well release.

Despite the likely increased dispersion rate on the afternoon of April 9th, we again detected enhanced CH_4 and NMVOC concentration in the middle of the day that clearly traced back to

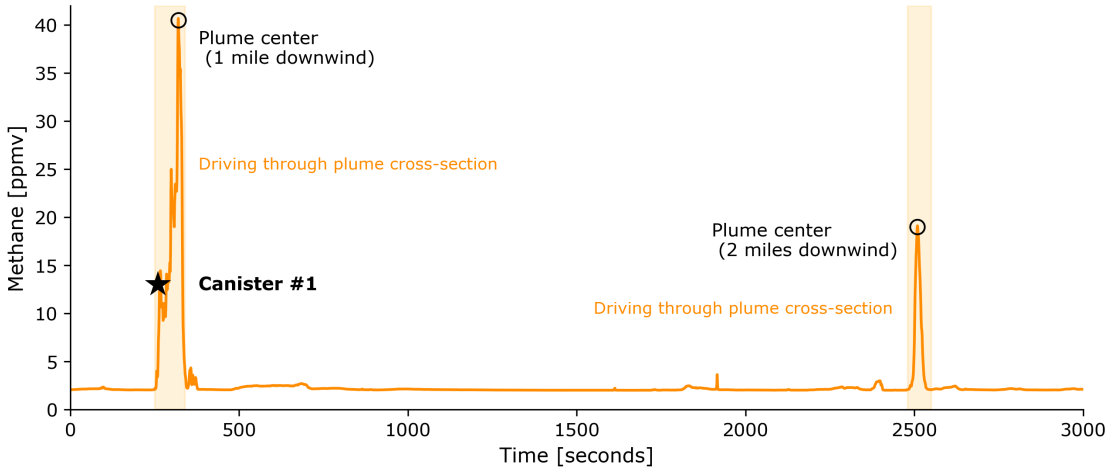

Figure 4.6: Time series of the blowout plume cross-sections on April 8, 2025 in Galeton, CO. The whole air canister sample (black star) and plume centers from one and two miles downwind are shown, along with the time driving through the plume (orange shading). Zero seconds on the plot corresponding to 7:48 PM.

the well. As seen in Figures 4.2 and 4.3, we intercepted the plume multiple times between approximately one to three miles, and possibly four miles, downwind of the blowout. The highest CH_4 and ethane concentrations were 10 ppmv and 1925 ppbv, respectively, in the plume transect approximately one-mile downwind. Additionally, we intercepted the plume over two-miles downwind in two locations with peak one-second average CH_4 concentrations of 4-5 ppmv (Figure 4.2) and peak ethane concentrations of 520-540 ppbv (Figure 4.3). The in-plume canister we collected during this drive with the largest CH_4 and NMVOC concentrations had 9.8 ppmv of CH_4, 1727 ppbv of ethane, 131 ppbv of *n*-hexane, 22 ppbv of benzene, and 59 ppbv of toluene near the plume center one-mile downwind of the well (Canister 5; Table 4.2). Since there are practical difficulties in collecting a canister sample in the most concentrated portion of each plume intercept, we can use the real-time CH_4 concentrations to estimate in-plume values for other species of interest using their observed relationship to CH_4.

Leveraging the whole air canister samples and real-time CH_4 measurements, we are able to extrapolate the maximum NMVOC and HAP concentrations in the center of the plume. To account for the underlying regional influence from O&G, urban, agricultural, and other emissions, we background-corrected the measurements using the upwind canister sample from Galeton Elementary School collected during the same drive. This extrapolation method assumes that the chemical

composition throughout the plume width is constant, which we believe adequately holds given the large concentration magnitudes in the plume. The equation for the extrapolation method is below, where $[VOC]_{center}$ is the extrapolated concentration of the VOC at the plume center, $[VOC]_{plume}$ and $[CH_4]_{plume}$ are in-plume canister sample measurements of VOC and CH_4, $[VOC]_{bkgd}$ and $[CH_4]_{bkgd}$ are VOC and CH_4 concentrations from the upwind canister sample, and $[CH_4]_{center}$ is the peak real-time CH_4 measurement in the plume cross-section.

$$[CH_4]_{\text{center}} = \frac{[VOC]_{\text{plume}} - [VOC]_{\text{bkgd}}}{[CH_4]_{\text{plume}} - [CH_4]_{\text{bkgd}}} \times ([CH_4]_{\text{center}} - [CH_4]_{\text{bkgd}}) + [VOC]_{\text{center}} \qquad (4.1)$$

Applying our extrapolation method (Equation 4.1), we explore the maximum concentrations of branched alkanes and various HAPs in the plume cross-sections one-mile downwind of the blowout (Table 4.3). This results in concentrations slightly over three times higher than the in-plume canister sample from the evening of April 8 (Canister 1; Table 4.2) with 8733 ppbv of ethane, 605 ppbv of *n*-hexane, 116 ppbv of benzene, and 297 ppbv of toluene on the evening of April 8 (Table 4.3). Since we collected the canister sample closer to the plume center on the afternoon of April 9 (Canister 5; Table 4.2), the extrapolation NMVOC values are more similar to the canister concentrations with 1761 ppbv of ethane, 134 ppbv of *n*-hexane, 23 ppbv of benzene, 60 ppbv of toluene at the plume center (Table 4.3). In addition to characterizing the chemical composition of the blowout plume, this event presents an opportunity to investigate the ratios of key NMVOCs in concentrated, uncontrolled O&G emissions.

4.4 VOC ratios within the blowout plume

To further characterize the blowout plume composition, we evaluate NMVOC ratios from the blowout plume and contrast them against values previously measured in plumes from O&G pre-production processes. As introduced in Section 3.4.a, the *i*/*n*-pentane ratio is a robust indicator of the relative influence of O&G activity and urban combustion emissions on air samples. The ratio of

Table 4.2: In-plume and background concentrations of CH_4 [ppmv] and NMVOCs [ppbv] measured with whole air canisters during the O&G blowout in Galeton, CO.[1]

Species	Canister 1	Canister 2	Canister 3	Canister 4	Canister 5	Canister 6
Methane	13.9	2.1	2.1	2.2	9.8	3.9
Ethane	2670	2.1	2.2	45.2	1730	431
Propane	1420	0.72	0.73	26.4	1010	254
i-Butane	239	0.07	0.07	3.9	151	37.8
n-Butane	693	0.18	0.14	11.7	457	115
i-Pentane	225	0.05	0.05	3.9	155	39.1
n-Pentane	371	0.05	0.04	6.2	248	62.8
n-Hexane	185	0.006	0.004	2.6	131	29.8
n-Nonane	68.6	0.002	0.009	1.4	55.5	14.5
Benzene	35.5	0.04	0.06	0.6	22.3	5.4
Toluene	90.9	0.008	0.03	1.5	59.1	15.1
m+*p*-Xylene	98.1	0.003	0.007	1.6	64.8	15.5
o-Xylene	35.7	0.002	0.002	0.6	24.8	6.5
Ethylbenzene	17.8	0.001	0.002	0.4	12.9	3.4

[1] CH_4 and NMVOC concentrations are not background corrected. In-plume samples include Canisters 2 and 4-6, and background, upwind samples include Canisters 1 and 3. For more canister information see Table 4.1.

Table 4.3: Peak concentrations of CH_4 [ppmv] and NMVOCs [ppbv] at the center of the O&G blowout plume one mile downwind of the Bishop well in Galeton, CO on April 8, 2025 and April 9, 2025.[1]

Species	Peak on April 8	Peak on April 9
Methane	40.7	10.0
Ethane	8733	1761
Propane	4635	1034
i-Butane	782	154
n-Butane	2266	466
i-Pentane	736	156
n-Pentane	1213	253
n-Hexane	605	134
n-Nonane	224	57
Benzene	116	23
Toluene	297	60
m+*p*-Xylene	321	66
o-Xylene	117	25
Ethylbenzene	58	13

[1] The maximum NMVOC concentrations at the center of the plume are extrapolated (Equation 4.1) using the one-second average CH_4 measurement from the LI-COR and Canister 1 on April 8 and the one-second average CH_4 measurement from the MIRA and Canister 5 on April 9.

toluene to benzene (toluene/benzene) is similarly used for source apportionment in the CNFR with some considerations (Halliday et al., 2016). Toluene degrades in the atmosphere more rapidly than benzene (Warneke et al., 2007), and thus their ratio is also an indicator of the photochemical age of an air mass (Roberts et al., 1984), making this aromatic ratio less robust for source determination than *i*/*n*-pentane. Given the amplitude of fresh emissions from the well and the short transport time from emission to plume interception, we still calculate toluene/benzene ratios for the in-plume whole air canister samples since little chemical evolution is expected prior to plume sample collection. We can then contrast the *i*/*n*-pentane and toluene/benzene ratios from the Bishop Well emissions against ratios from previous studies focused on pad-level, activity specific measurements from the DJ Basin (Hecobian et al., 2019; Ku et al., 2024).

As the Bishop Well was in preparation for the flowback pre-production operation stage during the time of the blowout, we focus our comparison on measurements collected in the DJ basin during flowback operations. Often associated with high VOC emissions (Hecobian et al., 2019; Ku et al., 2024), flowback is the process following hydraulic fracturing (fracking) when injected fracturing fluids and produced water from the formation are returned to the surface. Similar to our study, Hecobian et al. (2019) and Ku et al. (2024) used 1.4-L Silonite®-coated stainless steel canisters to measure a suite of NMVOCs during various O&G operations, including flowback, from various wellpads in the Front Range from 2014-2016 (36 samples) and Broomfield, CO, in 2020-2022 (23 samples), respectively. The samples in both studies were triggered upon detection of plumes and represent relatively concentrated emissions. These measurements are somewhat analogous to the Galeton sampling situation except for the emissions control measures in place during controlled flowback operations. We report the background-corrected *i*/*n*-pentane and toluene/benzene ratios for the Galeton samples in Table 4.4 and the averages and ranges of ratio for the prior studies in Table 4.5.

The Galeton in-plume samples have relatively consistent *i*/*n*-pentane and toluene/benzene ratios that fall within previously measured ratios in Northern Colorado. The *i*/*n*-pentane ratio from the April 8 sample is 0.61 and spans from 0.62 to 0.63 on April 9 with an average value of 0.62

for both days (Table 4.4). In comparison, the pentane isomer ratios range from 0.61 to 1.11 in the samples from Hecobian et al. (2019) with an average value of 0.76, while the ratios from Ku et al. (2024) are 0.73 on average and span from 0.65-0.97 (Table 4.5). The toluene/benzene ratio from the April 8 sample is 2.56 and spans from 2.64 to 2.80 on April 9 (Table 4.5). The Bishop Well blowout emissions had an average toluene/benzene ratio of 2.66, which is larger than the average ratio of 1.40 measured from recent flowback emissions in Broomfield, and more similar to the value of 2.36 from the earlier Hecobian et al. study (Table 4.5). Furthermore, Galeton plume toluene/benzene ratios are within the range of 1.53 to 3.91 in the Hecobian et al. (2019) study and larger than the range of 0.001 to 2.08 in Broomfield (Table 4.5).

Table 4.4: Toluene/benzene and *i*/*n*-pentane ratios for the canister samples collected during the O&G blowout in Galeton, CO.[1]

Species	Canister 1	Canister 2	Canister 3	Canister 4	Canister 5	Canister 6
Toluene/Benzene	2.56	0.23	0.54	2.64	2.66	2.80
i/*n*-Pentane	0.61	0.98	1.16	0.63	0.62	0.62

[1] The in-plume canister samples (Canister 1, 4-6) are background-corrected using the upwind samples from the same drive (Canisters 2 and 3). For more canister information see Table 4.1.

Table 4.5: Toluene/benzene and *i*/*n*-pentane ratios from the DJ Basin (Hecobian et al., 2019) and Broomfield (Ku et al., 2024).[1]

Ratio	DJ Basin mean	DJ Basin range	Broomfield mean	Broomfield range
Years	*2014-2016*		*2020-2022*	
Toluene/Benzene	2.36	1.53 – 3.81	1.40	0.001 – 2.08
i/*n*-Pentane	0.76	0.61 – 1.11	0.73	0.65 – 0.97

[1] The concentrations were background corrected prior to calculating the ratios. For Hecobian et al. (2019), the upwind samples were subtracted from the downwind measurements on each day at various wellpads in the DJ Basin from 2014-2016. For Ku et al. (2024), the weekly-average concentrations from the background site were subtracted from the triggered canister samples during flowback in Broomfield, CO from 2018-2022.

We postulate that the differences in toluene/benzene ratios may partially be due to changes in management practices to limit on-pad flowback emissions. The wellpads in Broomfield employed

a closed-loop, tankless fluid handling system during flowback operations, while the green compliance practices in Colorado allowed for prolonged storage of flowback liquids in tanks on the pad during the earlier study (Hecobian et al., 2019; Ku et al., 2024). Thus, given the uncontrolled manner of flowback fluid explosion during the blowout event in Galeton, it is not surprising that the blowout samples have toluene/benzene ratios more consistent with flowback emissions collected before implementation of more active emission control measures using a closed-loop tankless system in Broomfield.

4.5 The fallout: potential exposure and modeling study

Collectively, the CH_4 and NMVOC observations and plume-center estimates indicate that near the surface, the blowout plume traveled several miles downwind of the well with high HAPs concentrations, increasing potential acute exposure to residents outside of the evacuation zone. Acute exposure represents intermittent contact that occurs repeatedly for a few hours to a few days. The non-carcinogenic acute health guideline values (HGV) for preliminary risk assessments in Colorado are 5400 ppbv for *n*-hexane, 3000 ppbv for *n*-nonane, 9 ppbv for benzene, 2000 ppbv for toluene, 2000 ppbv for xylene isomers, and 5000 for ethylbenzene (CDPHE, 2019). The U.S. EPA defines these values as the daily exposure levels that are likely to be without appreciable risk of adverse non-cancer health effects in an exposed population, including sensitive individuals, and are meant to serve as screening tools. Directly evaluating our measurements against the acute health guideline values is misleading as the sampling durations are shorter than what the guideline values represent. Still, the fact that we detected episodes of high benzene concentrations in the plume on both days is cause for further investigation since even several minutes of exposure at the plume center would yield an hourly average potential exposure exceeding the acute HGV for benzene.

Due to the rarity of the blowout event and the dynamic atmospheric conditions, we do not know the amount of time individuals were actually exposed to the plume (the plume was moving with the wind) and the extent to which it may have caused acute adverse health impacts. As we alluded to above, future work should involve simulating plume dispersion constrained with

meteorological observations and CH_4 and NMVOC measurements to further address questions regarding potential human health impacts. Such a model could be used to quantify emission rates and exposure estimates that would aid future health impact studies. In addition to the air quality monitoring we present above, other governmental and private groups collected various air quality samples during the majority of the blowout event in Galeton which could be utilized to further constrain dispersion model simulations.

Briefly, the governmental and private data from the event we are currently aware of include various air quality measurements from canisters and real-time instruments as well as oil samples collected on and near the well pad. First, composed of the Galeton Fire District, U.S. EPA, ECMC, and CDPHE, and Weld County, the Unified Command collected three types of data during the blowout event (i.e., fixed monitoring of total VOCs, 24-hour whole air canister samples, and hand-held PID sensor for total VOC measurements all collected near the well pad and residential areas), starting on April 7. Additionally, CDPHE deployed their Mobile Optical Oil and gas Sensor of Emissions (MOOSE) van to sample HAPs on April 9-11 and returned after the well was successfully secured on both April 18 and 21 to measure methane and benzene. During two separate deployments of the MOOSE (April 9 and 10), CDPHE observed 1.5-minute averaged benzene concentrations of 9.35 ppbv about 1.38 miles downwind of the well (CDPHE's Air toxics and ozone precursor program (ATOP) summary report; CDPHE, 2025a). CDPHE also used their stationary Remote Air Tracking Trailer for Localized Emissions Recording (RATTLER) to measure benzene and installed SPODs (similar to what we describe in Section 2.5) to measure a proxy for total VOCs and meteorological variables starting on April 11 through May 22, after well containment (CDPHE, 2025a). At the time of the incident, the operator was conducting regular monitoring required by Regulation 7 at 13 monitoring sites across four adjacent well pads in Galeton, including the one with the explosion; they measured a total VOC proxy with PID sensors (similar to what we describe in Section 2.5) and measured benzene and BTEX compounds in seven 1-hour integrated whole air canisters. Two of the canisters from April 6 (collected at 18:34 about 890 m from the well pad with the blowout) and April 9 (collected at 4:02 about 1.38 miles from the

well pad with the blowout) contained benzene concentrations above the HGV with 17.8 and 13.2 ppbv, respectively. Additionally, the private company, Project Canary Foundation, collected five trigger canisters during the blowout event. Lastly, Chevron collected an oil sample from the well pad and another from an emergency diversion ditch near the pad on April 8 (Chevron's 'Analytical of Source Material' documentation; ECMC, 2025b). The additional air quality data may aid in constraining future modeling analysis and oil composition could be evaluated against the in-plume canisters we collected during the event.

Following containment, attention regarding the blowout shifted away from emergency management to address immediate safety concerns to legal examinations and clean up efforts. The event garnered both local and international media attention regarding the perceived immediate human health concerns for people living in the area (e.g., Jaffe, 2025a,b; Solomon, 2025; Thomas, 2025) and nondisclosure violation of fracking liquid composition (Fassler, 2025). Two months after the blowout, the ECMC, the agency with statutory authority to regulate Colorado O&G operations, including the investigation and remediation of spills, issued a Notice of Alleged Violation (NOAV) citing six rule violations against Noble Energy Inc. and Chevron (ECMC, 2025e). The alleged violations include: Rule 428 - Well control, Rule 602.c. - General safety requirements, Rule 608.e. - Oil and gas facilities, Rule 902.a.b.c. - Pollution, Rule 902.d. - Pollution (water), and Rule 903 - Venting or flaring natural gas. Under the Colorado Oil and Gas Conservation Act, the operator is responsible for all soil and water remediation efforts which they must complete by spring 2030 and will require a multi-faceted approach.

Chapter 5

Conclusion

Applying stationary and mobile VOC monitoring techniques, this work explored the potential for chronic and acute air toxics exposure in the CNFR. We used whole air canister samples to address questions regarding VOC seasonal and spatial trends across the region and characterize their sources. We used real-time CH_4 and VOC measurements to investigate short-term concentrated, uncontrolled O&G emissions in a rural town in Colorado.

By employing a unique dataset of weekly-integrated canister measurements, this work examines the seasonal and spatial trends in ambient concentrations of CH_4 and NMVOCs in the CNFR. This analysis includes measurements from sites near O&G wells, a large gas station, an urban school adjacent to an automobile repair shop, and a suburban site at the base of the Rocky Mountains. We find that CH_4 and the most abundant NMVOCs show strong seasonal patterns that are driven by meteorological and emission patterns, with concentrations generally peaking in the winter. Reflecting the regional distribution of O&G activity, there is a strong eastward increasing gradient in CH_4 and NMVOCs moving from the west side of Fort Collins to Greeley, with an order of magnitude difference between these sites. Highlighting the influence from traffic and point emission sources and disrupting these regional trends, the samples collected near a large gas station in Timnath, between Fort Collins and Greeley, have the largest ambient concentrations observed across the study region for several HAPs species. They also display divergent seasonality compared to other sampling locations.

Laboratory headspace analyses of gasoline and diesel fuels reveal that the ambient gas station samples exhibit a distinct compositional NMVOC signature partly resembling a gasoline evaporative emissions fingerprint. Compared to urban and suburban site samples, the gas station samples contained larger relative contributions from C_4-C_6 branched alkanes and HAPs, indicative of influence from a combination of vehicular combustion and gasoline evaporation. Among the HAPs we analyzed, benzene, toluene, and *n*-hexane have the highest abundance in the ambient measure-

ments from the gas station. Benzene, *n*-nonane, and the xylene isomers have concentrations closest to established chronic exposure health guideline values.

Two source attribution methods reveal that both O&G and traffic and urban combustion emissions have a large-scale impact on air quality in the CNFR. Low *i*/*n*-pentane ratios indicate a mix of O&G activity and urban and traffic combustion emissions across the region. The lowest ratios occur in Greeley, close to O&G activity, and the highest ratios are observed at the Timnath gas station, reflecting the prevalence of traffic and fuel evaporative emissions. PMF analysis results show four factors best describe sample VOC composition; we labeled these as representing O&G activity, traffic + urban combustion, fueling station, and biogenic + background. Spatial gradients in the annual-average source contributions for total VOCs and HAPs such as benzene, toluene, and *n*-hexane reflect the regional distribution of O&G activity and influence from traffic and point emission sources. On a regional-scale, benzene concentrations show large-scale influence from a mixture of O&G and urban and traffic combustion, with generally larger impact from O&G moving eastward. Urban and traffic combustion plus biogenic and background emissions have the largest impact on ambient toluene concentrations. Ambient n-hexane concentrations are more strongly influenced by emissions from O&G activities. The gas station samples and the resulting fueling station PMF factor allow us to identify and quantify the range of abundances of HAPs from fueling stations in the urban and suburban samples and may be useful for predicting chronic exposure for individuals living and working near gas stations.

While our stationary monitoring network measurements did not find any HAPs concentrations exceeding chronic health guideline values, previous studies suggest that acute high exposure events might be more likely to pose health risks (Garcia-Gonzales et al., 2019; Ku et al., 2024; Weisner et al., 2025). The well blowout incident in Galeton provided a rare opportunity to investigate concentrated, uncontrolled O&G emissions. Collectively, the CH_4 and NMVOC observations indicate that the blowout plume traveled several miles downwind of the well with high HAPs concentrations, increasing potential acute exposure to residents outside of an evacuation zone. Due to the rarity of the blowout event and the dynamic atmospheric conditions, both the amount of time indi-

viduals were exposed to the plume and the extent to which it may have caused acute adverse health impacts are uncertain. Still, the fact that we detected episodes of high benzene concentrations in the plume on both days is cause for further investigation. Future work should involve simulating plume dispersion to further address questions regarding potential human health impacts.

The Bishop Well blowout was the largest spill recorded in Colorado, but smaller air pollution emissions are frequently associated with O&G activities and have potential to cause health impacts for residents living near O&G development (Garcia-Gonzales et al., 2019; Ku et al., 2024; Weisner et al., 2025). Furthermore, population influx and urban sprawl are expanding the convergence of residential housing and O&G extraction and increasing the chance of incidents of this nature to impact households along the CNFR. Galeton is a small town with a population of approximately 244 people (US Census Bureau, 2020), and it falls within a low-income population census track (Colorado EnviroScreen 2.0; CDPHE, 2025d). An accident similar to this blowout at a wellpad near a more populated urban center in Colorado could have exposed a much larger population to high HAPs concentrations. This is an example of tensions between economic and political realities that favor an active O&G industry and human health and environmental justice concerns.

5.1 Future work directions

Given the heterogeneity of VOC and HAP concentrations in the CNFR, subsequent studies would benefit from expanding the spatial extent of the air monitoring network we used in this work. In addition to the eight sampling locations included in this analysis, we have been collecting weekly-integrated canisters in downtown Fort Collins, which by the end of the sampling campaign, will comprise a year of data. The site is adjacent to train tracks (50 ft away) and heavily used roads (the nearest road is 20 ft away) and on the perimeter of the CSU downtown campus. Hence, the samples are strongly influenced by a variety of traffic and urban emissions, ranging from mobile sources (e.g., traffic combustion from the trains, vehicles driving on the road, and vehicles idling when stopped for the train), commercial, industrial, and manufacturing sources (e.g., urban combustion and chemical product usage at surrounding gas stations, restaurants, and automotive repair

shops), and utilities sources (e.g., a wastewater treatment plant that is 1.6 km away). Incorporating these urban canister samples into the dataset used here may facilitate untangling different combustion source types and help to isolate emissions from non-combustion urban activities in further PMF analysis. Analogously, installing a second monitoring site that is primarily impacted by O&G activities in Weld County would benefit further exploration into the range of abundances of HAPs in the ambient atmosphere regionally. Integrating more samples impacted by various O&G activities into subsequent PMF analysis may assist in separating long-lived, short-lived, and process-specific O&G emissions.

Along with collecting more weekly-integrated canisters, adding high time-resolution speciated VOC measurements in Greeley and Fort Collins seasonally would aid in source profile identification and allow future studies to investigate questions regarding regional VOC transport. Previous studies in the CNFR have used Proton-Transfer-Reaction Mass Spectrometry (PTR-MS) and real-time GC-MS (e.g., Gilman et al., 2013; Halliday et al., 2016; Ku et al., 2024) to analyze hourly-averaged speciated VOC concentrations. When coupled with co-located meteorological measurements (e.g., wind speed and direction), information gained from temporal and atmospheric dynamics patterns would help researchers identify PMF emission profiles using diurnal patterns and provide insight into long-range westward transport from O&G production along the CNFR. During the summer in periods of weak synoptic flow, mountain-valley circulation effects drive upslope flow that transport air masses with emission from the eastern plains toward the Rocky Mountains, which are subject to photochemical processing (Flocke et al., 2019 and references therein). In Summer 2025, the Front Range OZone Experiment (FROZÉ) campaign included measurements of speciated VOCs from a real-time GC at our Fort Collins West site, along with a suite of particulate matter, NO_x, O_3, and other trace gas observations. The summer campaign was periodically impacted by wildfire smoke and the data may be used to identify a potential source profile for biomass burning. Thus, expanding the air toxics focus of this thesis, the FROZÉ dataset should be leveraged in a separate PMF modeling study to explore the influence of regional VOC transport in order to address O_3 and fine particle air pollution concerns. Adding real-time speciated VOC mea-

surements at a site in Weld County, could help further address the temporal and spatial influence of O&G emissions and their relevance to broader air quality issues in the region.

The drivers of O_3 formation in the CNFR, in particular the importance of VOC emissions from urban and O&G sources, are open issues that impact human and ecological health. Subsequent analysis could utilize the PMF source factor profiles from this work to characterize and quantify VOC reactivity with hydroxyl radicals (OH) as demonstrated in Pan et al., 2023. This analysis could help inform VOC emissions regulation to effectively reduce O_3 regionally.

To expand the gas station analysis of HAPs in this work and explore the effectiveness of current emission regulations, future work should include collecting more canister samples from gas stations in the CNFR. Starting in 2024, the EPA required gas stations in CNFR within the non-attainment zone to carry summer-blend and winter-blend fuels in an effort to control O_3 formation. In addition to the winter-formula gasoline and diesel fuel samples presented in this study, we conducted headspace analysis of a summer-formula gasoline fuel sample. Collecting supplemental ambient samples from gas stations could provide an opportunity to compare fuel formulations between the 2015-2016 samples and more recent measurements, as well as to examine potential differences introduced by the seasonal gasoline mandate. The range of abundances of HAPs from fueling stations in several of the urban and suburban samples in this work underscores the importance of further investigation into emissions from gas stations.

While this work did not explore the continuous total VOC measurements or trigger canisters described in Section 2.5, the data should be used to further characterize the HAPs at the sites near schools in Greeley and Loveland.

Last, the uncertainties regarding the amount of acute exposure residents living downwind of the blowout plume in Galeton had to HAPs warrants further consideration. In Section 4.5, we advocate that supplementary analysis include plume dispersion simulations constrained by the numerous observations collected during the event to quantify emission rates and exposure estimates for human health studies. To complement this proposed modeling study, satellite-derived measure-

ments of CH_4 from MethaneSAT should be analyzed to examine the magnitude and spatial impact of this unique event.

Bibliography

[Abeleira et al., 2017] Abeleira, A., Pollack, I. B., Sive, B., Zhou, Y., Fischer, E. V., & Farmer, D. K. (2017). Source characterization of volatile organic compounds in the Colorado Northern Front Range Metropolitan Area during spring and summer 2015. *Journal of Geophysical Research: Atmospheres*, 122(6), 3595–3613. https://doi.org/10.1002/2016JD026227

[Adgate et al., 2014] Adgate, J. L., Goldstein, B. D., & McKenzie, L. M. (2014). Potential Public Health Hazards, Exposures and Health Effects from Unconventional Natural Gas Development. *Environmental Science & Technology*, 48(15), 8307–8320. https://doi.org/10.1021/es404621d

[Allshouse et al., 2017] Allshouse, W. B., Adgate, J. L., Blair, B. D., & McKenzie, L. M. (2017). Spatiotemporal Industrial Activity Model for Estimating the Intensity of Oil and Gas Operations in Colorado. *Environmental Science & Technology*, 51(17), 10243–10250. https://doi.org/10.1021/acs.est.7b02084

[Atkinson et al., 1990] Atkinson, R. (1990). Gas-phase tropospheric chemistry of organic compounds: A review. *Atmospheric Environment. Part A. General Topics*, 24(1), 1–41. https://doi.org/10.1016/0960-1686(90)90438-S

[ATSDR, 2025] ATSDR. (2025, January 14). Calculating Hazard Quotients and Cancer Risk Estimates. CDC. *https://www.atsdr.cdc.gov/pha-guidance/conducting_scientific_evaluations/epcs_and_exposure_calculations/hazardquotients_cancerrisk.html*

[Baker et al., 2008] Baker, A. K., Beyersdorf, A. J., Doezema, L. A., Katzenstein, A., Meinardi, S., Simpson, I. J., Blake, D. R., & Sherwood Rowland, F. (2008). Measurements of nonmethane hydrocarbons in 28 United States cities. *Atmospheric Environment*, 42(1), 170–182. https://doi.org/10.1016/j.atmosenv.2007.09.007

[Benedict et al., 2019] Benedict, K. B., Zhou, Y., Sive, B. C., Prenni, A. J., Gebhart, K. A., Fischer, E. V., Evanoski-Cole, A., Sullivan, A. P., Callahan, S., Schichtel, B. A., Mao, H., Zhou, Y., & Collett Jr., J. L. (2019). Volatile organic compounds and ozone in Rocky Mountain National Park during FRAPPÉ. *Atmospheric Chemistry and Physics*, 19(1), 499–521. https://doi.org/10.5194/acp-19-499-2019

[Bon et al., 2011] Bon, D. M., Ulbrich, I. M., de Gouw, J. A., Warneke, C., Kuster, W. C., Alexander, M. L., Baker, A., Beyersdorf, A. J., Blake, D., Fall, R., Jimenez, J. L., Herndon, S. C., Huey, L. G., Knighton, W. B., Ortega, J., Springston, S., & Vargas, O. (2011). Measurements of volatile organic compounds at a suburban ground site (T1) in Mexico City during the MILAGRO 2006 campaign: Measurement comparison, emission ratios, and source attribution. *Atmospheric Chemistry and Physics*, 11(6), 2399–2421. https://doi.org/10.5194/acp-11-2399-2011

[Brantley et al., 2015] Brantley, H. L., Thoma, E. D., & Eisele, A. P. (2015). Assessment of volatile organic compound and hazardous air pollutant emissions from oil and natural gas well pads using mobile remote and on-site direct measurements. *Journal of the Air & Waste Management Association*, 65(9), 1072–1082. https://doi.org/10.1080/10962247.2015.1056888

[Brown et al., 2007] Brown, S. G., Frankel, A., & Hafner, H. R. (2007). Source apportionment of VOCs in the Los Angeles area using positive matrix factorization. *Atmospheric Environment*, 41(2), 227–237. https://doi.org/10.1016/j.atmosenv.2006.08.021

[Brown et al., 2013] Brown, S. S., Thornton, J. A., Keene, W. C., Pszenny, A. A. P., Sive, B. C., Dubé, W. P., Wagner, N. L., Young, C. J., Riedel, T. P., Roberts, J. M., VandenBoer, T. C., Bahreini, R., Öztürk, F., Middlebrook, A. M., Kim, S., Hübler, G., & Wolfe, D. E. (2013). Nitrogen, Aerosol Composition, and Halogens on a Tall Tower (NACHTT): Overview of a wintertime air chemistry field study in the front range urban corridor of Colorado. *Journal of Geophysical Research: Atmospheres*, 118(14), 8067–8085. https://doi.org/10.1002/jgrd.50537

[Bryant et al., 2023] Bryant, D. J., Nelson, B. S., Swift, S. J., Budisulistiorini, S. H., Drysdale, W. S., Vaughan, A. R., Newland, M. J., Hopkins, J. R., Cash, J. M., Langford, B., Nemitz, E., Acton, W. J. F., Hewitt, C. N., Mandal, T., Gurjar, B. R., Shivani, Gadi, R., Lee, J. D., Rickard, A. R., & Hamilton, J. F. (2023). Biogenic and anthropogenic sources of isoprene and monoterpenes and their secondary organic aerosol in Delhi, India. *Atmospheric Chemistry and Physics*, 23(1), 61–83. https://doi.org/10.5194/acp-23-61-2023

[CDPHE, 2019] CDPHE. (2019, September 20). *Re: Updated acute and chronic health guideline values for use in preliminary risk assessments (referred to as "FA2019 HGVs").* Oil and Gas Health Information Response Program, Toxicology and Risk Assessment Section, Colorado Department of Public Health and Environment. https://docs.google.com/document/d/185dUdlVJtvh-oCBwVW_ECXWproGgTmbL_afhCSZjNkjw/edit?usp=sharing

[CDPHE, 2024] CDPHE. (2024). *Reported air toxics emissions data.* CDPHE. https://cdphe.colorado.gov/air-toxics/reporting/data

[CDPHE, 2025a] CDPHE. (2025a). *Air toxics*. https://cdphe.colorado.gov/air-toxics

[CDPHE, 2025b] CDPHE. (2025b). *Air Toxics and Ozone Precursor Data Repository* [Dataset]. Ozone Precursor Monitoring Data & Reports. https://www.colorado.gov/airquality/air_toxics_repo.aspx

[CDPHE, 2025c] CDPHE. (2025c). *Colorado EnviroScreen 2.0* [Dataset]. https://cdphe.colorado.gov/enviroscreen

[CDPHE, 2025d] CDPHE. (2025d, July 15). *Air monitoring data summary report Noble/Chevron Bishop.* https://www.colorado.gov/airquality/air_toxics_repo.aspx?action=open&file=Galeton+Report.pdf

[Cheadle et al., 2017] Cheadle, L. C., Oltmans, S. J., Pétron, G., Schnell, R. C., Mattson, E. J., Herndon, S. C., Thompson, A. M., Blake, D. R., & McClure-Begley, A. (2017). Surface

ozone in the Colorado northern Front Range and the influence of oil and gas development during FRAPPE/DISCOVER-AQ in summer 2014. *Elementa: Science of the Anthropocene*, 5, 61. https://doi.org/10.1525/elementa.254

[Chen et al., 2017] Chen, J., Li, C., Ristovski, Z., Milic, A., Gu, Y., Islam, M. S., Wang, S., Hao, J., Zhang, H., He, C., Guo, H., Fu, H., Miljevic, B., Morawska, L., Thai, P., Lam, Y. F., Pereira, G., Ding, A., Huang, X., & Dumka, U. C. (2017). A review of biomass burning: Emissions and impacts on air quality, health and climate in China. *Science of The Total Environment*, 579, 1000–1034. https://doi.org/10.1016/j.scitotenv.2016.11.025

[Chevron, 2025] Chevron. (2025). *Bishop Well Incident*. https://colorado.chevron.com/bishop-well-incident

[Chin and Batterman, 2012] Chin, J.-Y., & Batterman, S. A. (2012). VOC composition of current motor vehicle fuels and vapors, and collinearity analyses for receptor modeling. *Chemosphere*, 86(9), 951–958. https://doi.org/10.1016/j.chemosphere.2011.11.017

[Cohen et al., 2017] Cohen, A. J., Brauer, M., Burnett, R., Anderson, H. R., Frostad, J., Estep, K., Balakrishnan, K., Brunekreef, B., Dandona, L., Dandona, R., Feigin, V., Freedman, G., Hubbell, B., Jobling, A., Kan, H., Knibbs, L., Liu, Y., Martin, R., Morawska, L., ... Forouzanfar, M. H. (2017). Estimates and 25-year trends of the global burden of disease attributable to ambient air pollution: An analysis of data from the Global Burden of Diseases Study 2015. *Lancet (London, England)*, 389(10082), 1907–1918. https://doi.org/10.1016/S0140-6736(17)30505-6

[Community Foundation of Northern Colorado, 2024] Community Foundation of Northern Colorado. (2024). *Interations Report 2024*. https://nocofoundation.org/wp-content/uploads/2024-Intersections-Report.pdf

[Conner et al., 1995] Conner, T. L., Lonneman, W. A., & Seila, R. L. (1995). Transportation-Related Volatile Hydrocarbon Source Profiles Measured in Atlanta. *Journal of the Air & Waste Management Association*, 45(5), 383–394. https://doi.org/10.1080/10473289.1995.10467370

[Dockery, 2001] Dockery, D. W. (2001). Epidemiologic evidence of cardiovascular effects of particulate air pollution. *Environmental Health Perspectives*, 109(suppl 4), 483–486. https://doi.org/10.1289/ehp.01109s4483

[ECMC, 2025a] ECMC. (2025a). *Active Well Count by County and Year Report*. https://ecmc.colorado.gov/data-maps/downloadable-data-documents/county-active

[ECMC, 2025b] ECMC. (2025b). *Bishop Well Control Incident (last update 7/7/2025)*. https://ecmc.colorado.gov/bishop-well-control-incident

[ECMC, 2025c] ECMC. (2025c). *ECMC Data Downloads* [Dataset]. Well Surface Location Data (Updated Daily). https://ecmc.state.co.us/data2.html#/downloads

[ECMC, 2025d] ECMC. (2025d). *Production By County* [Dataset]. https://ecmc.colorado.gov/data-maps/production-by-county

[ECMC, 2025e] ECMC. (2025e, June 26). *State Regulatory Agency Issues Notice of Alleged Violation to Noble Energy, Inc., Upon Investigation of the Bishop Well Incident*. https://ecmc.colorado.gov/press-release/state-regulatory-agency-issues-notice-of-alleged-violation-to-noble-energy-inc-upon

[Erickson et al., 2022] Erickson, C. L., Barron, I. G., & Zapata, I. (2022). The Effects of Hydraulic Fracturing Activities on Birth Outcomes are Evident in a Non-Individualized County-Wide Aggregate Data Sample from Colorado. *Journal of Public Health Research*, 11(1), jphr.2021.2551. https://doi.org/10.4081/jphr.2021.2551

[Evans and Helmig, 2017] Evans, J. M., & Helmig, D. (2017). Investigation of the influence of transport from oil and natural gas regions on elevated ozone levels in the northern Colorado front range. *Journal of the Air & Waste Management Association*, 67(2), 196–211. https://doi.org/10.1080/10962247.2016.1226989

[Fassler, 2025] Fassler, J. (2025, May 20). US oil firms pumping secret chemicals into ground and not fully reporting it. *The Guardian*. https://www.theguardian.com/us-news/2025/may/20/us-oil-firms-chemicals-colorado

[Flocke et al., 2020] Flocke, F., Pfister, G., Crawford, J. H., Pickering, K. E., Pierce, G., Bon, D., & Reddy, P. (2020). Air Quality in the Northern Colorado Front Range Metro Area: The Front Range Air Pollution and Photochemistry Éxperiment (FRAPPÉ). *Journal of Geophysical Research: Atmospheres*, 125(2), e2019JD031197. https://doi.org/10.1029/2019JD031197

[Fraser et al., 1998] Fraser, M. P., Cass, G. R., & Simoneit, B. R. T. (1998). Gas-Phase and Particle-Phase Organic Compounds Emitted from Motor Vehicle Traffic in a Los Angeles Roadway Tunnel. *Environmental Science & Technology*, 32(14), 2051–2060. https://doi.org/10.1021/es970916e

[Frischmon and Hannigan, 2024] Frischmon, C., & Hannigan, M. (2024). VOC source apportionment: How monitoring characteristics influence positive matrix factorization (PMF) solutions. *Atmospheric Environment: X, 21*, 100230. https://doi.org/10.1016/j.aeaoa.2023.100230

[Garcia-Gonzales et al., 2019] Garcia-Gonzales, D. A., Shonkoff, S. B. C., Hays, J., & Jerrett, M. (2019). Hazardous Air Pollutants Associated with Upstream Oil and Natural Gas Development: A Critical Synthesis of Current Peer-Reviewed Literature. *Annual Review of Public Health*, 40(Volume 40, 2019), 283–304. https://doi.org/10.1146/annurev-publhealth-040218-043715

[Gentner et al., 2009] Gentner, D. R., Harley, R. A., Miller, A. M., & Goldstein, A. H. (2009). Diurnal and Seasonal Variability of Gasoline-Related Volatile Organic Compound Emissions in River-

side, California. *Environmental Science & Technology*, 43(12), 4247–4252. https://doi.org/10.1021/es9006228

[Gentner et al., 2013] Gentner, D. R., Worton, D. R., Isaacman, G., Davis, L. C., Dallmann, T. R., Wood, E. C., Herndon, S. C., Goldstein, A. H., & Harley, R. A. (2013). Chemical Composition of Gas-Phase Organic Carbon Emissions from Motor Vehicles and Implications for Ozone Production. *Environmental Science & Technology*, 47(20), 11837–11848. https://doi.org/10.1021/es401470e

[Gilman et al., 2013] Gilman, J. B., Lerner, B. M., Kuster, W. C., & de Gouw, J. A. (2013). Source Signature of Volatile Organic Compounds from Oil and Natural Gas Operations in Northeastern Colorado. *Environmental Science & Technology*, 47(3), 1297–1305. https://doi.org/10.1021/es304119a

[Guenther et al., 1995] Guenther, A., Hewitt, C. N., Erickson, D., Fall, R., Geron, C., Graedel, T., Harley, P., Klinger, L., Lerdau, M., Mckay, W. A., Pierce, T., Scholes, B., Steinbrecher, R., Tallamraju, R., Taylor, J., & Zimmerman, P. (1995). A global model of natural volatile organic compound emissions. *Journal of Geophysical Research: Atmospheres*, 100(D5), 8873–8892. https://doi.org/10.1029/94JD02950

[Guha et al., 2015] Guha, A., Gentner, D. R., Weber, R. J., Provencal, R., & Goldstein, A. H. (2015). Source apportionment of methane and nitrous oxide in California's San Joaquin Valley at CalNex 2010 via positive matrix factorization. *Atmospheric Chemistry and Physics*, 15(20), 12043–12063. https://doi.org/10.5194/acp-15-12043-2015

[Halliday et al., 2016] Halliday, H. S., Thompson, A. M., Wisthaler, A., Blake, D. R., Hornbrook, R. S., Mikoviny, T., Müller, M., Eichler, P., Apel, E. C., & Hills, A. J. (2016). Atmospheric benzene observations from oil and gas production in the Denver-Julesburg Basin in July and August 2014. *Journal of Geophysical Research: Atmospheres*, 121(18), 11,055-11,074. https://doi.org/10.1002/2016JD025327

[Harley et al., 2000] Harley, R. A., Coulter-Burke, S. C., & Yeung, T. S. (2000). Relating Liquid Fuel and Headspace Vapor Composition for California Reformulated Gasoline Samples Containing Ethanol. *Environmental Science & Technology*, 34(19), 4088–4094. https://doi.org/10.1021/es000 9875

[Hecobian et al., 2019] Hecobian, A., Clements, A. L., Shonkwiler, K. B., Zhou, Y., MacDonald, L. P., Hilliard, N., Wells, B. L., Bibeau, B., Ham, J. M., Pierce, J. R., & Collett, J. L. Jr. (2019). Air Toxics and Other Volatile Organic Compound Emissions from Unconventional Oil and Gas Development. *Environmental Science & Technology Letters*, 6(12), 720–726. https://doi.org/10.1021/ac s.estlett.9b00591

[Helmig, 2020] Helmig, D. (2020). Air quality impacts from oil and natural gas development in Colorado. *Elementa: Science of the Anthropocene*, 8, 4. https://doi.org/10.1525/elementa.398

[Helmig et al., 2025] Helmig, D., Greenberg, G., Hueber, J., Blanchard, B., Chopra, J., Simoncic, S., Angot, H., Darby, L. S., Ortega, J., & Caputi, D. (2025). Methane and volatile organic compounds and their influence on air quality in Boulder, Colorado. *Elementa: Science of the Anthropocene*, 13(1), 00117. https://doi.org/10.1525/elementa.2023.00117

[Holder et al., 2019] Holder, C., Hader, J., Avanasi, R., Hong, T., Carr, E., Mendez, B., Wignall, J., Glen, G., Guelden, B., & Wei, Y. (2019). Evaluating potential human health risks from modeled inhalation exposures to volatile organic compounds emitted from oil and gas operations. *Journal of the Air & Waste Management Association*, 69(12), 1503–1524. https://doi.org/10.1080/10962247.2 019.1680459

[Hopke, 2016] Hopke, P. K. (2016). Review of receptor modeling methods for source apportionment. *Journal of the Air & Waste Management Association*, 66(3), 237–259. https://doi.org/10.108 0/10962247.2016.1140693

[Huangfu et al.,] Huangfu, Y., Yuan, B., Wang, S., Wu, C., He, X., Qi, J., de Gouw, J., Warneke, C., Gilman, J. B., Wisthaler, A., Karl, T., Graus, M., Jobson, B. T., & Shao, M. (2021). Revisiting Acetonitrile as Tracer of Biomass Burning in Anthropogenic-Influenced Environments. *Geophysical Research Letters*, 48(11), e2020GL092322. https://doi.org/10.1029/2020GL092322

[Jaffe, 2025a] Jaffe, M. (2025a, May 12). Weld County oil well blowout exposed people miles away to high levels of benzene, researchers say. *The Colorado Sun*. https://coloradosun.com/2025/05/12/oil-well-blowout-galeton-weld-county-bishop-chevron/

[Jaffe, 2025b] Jaffe, M. (2025b, June 27). Colorado regulators move to hold Chevron accountable for massive Weld County well blow out. *The Colorado Sun*. https://coloradosun.com/2025/06/27/chevron-blowout-colorado-weld-county-galeton/

[Kohut, 2007] Kohut, R. (2007). Assessing the risk of foliar injury from ozone on vegetation in parks in the U.S. National Park Service's Vital Signs Network. *Environmental Pollution*, 149(3), 348–357. https://doi.org/10.1016/j.envpol.2007.04.022

[Kroepsch et al., 2019] Kroepsch, A. C., Maniloff, P. T., Adgate, J. L., McKenzie, L. M., & Dickinson, K. L. (2019). Environmental Justice in Unconventional Oil and Natural Gas Drilling and Production: A Critical Review and Research Agenda. *Environmental Science & Technology*, 53(12), 6601–6615. https://doi.org/10.1021/acs.est.9b00209

[Ku et al., 2024] Ku, I.-T., Zhou, Y., Hecobian, A., Benedict, K., Buck, B., Lachenmayer, E., Terry, B., Frazier, M., Zhang, J., Pan, D., Low, L., Sullivan, A., & Collett, J. L. (2024). Air quality impacts from the development of unconventional oil and gas well pads: Air toxics and other volatile organic compounds. *Atmospheric Environment*, 317, 120187. https://doi.org/10.1016/j.atmosenv.2023.120187

[Kumar et al., 2020] Kumar, A., Sinha, V., Shabin, M., Hakkim, H., Bonsang, B., & Gros, V. (2020). Non-methane hydrocarbon (NMHC) fingerprints of major urban and agricultural emission

sources for use in source apportionment studies. *Atmospheric Chemistry and Physics*, 20(20), 12133–12152. https://doi.org/10.5194/acp-20-12133-2020

[Lachenmayer et al., 2024] Lachenmayer, E., Ku, I.-T., Hecobian, A., Benedict, K. B., Zhou, Y., Buck, B., & Collett, J. L. (2024). Source apportionment of airborne volatile organic compounds near unconventional oil and gas development. *Environmental Research Communications*, 6(10), 101013. https://doi.org/10.1088/2515-7620/ad82b2

[Lindaas et al., 2019] Lindaas, J., Farmer, D. K., Pollack, I. B., Abeleira, A., Flocke, F., & Fischer, E. V. (2019). Acyl Peroxy Nitrates Link Oil and Natural Gas Emissions to High Ozone Abundances in the Colorado Front Range During Summer 2015. *Journal of Geophysical Research: Atmospheres*, 124(4), 2336–2350. https://doi.org/10.1029/2018JD028825

[Lindaas et al., 2017] Lindaas, J., Farmer, D. K., Pollack, I. B., Abeleira, A., Flocke, F., Roscioli, R., Herndon, S., & Fischer, E. V. (2017). Changes in ozone and precursors during two aged wildfire smoke events in the Colorado Front Range in summer 2015. *Atmospheric Chemistry and Physics*, 17(17), 10691–10707. https://doi.org/10.5194/acp-17-10691-2017

[LTE, 2007] LTE. (2007). *Greater Wattenberg Area Baseline Study*. LT Environmental, Inc.; ECMC. https://ecmc.state.co.us/documents/library/AreaReports/DenverBasin/GWA/Greater_Wattenberg_Baseline_Study_Report_062007.pdf

[Lyu et al., 2021] Lyu, C., Capps, S. L., Kurashima, K., Henze, D. K., Pierce, G., Hakami, A., Zhao, S., Resler, J., Carmichael, G. R., Sandu, A., Russell, A. G., Chai, T., & Milford, J. (2021). Evaluating oil and gas contributions to ambient nonmethane hydrocarbon mixing ratios and ozone-related metrics in the Colorado Front Range. *Atmospheric Environment*, 246, 118113. https://doi.org/10.1016/j.atmosenv.2020.118113

[Malin, 2020] Malin, S. A. (2020). Depressed democracy, environmental injustice: Exploring the negative mental health implications of unconventional oil and gas production in the United States. *Energy Research & Social Science*, 70, 101720. https://doi.org/10.1016/j.erss.2020.101720

[Mayer et al., 2021] Mayer, A., Malin, S., McKenzie, L., Peel, J., & Adgate, J. (2021). Understanding Self-Rated Health and Unconventional Oil and Gas Development in Three Colorado Communities. *Society & Natural Resources*, 34(1), 60–81. https://doi.org/10.1080/08941920.2020.1734702

[McDuffie et al., 2016] McDuffie, E. E., Edwards, P. M., Gilman, J. B., Lerner, B. M., Dubé, W. P., Trainer, M., Wolfe, D. E., Angevine, W. M., deGouw, J., Williams, E. J., Tevlin, A. G., Murphy, J. G., Fischer, E. V., McKeen, S., Ryerson, T. B., Peischl, J., Holloway, J. S., Aikin, K., Langford, A. O., . . . Brown, S. S. (2016). Influence of oil and gas emissions on summertime ozone in the Colorado Northern Front Range. *Journal of Geophysical Research: Atmospheres*, 121(14), 8712–8729. https://doi.org/10.1002/2016JD025265

[McKenzie et al., 2024] McKenzie, L. M., Allshouse, W. B., Abrahams, B., & Tompkins, C. (2024). Oil and gas development exposure and atrial fibrillation exacerbation: A retrospective study of atrial fibrillation exacerbation using Colorado's all payer claims dataset. *Frontiers in Epidemiology*, 4. https://doi.org/10.3389/fepid.2024.1379271

[McKenzie et al., 2016] McKenzie, L. M., Allshouse, W. B., Burke, T., Blair, B. D., & Adgate, J. L. (2016). Population Size, Growth, and Environmental Justice Near Oil and Gas Wells in Colorado. *Environmental Science & Technology*, 50(21), 11471–11480. https://doi.org/10.1021/acs.est.6b04391

[McKenzie et al., 2017] McKenzie, L. M., Allshouse, W. B., Byers, T. E., Bedrick, E. J., Serdar, B., & Adgate, J. L. (2017). Childhood hematologic cancer and residential proximity to oil and gas development. *PLOS ONE*, 12(2), e0170423. https://doi.org/10.1371/journal.pone.0170423

[McKenzie et al., 2025] McKenzie, L. M., Allshouse, W. B., Johnson, D. R., DeVoe, C. C., Cockburn, M., & Ghosh, D. (2025). Exposures from Oil and Gas Development and Childhood Leukemia Risk in Colorado: A Population-Based Case–Control Study. *Cancer Epidemiology, Biomarkers & Prevention*, 34(5), 658–668. https://doi.org/10.1158/1055-9965.EPI-24-1583

[McKenzie et al., 2019] McKenzie, L. M., Allshouse, W., & Daniels, S. (2019). Congenital heart defects and intensity of oil and gas well site activities in early pregnancy. *Environment International*, 132, 104949. https://doi.org/10.1016/j.envint.2019.104949

[McKenzie et al., 2018] McKenzie, L. M., Blair, B., Hughes, J., Allshouse, W. B., Blake, N. J., Helmig, D., Milmoe, P., Halliday, H., Blake, D. R., & Adgate, J. L. (2018). Ambient Nonmethane Hydrocarbon Levels Along Colorado's Northern Front Range: Acute and Chronic Health Risks. *Environmental Science & Technology*, 52(8), 4514–4525. https://doi.org/10.1021/acs.est.7b05983

[McKenzie et al., 2014] McKenzie, L. M., Guo, R., Witter, R. Z., Savitz, D. A., Newman, L. S., & Adgate, J. L. (2014). Birth Outcomes and Maternal Residential Proximity to Natural Gas Development in Rural Colorado. *Environmental Health Perspectives*, 122(4), 412–417. https://doi.org/10.1289/ehp.1306722

[McLaren et al., 1996] McLaren, R., Gertler, A. W., Wittorff, D. N., Belzer, W., Dann, T., & Singleton, D. L. (1996). Real-World Measurements of Exhaust and Evaporative Emissions in the Cassiar Tunnel Predicted by Chemical Mass Balance Modeling. *Environmental Science & Technology*, 30(10), 3001–3009. https://doi.org/10.1021/es960036k

[McMullin et al., 2018] McMullin, T. S., Bamber, A. M., Bon, D., Vigil, D. I., & Van Dyke, M. (2018). Exposures and Health Risks from Volatile Organic Compounds in Communities Located near Oil and Gas Exploration and Production Activities in Colorado (U.S.A.). *International Journal of Environmental Research and Public Health*, 15(7), 1500. https://doi.org/10.3390/ijerph15071500

[Monks et al., 2015] Monks, P. S., Archibald, A. T., Colette, A., Cooper, O., Coyle, M., Derwent, R., Fowler, D., Granier, C., Law, K. S., Mills, G. E., Stevenson, D. S., Tarasova, O., Thouret, V., von Schneidemesser, E., Sommariva, R., Wild, O., & Williams, M. L. (2015). Tropospheric ozone and its precursors from the urban to the global scale from air quality to short-lived climate forcer. *Atmospheric Chemistry and Physics*, 15(15), 8889–8973. https://doi.org/10.5194/acp-15-8889-2015

[Montells et al., 2000] Montells, R., Aceves, M., & Grimalt, J. O. (2000). Sampling and Analysis of Volatile Organic Compounds Emitted from Leaded and Unleaded Gasoline Powered Motor Vehicles. *Environmental Monitoring and Assessment*, 62(1), 1–14. https://doi.org/10.1023/A:1006201100174

[Na et al., 2004] Na, K., Kim, Y. P., Moon, I., & Moon, K.-C. (2004). Chemical composition of major VOC emission sources in the Seoul atmosphere. *Chemosphere*, 55(4), 585–594. https://doi.org/10.1016/j.chemosphere.2004.01.010

[Norris et al., 2015] Norris, G., Duvall, R., Brown, S., & Bai, S. (2015, February 4). *EPA Positive Matrix Factorization 5.0 Fundamentals and User Guide*. U.S. EPA Office of Research and Development. https://www.epa.gov/air-research/epa-positive-matrix-factorization-50-fundamentals-and-user-guide

[Oltmans et al., 2019] Oltmans, S. J., Cheadle, L. C., Johnson, B. J., Schnell, R. C., Helmig, D., Thompson, A. M., Cullis, P., Hall, E., Jordan, A., Sterling, C., McClure-Begley, A., Sullivan, J. T., McGee, T. J., & Wolfe, D. (2019). Boundary layer ozone in the Northern Colorado Front Range in July–August 2014 during FRAPPE and DISCOVER-AQ from vertical profile measurements. *Elementa: Science of the Anthropocene*, 7, 6. https://doi.org/10.1525/elementa.345

[Orak et al., 2021] Orak, N. H., Reeder, M., & Pekney, N. J. (2021). Identifying and quantifying source contributions of air quality contaminants during unconventional shale gas extraction. *Atmospheric Chemistry and Physics*, 21(6), 4729–4739. https://doi.org/10.5194/acp-21-4729-2021

[Pan et al., 2023] Pan, D., Pollack, I. B., Sive, B. C., Marsavin, A., Naimie, L. E., Benedict, K. B., Zhou, Y., Sullivan, A. P., Prenni, A. J., Cope, E. J., Juncosa Calahorrano, J. F., Fischer, E. V., Schichtel, B. A., & Collett Jr., J. L. (2023). Source characterization of volatile organic compounds at Carlsbad Caverns National Park. *Journal of the Air & Waste Management Association*, 73(12), 914–929. https://doi.org/10.1080/10962247.2023.2266696

[Parrish et al., 2007] Parrish, D. D., Stohl, A., Forster, C., Atlas, E. L., Blake, D. R., Goldan, P. D., Kuster, W. C., & de Gouw, J. A. (2007). Effects of mixing on evolution of hydrocarbon ratios in the troposphere. *Journal of Geophysical Research: Atmospheres*, 112(D10). https://doi.org/10.1029/2006JD007583

[Payne et al., 2017] Payne, B. F., Ackley, R., Paige Wicker, A., Hildenbrand, Z. L., Carlton, D. D., & Schug, K. A. (2017). Characterization of methane plumes downwind of natural gas compressor stations in Pennsylvania and New York. *Science of The Total Environment*, 580, 1214–1221. https://doi.org/10.1016/j.scitotenv.2016.12.082

[Permar et al., 2021] Permar, W., Wang, Q., Selimovic, V., Wielgasz, C., Yokelson, R. J., Hornbrook, R. S., Hills, A. J., Apel, E. C., Ku, I.-T., Zhou, Y., Sive, B. C., Sullivan, A. P., Collett Jr, J. L., Campos, T. L., Palm, B. B., Peng, Q., Thornton, J. A., Garofalo, L. A., Farmer, D. K., … Hu, L. (2021). Emissions of Trace Organic Gases From Western U.S. Wildfires Based on WE-CAN Aircraft Measurements. *Journal of Geophysical Research: Atmospheres*, 126(11), e2020JD033838. https://doi.org/10.1029/2020JD033838

[Pétron et al., 2012] Pétron, G., Frost, G., Miller, B. R., Hirsch, A. I., Montzka, S. A., Karion, A., Trainer, M., Sweeney, C., Andrews, A. E., Miller, L., Kofler, J., Bar-Ilan, A., Dlugokencky, E. J., Patrick, L., Moore Jr., C. T., Ryerson, T. B., Siso, C., Kolodzey, W., Lang, P. M., … Tans, P. (2012). Hydrocarbon emissions characterization in the Colorado Front Range: A pilot study. *Journal of Geophysical Research: Atmospheres*, 117(D4). https://doi.org/10.1029/2011JD016360

[Pétron et al., 2014] Pétron, G., Karion, A., Sweeney, C., Miller, B. R., Montzka, S. A., Frost, G. J., Trainer, M., Tans, P., Andrews, A., Kofler, J., Helmig, D., Guenther, D., Dlugokencky, E., Lang, P., Newberger, T., Wolter, S., Hall, B., Novelli, P., Brewer, A., ... Schnell, R. (2014). A new look at methane and nonmethane hydrocarbon emissions from oil and natural gas operations in the Colorado Denver-Julesburg Basin. *Journal of Geophysical Research: Atmospheres*, 119(11), 6836–6852. https://doi.org/10.1002/2013JD021272

[Pfister et al., 2017] Pfister, G. G., Reddy, P. J., Barth, M. C., Flocke, F. F., Fried, A., Herndon, S. C., Sive, B. C., Sullivan, J. T., Thompson, A. M., Yacovitch, T. I., Weinheimer, A. J., & Wisthaler, A. (2017). Using Observations and Source-Specific Model Tracers to Characterize Pollutant Transport During FRAPPÉ and DISCOVER-AQ. *Journal of Geophysical Research: Atmospheres*, 122(19), 10,510-10,538. https://doi.org/10.1002/2017JD027257

[Polissar et al., 1998] Polissar, A. V., Hopke, P. K., Paatero, P., Malm, W. C., & Sisler, J. F. (1998). Atmospheric aerosol over Alaska: 2. Elemental composition and sources. *Journal of Geophysical Research: Atmospheres*, 103(D15), 19045–19057. https://doi.org/10.1029/98JD01212

[Pollack et al., 2021] Pollack, I. B., Helmig, D., O'Dell, K., & Fischer, E. V. (2021). Seasonality and Source Apportionment of Nonmethane Volatile Organic Compounds at Boulder Reservoir, Colorado, Between 2017 and 2019. *Journal of Geophysical Research: Atmospheres*, 126(9), e2020JD034234. https://doi.org/10.1029/2020JD034234

[Pope, 2000] Pope, C. A. (2000). Epidemiology of Fine Particulate Air Pollution and Human Health: Biologic Mechanisms and Who's at Risk? *Environmental Health Perspectives*, 108, 713–723. https://doi.org/10.2307/3454408

[Roberts et al., 1984] Roberts, J. M., Fehsenfeld, F. C., Liu, S. C., Bollinger, M. J., Hahn, C., Albritton, D. L., & Sievers, R. E. (1984). Measurements of aromatic hydrocarbon ratios and NOx concentrations in the rural troposphere: Observation of air mass photochemical aging and NOx

removal. *Atmospheric Environment (1967)*, 18(11), 2421–2432. https://doi.org/10.1016/0004-6981(84)90012-X

[Rodriguez et al., 2009] Rodriguez, M. A., Barna, M. G., & Moore, T. (2009). Regional Impacts of Oil and Gas Development on Ozone Formation in the Western United States. *Journal of the Air & Waste Management Association*, 59(9), 1111–1118. https://doi.org/10.3155/1047-3289.59.9.1111

[Rossabi and Helmig, 2018] Rossabi, S., & Helmig, D. (2018). Changes in Atmospheric Butanes and Pentanes and Their Isomeric Ratios in the Continental United States. *Journal of Geophysical Research: Atmospheres*, 123(7), 3772–3790. https://doi.org/10.1002/2017JD027709

[Rubin et al., 2006] Rubin, J. I., Kean, A. J., Harley, R. A., Millet, D. B., & Goldstein, A. H. (2006). Temperature dependence of volatile organic compound evaporative emissions from motor vehicles. *Journal of Geophysical Research: Atmospheres*, 111(D3). https://doi.org/10.1029/2005JD006458

[Sakas, 2020] Sakas, M. E. (2020, July 30). Safety Fears Hang In The Air After A Benzene Spike At A Greeley School With A Neighboring Oil And Gas Well. *Colorado Public Radio*. https://www.cpr.org/2020/07/30/safety-fears-hang-in-the-air-after-a-benzene-spike-at-a-greeley-school-with-a-neighboring-oil-and-gas-well/

[Sansone-Poe et al., 2025] Sansone-Poe, D. M., Walters, H. L., Adgate, J. L., Allshouse, W. B., McKenzie, L. M., & Dickinson, K. L. (2025). Variation in Proximity to Oil and Gas Well Pads across Race-Ethnicity and Income Groups in Colorado: An Inquiry into Distributive Environmental Justice Patterns. *Environmental Science & Technology*, 59(5), 2494–2504. https://doi.org/10.1021/acs.est.4c10007

[Sive et al., 2005] Sive, B. C., Zhou, Y., Troop, D., Wang, Y., Little, W. C., Wingenter, O. W., Russo, R. S., Varner, R. K., & Talbot, R. (2005). Development of a Cryogen-Free Concentration System for Measurements of Volatile Organic Compounds. *Analytical Chemistry*, 77(21), 6989–6998. https://doi.org/10.1021/ac0506231

[Solomon, 2025] Solomon, R. (2025, June 23). *"A spike in air pollution:" Galeton well cleanup continues but concerns linger*. KUNC. https://www.kunc.org/news/2025-06-23/air-quality-and-public-health-are-a-concern-in-the-wake

[Sullivan et al., 2016] Sullivan, J. T., McGee, T. J., Langford, A. O., Alvarez II, R. J., Senff, C. J., Reddy, P. J., Thompson, A. M., Twigg, L. W., Sumnicht, G. K., Lee, P., Weinheimer, A., Knote, C., Long, R. W., & Hoff, R. M. (2016). Quantifying the contribution of thermally driven recirculation to a high-ozone event along the Colorado Front Range using lidar. *Journal of Geophysical Research: Atmospheres*, 121(17), 10,377-10,390. https://doi.org/10.1002/2016JD025229

[Sultana and Hoover, 2024] Sultana, D., & Hoover, S. (2024). Analysis of gasoline-related pollutant exposures and risks in California between 1996 and 2014. *Journal of Exposure Science & Environmental Epidemiology*, 34(3), 518–528. https://doi.org/10.1038/s41370-023-00615-0

[Sun et al., 2025] Sun, Y., Guan, J., Yue, G., Xiu, Y., Wang, H., McHugh, T., & Ma, J. (2025). Chemical Composition and Fingerprints of Headspace Vapors of 37 Petroleum Products and Non-Aqueous Phase Liquid Samples. *Environmental Forensics*, 26(4), 485–500. https://doi.org/10.1080/15275922.2025.2459405

[Swarthout et al., 2013] Swarthout, R. F., Russo, R. S., Zhou, Y., Hart, A. H., & Sive, B. C. (2013). Volatile organic compound distributions during the NACHTT campaign at the Boulder Atmospheric Observatory: Influence of urban and natural gas sources. *Journal of Geophysical Research: Atmospheres*, 118(18), 10,614-10,637. https://doi.org/10.1002/jgrd.50722

[Thakore, 2025] Thakore, I. (2025, June 26). *State alleges Chevron subsidiary violated rules in April spill*. Colorado Public Radio. https://www.cpr.org/2025/06/26/colorado-oil-spill-rules-allegedly-violated-chevron-subsidiary/

[Thomas, 2025] Thomas, D. (2025, June 30). *Investigators release cause of Northern Colorado oil and gas leak, some residents remain displaced*. CBS Colorado. https://www.cbsnews.com/colorado/news/investigators-release-cause-northern-colorado-oil-gas-leak/

[Thompson et al., 2014] Thompson, C. R., Hueber, J., & Helmig, D. (2014). Influence of oil and gas emissions on ambient atmospheric non-methane hydrocarbons in residential areas of Northeastern Colorado. *Elementa: Science of the Anthropocene*, 3, 000035. https://doi.org/10.12952/journal.elementa.000035

[U.S. Census Bureau, 2020] U.S. Census Bureau. (2020). *Census Bureau Data* [Dataset]. https://data.census.gov/

[U.S. EPA, 1994] U.S. EPA. (1994). *Methods for Derivation of Inhalation Reference Concentrations and Application of Inhalation Dosimetry*. https://www.epa.gov/risk/methods-derivation-inhalation-reference-concentrations-and-application-inhalation-dosimetry

[U.S. EPA, 2023] U.S. EPA. (2023). *2020 NEI Supporting Data and Summaries* [Dataset]. https://www.epa.gov/air-emissions-inventories/2020-nei-supporting-data-and-summaries

[Warneke et al., 2014] Warneke, C., Geiger, F., Edwards, P. M., Dube, W., Pétron, G., Kofler, J., Zahn, A., Brown, S. S., Graus, M., Gilman, J. B., Lerner, B. M., Peischl, J., Ryerson, T. B., de Gouw, J. A., & Roberts, J. M. (2014). Volatile organic compound emissions from the oil and natural gas industry in the Uintah Basin, Utah: Oil and gas well pad emissions compared to ambient air composition. *Atmospheric Chemistry and Physics*, 14(20), 10977–10988. https://doi.org/10.5194/acp-14-10977-2014

[Warneke et al., 2007] Warneke, C., McKeen, S. A., de Gouw, J. A., Goldan, P. D., Kuster, W. C., Holloway, J. S., Williams, E. J., Lerner, B. M., Parrish, D. D., Trainer, M., Fehsenfeld, F. C., Kato, S., Atlas, E. L., Baker, A., & Blake, D. R. (2007). Determination of urban volatile organic

compound emission ratios and comparison with an emissions database. *Journal of Geophysical Research: Atmospheres*, 112(D10). https://doi.org/10.1029/2006JD007930

[Weber, 2018] Weber, D. T. (2018). *Volatile organic compound concentrations and the impacts of future oil and natural gas development in the Colorado Northern Front Range* [Colorado State University. Libraries]. https://hdl.handle.net/10217/189283

[Weisner et al., 2023] Weisner, M. L., Allshouse, W. B., Erjavac, B. W., Valdez, A. P., Vahling, J. L., & McKenzie, L. M. (2023). Health Symptoms and Proximity to Active Multi-Well Unconventional Oil and Gas Development Sites in the City and County of Broomfield, Colorado. *International Journal of Environmental Research and Public Health*, 20(3), 2634. https://doi.org/10.3390/ijerph20032634

[Weisner et al., 2025] Weisner, M. L., Varner, P. M., Ku, I.-T., Collett, J. L., Buck, B., & McKenzie, L. M. (2025). Cumulative Human Health Risk Assessment of Regional Ozone and Volatile Organic Compounds from Unconventional Oil and Gas Sites in Colorado's Front Range. *Environmental Health Perspectives*, 133(5), 057025. https://doi.org/10.1289/EHP16272

[Wells, 2017] Wells, D. (2017). *Consequences of the Evolution of Oil and Gas Control and Production Technology in the Denver Ozone Nonattainment Area.* https://vibe.cira.colostate.edu/ogec/docs/CDPHE/Consequences%20of%20the%20Evolution%20of%20Control%20and%20Production%20Technology%20in%20the%20Denver%20Ozone%20NAA.pdf

[Yuan et al., 2012] Yuan, B., Shao, M., de Gouw, J., Parrish, D. D., Lu, S., Wang, M., Zeng, L., Zhang, Q., Song, Y., Zhang, J., & Hu, M. (2012). Volatile organic compounds (VOCs) in urban air: How chemistry affects the interpretation of positive matrix factorization (PMF) analysis. *Journal of Geophysical Research: Atmospheres*, 117(D24). https://doi.org/10.1029/2012JD018236

[Zhou et al., 2005] Zhou, Y., Varner, R. K., Russo, R. S., Wingenter, O. W., Haase, K. B., Talbot, R., & Sive, B. C. (2005). Coastal water source of short-lived halocarbons in New England. *Journal of Geophysical Research: Atmospheres*, 110(D21). https://doi.org/10.1029/2004JD005603

Appendix A

Chapter 2

A.1 Descriptions of the eight sampling locations

Note that in the proceeding site descriptions we have excluded the specific location and names of several of the sites to protect the identities of individuals and organizations.

Fort Collins West (FCW): Located in Christman Field, FCW [40.592°N, -105.141°W] is approximately 350 m from a regularly used roadway to the south (Laporte Ave.) and a larger and more heavily trafficked roadway to the east about 600 m (S. Overland Trail). We secure the canisters to the roof of a mobile laboratory about 12 ft above the ground. The samples in this work consist of continuous weekly measurements from September 21, 2023 to May 1, 2025, however, the sample collection is ongoing at the time of thesis publication.

Fort Collins North (FCN): For the FCN samples, we collected canisters at two different but closely positioned sites. We mounted the canisters at the first sampling location on a fence post in a field, approximately 2 m above the ground, at the edge of a neighborhood. The site was 200-300 ft from the well. At the second site, we mounted the canisters on the top of a steel fence post inside a large dog kennel, approximately 2 m above the ground. We collected these samples near a small farm and a seldom used gravel road. The data consists of continuous weekly measurements from February 11, 2022 to April 25, 2025, and May 29, 2024 to September 13, 2024. Note that we used the dog kennel to protect co-located continuous monitoring equipment used to collect air samples during short pollution events (i.e., a SENSIT® SPOD with a photoionization detector (PID) sensor and coupled with evacuated Entech Instruments 1.4-L Silonite®-coated stainless steel canisters). A detailed description of a similar real-time monitoring system can be found in Ku et al. (2024) and a short description is in Section 2.5 of this thesis.

Greeley Residential Area (GRA): In southeast Greeley, CO, GRA is located in a rural residential neighborhood with multiple small private farms in the vicinity. Additionally, GRA is approx-

imately 3 km from the Greeley-Weld County airport. Similar to FCN, we mount the canisters on the top of a steel fence post inside a large dog kennel at approximately 2 m above the ground. At this site, we have also co-located continuous monitoring equipment (Section 2.5). The data in this work consists of discontinuous weekly measurements from February 23, 2023 to May 2, 2025, and continuous samples from September 7, 2023 to May 1, 2025. The sample collection at this site is ongoing.

Loveland Elementary School (LES): The elementary school in Loveland, CO [40.392°N, -105.055°W], is relatively close to the industrial development in the downtown area. We adhere the canisters to a fence on the campus at about 2 m above the ground. We also have co-located continuous monitoring equipment at this site (Section 2.5). The data in this work consists of continuous weekly measurements from July 11, 2024 to September 13, 2024 and December 19, 2024 to May 1, 2025. At the time of publication, sample collection is ongoing at this site.

The following information about 2015-2016 samples is adapted from Weber (2018).

Fossil Creek Reservoir Natural Area (FCNA): : At the time of sampling, FCNA [40.986°N, -105.009°W] was not in the immediate vicinity of dense O&G development and there were no active O&G wells within a 3 km radius of the site. Weber (2018) adhered the canisters about 2-m above the ground on a building adjacent to the Natural Area parking lot. The parking lot had a maximum capacity of 40 vehicles and was only used by staff and visitors. The maximum visitation was in April through June (43%) and dropped to a minimum from October to December (16%) (City of Fort Collins, 2003). The data consists of continuous weekly measurements from September 18, 2015 to November 25, 2015.

Timnath Elementary School (TES):The elementary school in Timnath, CO [40.515°N, -104.950°W], was surrounded by an actively developing residential neighborhood during the time of sampling. Weber (2018) affixed canisters to the northeast roof line of a mobile classroom roughly 3 m above the ground. The data consists of discontinuous weekly measurements, spanning slightly over a year, from July 31, 2015 to November 8, 2016.

Timnath Gas Station (TGS): Weber (2018) secured the canisters at the large gas station in Timnath, CO, to the back of a sign approximately 20-m north of the gasoline pumps. The data consists of discontinuous weekly measurements, spanning slightly over a year, from August 1, 2015 to November 8, 2016.

Soapstone Prairie Natural Area (SPNA): At SPNA [40.986°N, -105.009°W], Weber (2018) affixed the canisters about 1-m above the ground to a wooden pole outside of a shed used as the park ranger headquarters throughout the year. At the time of sampling, the building was seldom occupied and vehicular traffic was sparse on the surrounding dirt roads.

A.2 Method detection limits for GC analysis

Table A.1: The method detection limit (MDL) of CH_4 and the 51 NMVOCs measured by the GC systems for the canister samples from 2022 to 2025.

Species	MDL	MDL unit
Methane	0.0500	ppmv
Ethane	0.2082	ppbv
Propane	0.0419	ppbv
i-Butane	0.0147	ppbv
n-Butane	0.0216	ppbv
i-Pentane	0.0167	ppbv
n-Pentane	0.0054	ppbv
n-Hexane	0.0222	ppbv
n-Heptane	0.0173	ppbv
n-Octane	0.0121	ppbv
n-Nonane	0.0221	ppbv
n-Decane	0.0262	ppbv
Cyclopentane	0.0098	ppbv
Cyclohexane	0.0380	ppbv
Methylcyclohexane	0.0414	ppbv
2,*3*,*4*-Trimethylpentane	0.0211	ppbv
2,*2*,*4*-Trimethylpentane	0.0238	ppbv
2,*3*-Dimethylpentane	0.0320	ppbv
2,*4*-Dimethylpentane	0.0241	ppbv
2-Methylhexane	0.0100	ppbv
3-Methylhexane	0.0189	ppbv

Table A.2: The method detection limit (MDL) of CH_4 and the 51 NMVOCs measured by the GC systems for the canister samples from 2022 to 2025 continued.

Species	MDL	MDL unit
2-Methylheptane	0.0284	ppbv
3-Methylheptane	0.0091	ppbv
Ethene	0.0228	ppbv
Propene	0.0170	ppbv
t-2-Butene	0.0056	ppbv
1-Butene	0.0159	ppbv
c-2-Butene	0.0115	ppbv
t-2-Pentene	0.0079	ppbv
1-Pentene	0.0361	ppbv
c-2-Pentene	0.0139	ppbv
Benzene	0.0160	ppbv
Toluene	0.0177	ppbv
Ethylbenzene	0.0085	ppbv
m+p-Xylene	0.0207	ppbv
o-Xylene	0.0230	ppbv
Styrene	0.0153	ppbv
Isopropylbenzene	0.0184	ppbv
n-Propylbenzene	0.0247	ppbv
3-Ethyltoluene	0.0068	ppbv
4-Ethyltoluene	0.0306	ppbv
2-Ethyltoluene	0.0184	ppbv
1,*3*,*5*-Trimethylbenzene	0.0101	ppbv
1,*2*,*4*-Trimethylbenzene	0.0096	ppbv
1,*2*,*3*-Trimethylbenzene	0.1550	ppbv
1,*3*-Diethylbenzene	0.0226	ppbv
1,*4*-Diethylbenzene	0.0134	ppbv
Acetylene	0.0194	ppbv
Isoprene	0.0030	ppbv
Tetrachloroethylene	0.0898	pptv
Trichloroethylene	1.0000	pptv
Acetonitrile	0.222	ppbv

Table A.3: The method detection limit (MDL) of CH_4 and the 48 NMVOCs measured by the GC systems for the canister samples from 2015 to 2016.

Species	MDL	MDL unit
Ethane	0.105	ppbv
Propane	0.02	ppbv
i-Butane	0.008	ppbv
n-Butane	0.01	ppbv
i-Pentane	0.009	ppbv
n-Pentane	0.007	ppbv
n-Hexane	0.012	ppbv
n-Heptane	0.009	ppbv
n-Octane	0.016	ppbv
n-Nonane	0.01	ppbv
n-Decane	0.011	ppbv
Cyclopentane	0.009	ppbv
Cyclohexane	0.015	ppbv
Methylcyclohexane	0.019	ppbv
2,*3*,*4*-Trimethylpentane	0.009	ppbv
2,*2*,*4*-Trimethylpentane	0.018	ppbv
2,*3*-Dimethylpentane	0.013	ppbv
2,*4*-Dimethylpentane	0.004	ppbv
2-Methylhexane	0.01	ppbv
3-Methylhexane	0.014	ppbv
2-Methylheptane	0.022	ppbv
3-Methylheptane	0.016	ppbv
Ethene	0.053	ppbv
Propene	0.009	ppbv
t-2-Butene	0.018	ppbv
1-Butene	0.013	ppbv
c-2-Butene	0.022	ppbv
t-2-Pentene	0.014	ppbv
1-Pentene	0.023	ppbv
c-2-Pentene	0.012	ppbv
Benzene	0.01	ppbv
Toluene	0.017	ppbv
Ethylbenzene	0.019	ppbv
m+*p*-Xylene	0.014	ppbv
o-Xylene	0.006	ppbv
Styrene	0.014	ppbv
Isopropylbenzene	0.011	ppbv
n-Propylbenzene	0.012	ppbv

Table A.4: The method detection limit (MDL) of CH_4 and the 48 NMVOCs measured by the GC systems for the canister samples from 2015 to 2016 continued.

Species	MDL	MDL unit
3-Ethyltoluene	0.014	ppbv
4-Ethyltoluene	0.015	ppbv
2-Ethyltoluene	0.025	ppbv
1,*3*,*5*-Trimethylbenzene	0.012	ppbv
1,*2*,*4*-Trimethylbenzene	0.0124	ppbv
1,*2*,*3*-Trimethylbenzene	0.012	ppbv
1,*3*-Diethylbenzene	0.027	ppbv
1,*4*-Diethylbenzene	0.013	ppbv
Acetylene	0.013	ppbv
Isoprene	0.012	ppbv

A.3 Fuel composition analysis procedure

To prepare for the headspace fuel composition analysis, we cleaned amber glass vials (Restek® Pre-Cleaned Volatile Organic Analyte Sampling Vials, 20-mL, 24-400 Screw-Thread Open Top with 0.125" PTFE/Silicone Septa) with deionized (DI) water and dried the vials in an oven overnight at 95°C (Barnstead International Thermolyne® Model 62700 Basic Large Muffle Furnace).

In February 2025, we obtained the "regular" grade gasoline sample (winter-grade, 85 octane gasoline) from the same gas station in Timnath where Weber (2018) collected the weekly-integrated whole air gas samples used in this thesis. We filled a plastic 2-gallon container with gasoline for transport to the laboratory where we immediately transferred portions of the fuel sample into the glass vials in a fume hood. We completely filled the vials to minimize the amount of trapped ambient air inside during storage. To reduce reactivity of the liquid gasoline samples, we refrigerated the vials overnight at -18°C.

For the first round of analysis, we prepared two headspace samples. Within 24-hours, we pipetted 10 mL of the liquid gasoline sample into new clean and dry amber glass vials and let them sit at room temperature for about two hours. Once the volatile compounds in the liquid fuel sample had adequate time to evaporate into the air in the vial, we used a syringe to measure 1 mL of the

headspace gas from the vials for dilution. Using a zero air generator, we diluted each headspace sample inside an evacuated 1.4-L Silonite®-coated stainless steel canisters (Entech Instruments). We used a quick-connect compression fitting adapter (Entech Instruments Micro-QT) to attach the canister to the zero air generator for five seconds. With the canister still connected, we quickly injected the syringe with the headspace sample into the zero air generator via a Stainless Steel Ultra-Torr Tee (Swagelok), with a 11-mm Septa (Hewlett Packard) installed at one port of the Tee for the sample injection. The canisters were attached to the system for 20 seconds total. For quality control, we prepared a zero air blank sample following a similar procedure but instead injecting 1 mL of zero air into an evacuated canister. Then, we analyzed the diluted headspace and black samples using the GC methodology we describe in Section 2.2 of this thesis.

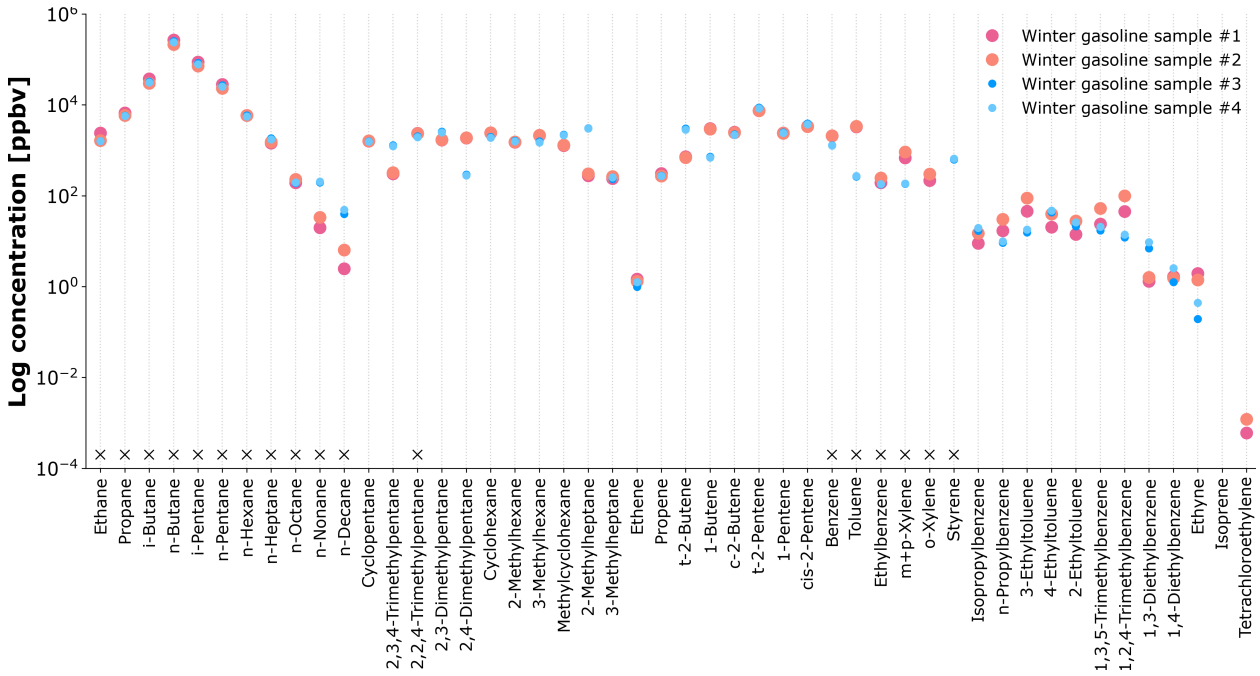

Figure A.1: Log concentrations [ppbv] of NMVOC in the headspace winter gasoline formula samples analyzed within 24 hours (reds) and after three months (blues). There are two samples for each analysis period. The cross symbols along the x-axis indicate the NMVOCs (i.e., light and heavy alkanes and HAPs) we use in Section 3.3.

To test the compositional stability of the liquid gasoline sample, we performed a second round of analysis on the fuel sample we stored in the refrigerator after about three months. Using the

remaining vials that were completely filled with gasoline, we prepared and analyzed two more headspace samples following the same procedure as outlined above. Figure A.1 has the results for the winter gasoline formula headspace samples. The light and heavy alkanes, *2*,*2*,*4*-trimethylpentane, benzene, ethylbenzene, in the gasoline samples are generally stable. The *n*-nonane, *n*-decane, toluene, *m*+*p*-xylene, *o*-xylene, and styrene concentrations change over the three months in the refrigerator. In particular, styrene concentrations were below MDL value in the 24-hour gasoline samples (#1-2) but comparable with other aromatics in the three month samples, and the opposite is true for *o*-xylene (#3-4; Figure A.1).

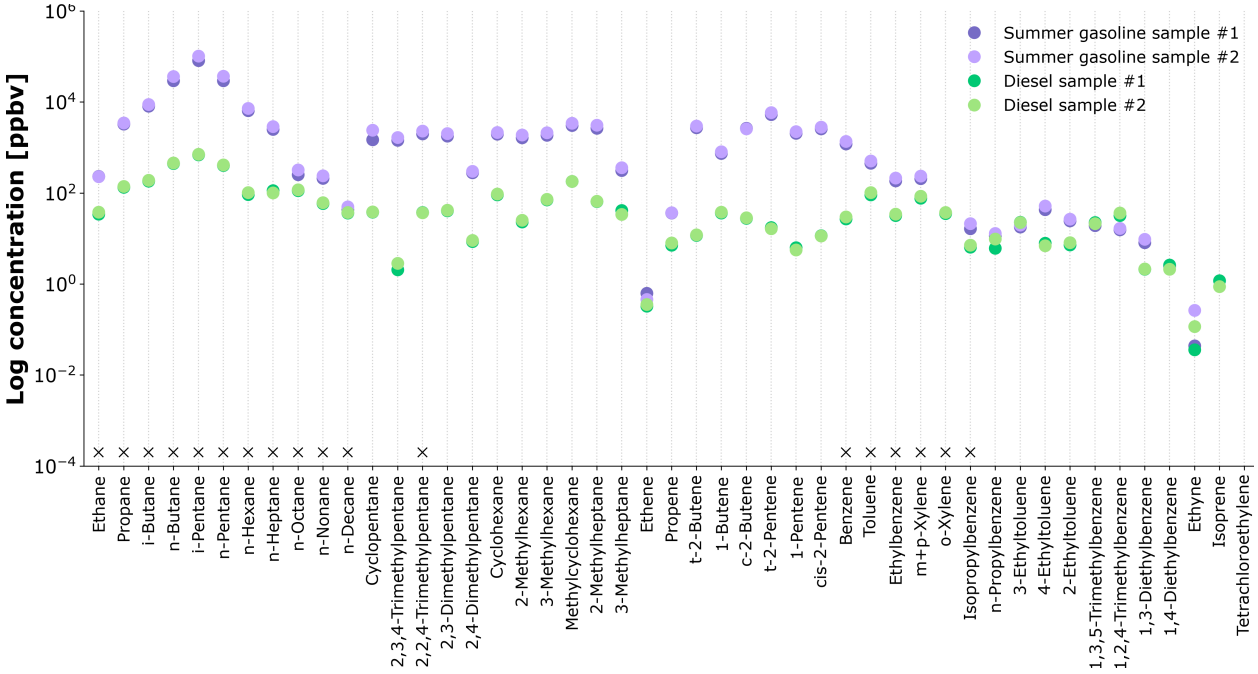

Figure A.2: Log concentrations [ppbv] of NMVOC in the headspace summer gasoline formula (purples) and diesel (greens) samples. There are two samples for each fuel type. The cross symbols along the x-axis indicate the NMVOCs (i.e., light and heavy alkanes and HAPs) we use in Section 3.3.

In July 2025, we performed a similar composition analysis on diesel and the summer formulation of "regular" grade gasoline samples (85 octane) we collected at the same gas station in Timnath. The summary of results for the diesel and summer gasoline formula headspace samples can be found in Figure A.2. Note that the diesel samples were analyzed within a week of collection

instead of within 24 hours. The compositional stability assessment is not complete for these two fuel samples at the time of thesis publication.

A.4 Considerations for interpreting PMF analysis

A.4.1 Choosing an appropriate number of factors for PMF analysis.

We run three tests to determine the number of PMF factors p that best explain the speciated VOC data described in Section 2.4. Ultimately, we found that the four-factor solution most clearly explained the VOC emission sources; however, we ran PMF analysis and tests for $p = 2\text{-}8$.

First, we evaluate how increasing p impacts the amount of information explained in the data using Q/Q_{exp} from the model output. In general, Q/Q_{exp} decreases as additional factors are considered. The change in Q/Q_{exp} or $\Delta Q/Q_{exp}$ with p is a better indicator for choosing the number of factors since a large decrease in Q/Q_{exp} with the addition of another factor implies the additional factor significantly improved the solution (Paatero and Tapper, 1993). Figure A.3 shows values for Q/Q_{exp} or $\Delta Q/Q_{exp}$ with p, indicating that there is not an obvious optimal number of factors. We apply the remaining tests for $p = 2\text{-}8$ and examine solutions for $p = 4$ and 5.

Second, to estimate effects from random variability and identify if a small subset of observations in the dataset disproportionately impacts the base PMF solution we perform a bootstrap analysis. The PMF program resamples the original dataset to create a new dataset of the same length that it runs through the PMF model to obtain bootstrap factor profiles which it compares to original or base factor profiles; the program repeats this process 100 times. We consider the solution stable if the base and bootstrap factors agree 80-100% of the time. Based on the bootstrap analysis, we determined that $p = 2\text{-}5$ solutions are stable.

Third, we performed a displacement analysis to explore sensitivity to small changes and effects of rotational ambiguity for each solution. For any pair of matrices, infinite variations of the pair can be generated by a simple rotation. Rotational ambiguity is caused by the existence of infinite solutions that are similar to the solution generated by PMF. Each value in the factor profile is adjusted and then the other values are computed to minimize Q. If a factor has large rotational

ambiguity, the factors will swap in the displacement analysis, indicating instability in the solution. Based on displacement analysis, we find that p = *2-8* solutions are stable.

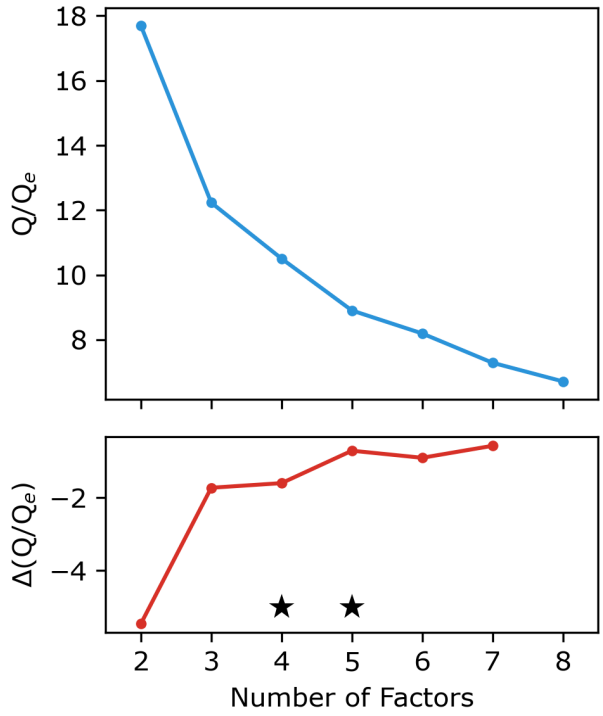

Figure A.3: Average Q/Q_{exp} and $\Delta Q/Q_{exp}$ for each number of factors (p) from 100 runs of the base model for each PMF solution for p = *2-8*. The black stars indicate the two solutions that we investigate further in Figure 3.5 (p = *4*) and Figure A.4 (p = *5*).

Since there was not an obvious optimal number of factors, we explored the NMVOCs in the profiles for each p solution. From VOC composition and proximity to particular source locations we determined that four factors best describe the canister samples. A three-factor PMF solution seems to group NMVOC emission for different sources. Alternatively, a five-factor PMF solution appears to split short-chain alkanes, abundant in long-lived O&G emission, from complex alkanes with shorter atmospheric lifetimes, but the i/n-pentane ratios complicate source attribution. The five-factor solution lowers the *i*/*n*-pentane ratio of the factor dominated by longer-lived alkanes to 0.77. However, the factor rich with complex alkane species has a ratio of 1.53, suggesting that the fifth factor contains shorter-lived alkanes from combustion sources instead of shorter-lived alkanes

from O&G emission (Figure A.4). Supporting this notion, we find that factor splitting in the five-source solution lowers the *i*/*n*-pentane ratio of both traffic + urban combustion and fueling station factors, indicating more mixed influence from O&G emissions.

Additional information about running PMF can be found in the EPA Positive Matrix Factorization (PMF) 5.0 Fundamentals and User Guide (Norris et al., 2014).

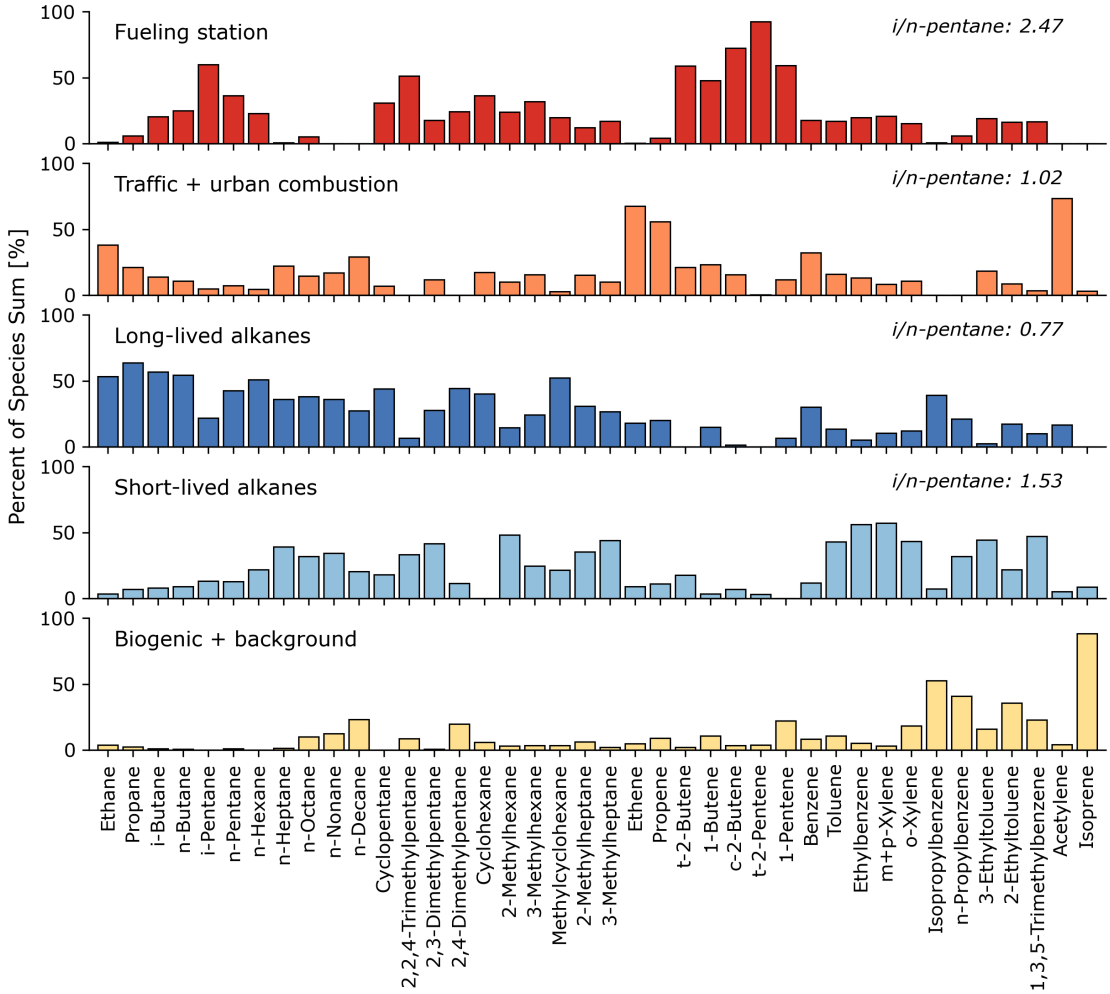

Figure A.4: The average percent of species sum of 40 NMVOCs for the five factor profiles calculated using PMF with their *i*/*n*-pentane ratios. The factors assignments include fueling station (red), traffic + urban combustion (orange), long-lived alkanes (dark blue), short-lived alkanes (light blue), and biogenic + background (yellow) sources. The NMVOC compounds with "weak" classification in the PMF model include *n*-decane, *3*-methylheptane, *1*-pentene, isopropylbenzene, *n*-propolbenzene, and *2*-ethyltoluene.

A.4.2 Uncertainty calculations used in PMF analysis.

If the concentration for an individual VOC is lower than the MDL value, the uncertainty calculation is Equation A.1 (Polissar et al., 1998). The MDL values for the 2015-2016 and 2022-2025 samples are in Tables A.1-A.4, respectively.

$$Unc = \frac{5}{6} \times MDL \tag{A.1}$$

If the concentration for an individual VOC is greater than the MDL value, the uncertainty calculation is Equation A.2, where the error fraction is 0.01 for CH_4 and 0.05 for NMVOCs. The MDL values for the 2015-2016 and 2022-2025 samples are in Tables A.1-A.4, respectively.

$$Unc = \sqrt{(Error fraction \times concentration)^2 + (0.5 \times MDL)^2} \tag{A.2}$$

A.4.3 Considerations for finalizing the list of VOC included in PMF.

As introduced in Section 2.4, following Hopke (2016), we used signal-to-noise ratio (*S/N*) and coefficient of determination (r^2) to determine which VOC species to exclude before running the PMF model. Applying these guidelines, compounds with *S/N* ratios > 1 are categorized as "good", *S/N* ratios < 0.5 are categorized as "bad", and 0.5 < *S/N* < 1 ratios are categorized as "weak." The bad compounds are excluded from PMF analysis and the imputed uncertainties (Section A.4.2) of the weak compounds are multiplied by three. From *S/N* ratio evaluation, we removed *1*,*3*-trimethylpentane and classified *1*-pentene, isopropylbenzene as weak. Similarly, we classified the compounds with r^2 < 0.3 between the observed and predicted values as weak; this included *n*-decane, *3*-methylheptane, *n*-propolbenzene, and *2*-ethyltoluene.

In addition, we removed species that appeared to reflect temporal trends and were not abundant at a majority of sampling locations. Due to the time difference between the 2015-2016 and 2022-2024 samples, we chose to exclude VOCs with large changes in concentrations between the two sampling periods which include *c-2*-pentene, *1*,*2*,*4*-trimethylbenzene, *1*,*4*-diethylbenzene, styrene, *2*,*3*,*4*-trimethylpentene, *4*-ethyltoluene. Based on MDL, we removed *2*,*3*,*4*-trimethylpentane, *4*-

ethyltoluene since five of the six sites had MDL values > 60%. Ultimately, we included 40 VOC species in the PMF analysis.

A.5 Triggered whole air canister sample examples

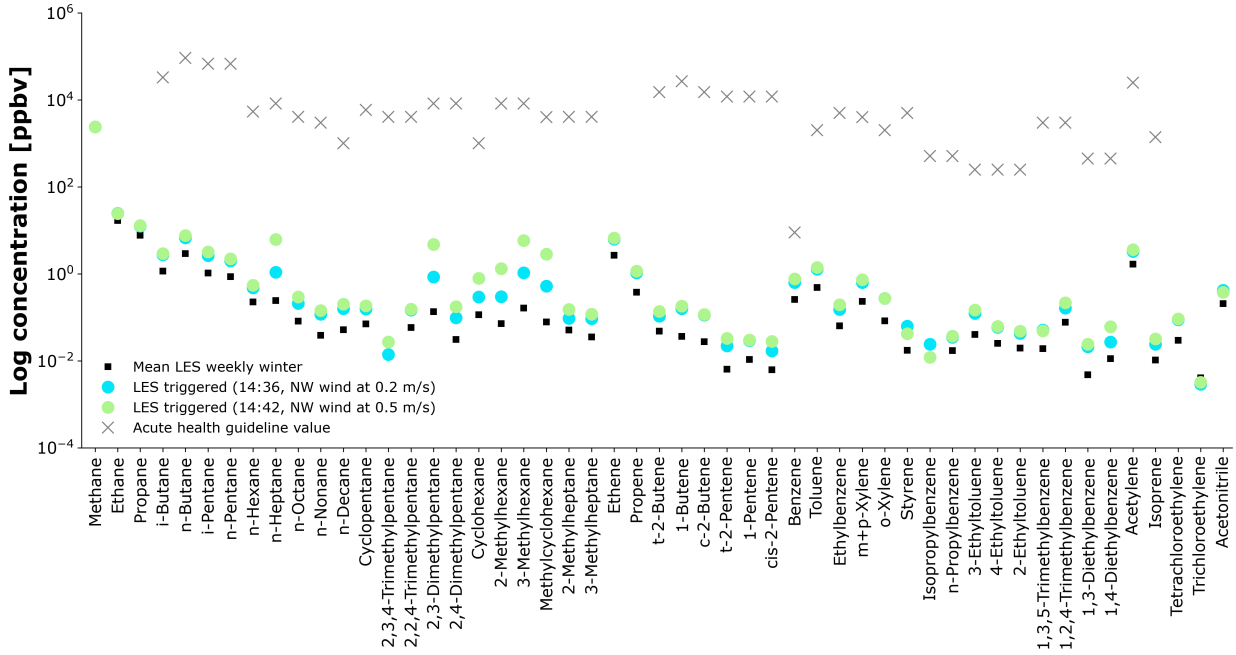

Figure A.5: CH_4 and NMVOC log concentrations [ppbv] from two triggered canister samples (blue and green circles) from Loveland Elementary School (LES) on 12/22/2024. The winter average weekly-integrated concentrations from LES (black squares) and noncarcinogenic chronic health guideline values (gray crosses; CDPHE, 2019) are included for reference.

Appendix B

Chapter 3

B.1 Average VOC concentrations by season and site

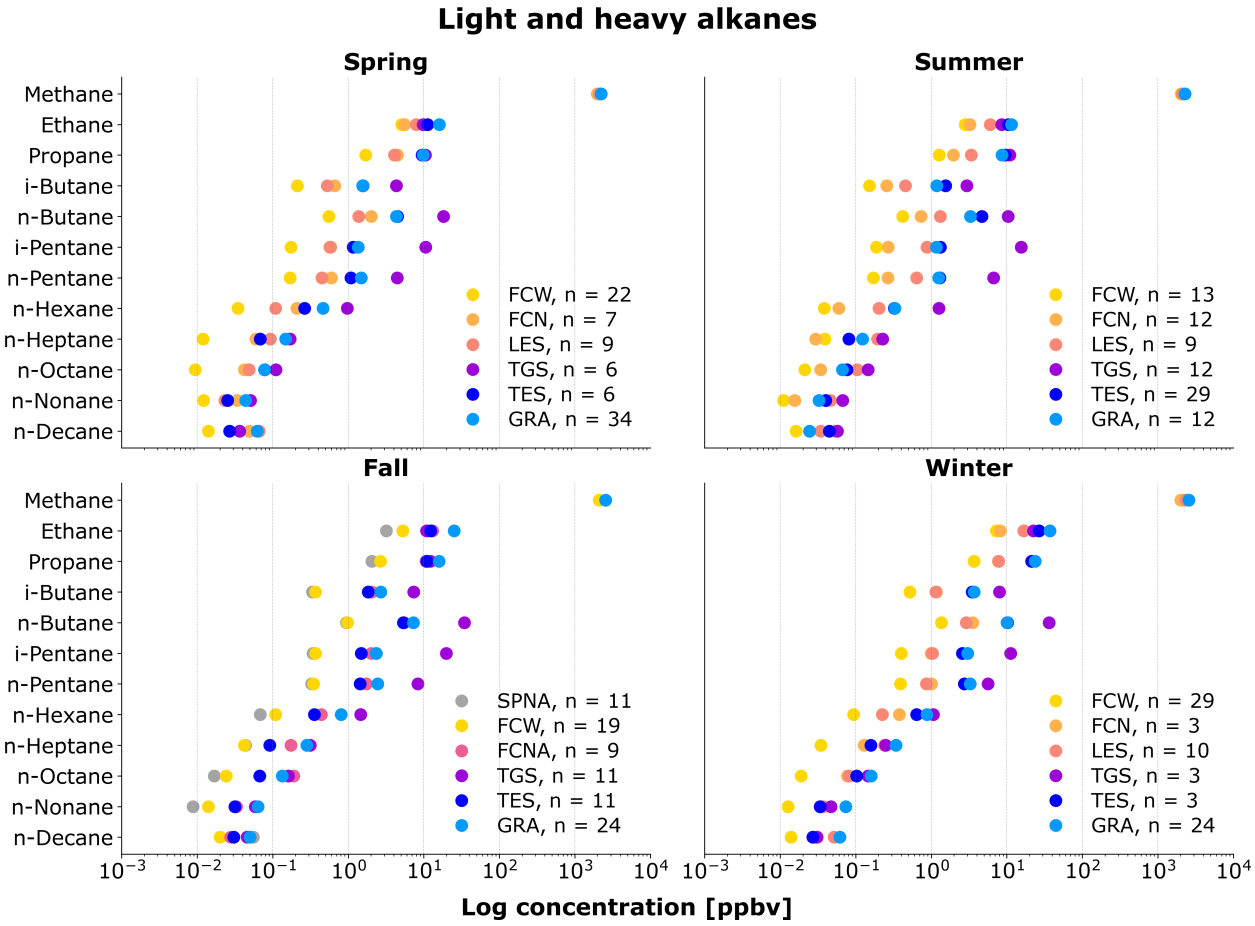

Figure B.1: Average log scale concentration [ppbv] of light and heavy alkanes by season Northern Colorado. Species concentrations below the detection limit are replaced with 1/2 of their MDL value. The site colors and name abbreviations correspond to the map in Figure 2.1. The samples collected in 2015-2016 were not analyzed for methane. Note, over 60% of the samples are below the MDL for: SPNA (fall *n*-nonane), FCW (spring *n*-heptane, *n*-octane, *n*-nonane, *n*-decane; summer *n*-decane; fall *n*-nonane, *n*-decane; winter *n*-nonane, *n*-decane), FCN (summer *n*-nonane; winter *n*-decane), and TES (summer *n*-nonane).

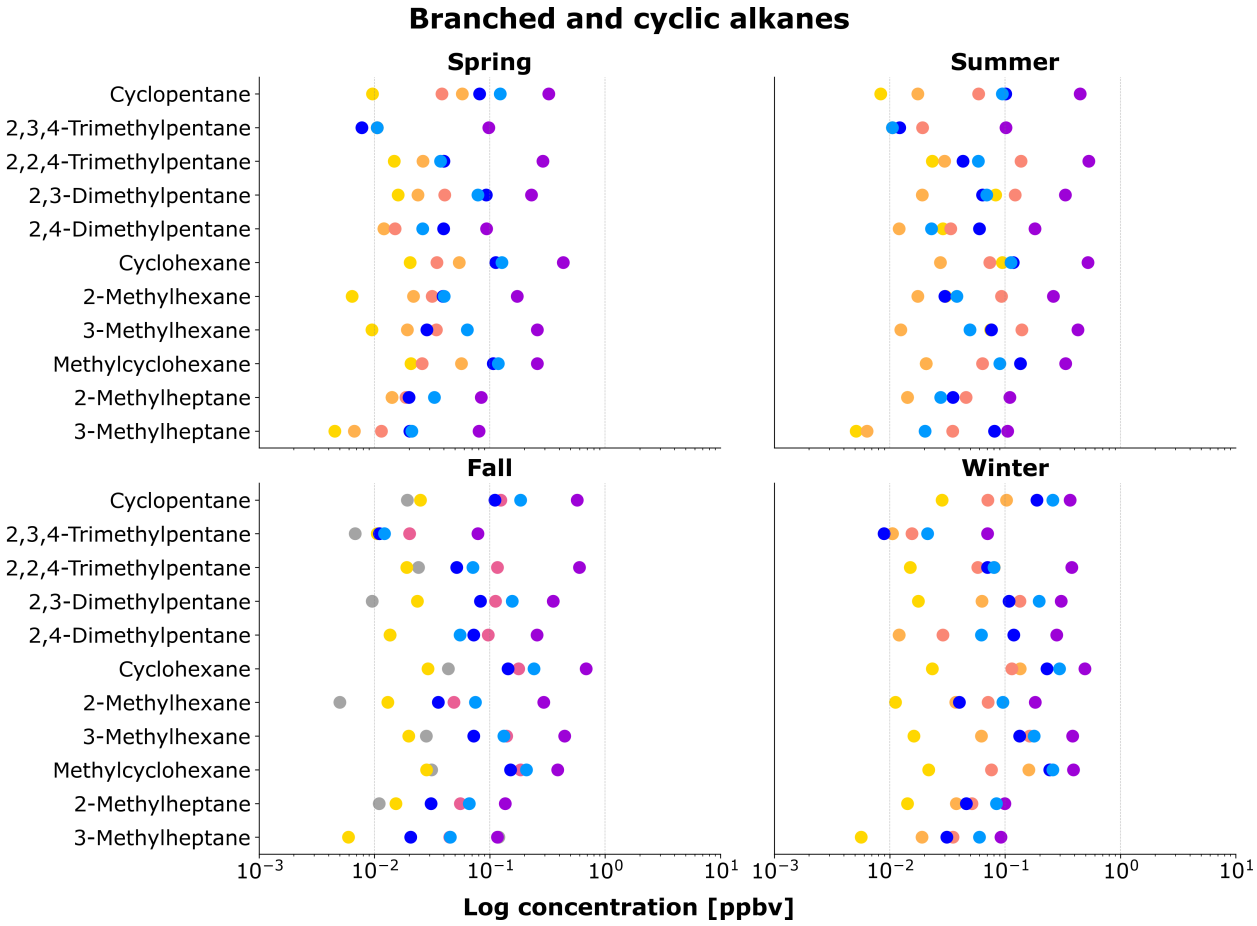

Figure B.2: Average log scale concentration [ppbv] of branched and cyclic alkanes by season Northern Colorado. Species concentrations below the detection limit are replaced with 1/2 of their MDL value. The site colors and name abbreviations correspond to the map in Figure 2.1. The number of samples for each site and season is found on Figure B.1. Over 60% of the samples are below the MDL for: SPNA (fall *2*,*3*,*4*-trimethylpentane, *2*,*2*,*4*-trimethylpentane, *2*,*3*-dimethylpentane, *2*-methylhexane, *3*-methylhexane, *2*-methylheptane), FCW (spring *2*,*3*,*4*-trimethylpentane, *2*,*2*,*4*-trimethylpentane, *2*,*3*-dimethylpentane, cyclohexane, *2*-methylhexane, *3*-methylhexane, methylcyclohexane, *2*-methylheptane, *3*-methylheptane; summer *2*,*3*,*4*-trimethylpentane, *2*,*3*-dimethylpentane, *2*,*4*-dimethylpentane, cyclohexane, *3*-methylhexane, methylcyclohexane, *2*-methylheptane, *3*-methylheptane; fall *2*,*3*,*4*-trimethylpentane, *2*,*3*-dimethylpentane, *2*,*4*-dimethylpentane, cyclohexane, methylcyclohexane, *2*-methylheptane, *3*-methylheptane; winter *2*,*3*,*4*-trimethylpentane, *2*,*2*,*4*-trimethylpentane, *2*,*3*-dimethylpentane, *2*,*4*-dimethylpentane, cyclohexane, *3*-methylhexane, methylcyclohexane, *2*-methylheptane, *3*-methylheptane), FCN (spring *2*,*3*,*4*-trimethylpentane, *2*,*3*-dimethylpentane, *3*-methylheptane; summer *2*,*3*,*4*-trimethylpentane, *2*,*3*-dimethylpentane, *2*,*4*-dimethylpentane, cyclohexane, *3*-methylhexane, methylcyclohexane, *2*-methylheptane, *3*-methylheptane; winter *2*,*3*,*4*-trimethylpentane, *2*,*4*-dimethylpentane), LES (spring *2*,*3*,*4*-trimethylpentane, *2*,*4*-dimethylpentane, methylcyclohexane, *2*-methylheptane; summer *2*,*3*,*4*-trimethylpentane; winter *2*,*3*,*4*-trimethylpentane), TGS (spring *2*,*2*,*4*-trimethylpentane), TES (spring *2*,*3*,*4*-trimethylpentane, *2*,*3*-dimethylpentane; summer *2*,*3*,*4*-trimethylpentane, *2*,*2*,*4*-trimethylpentane, cyclohexane, *2*-methylhexane, *2*-methylheptane, *3*-methylheptane; winter *2*,*3*,*4*-trimethylpentane), and GRA (spring *2*,*3*,*4*-trimethylpentane; fall *2*,*3*,*4*-trimethylpentane; summer *2*,*3*,*4*-trimethylpentane; winter *2*,*3*,*4*-trimethylpentane).

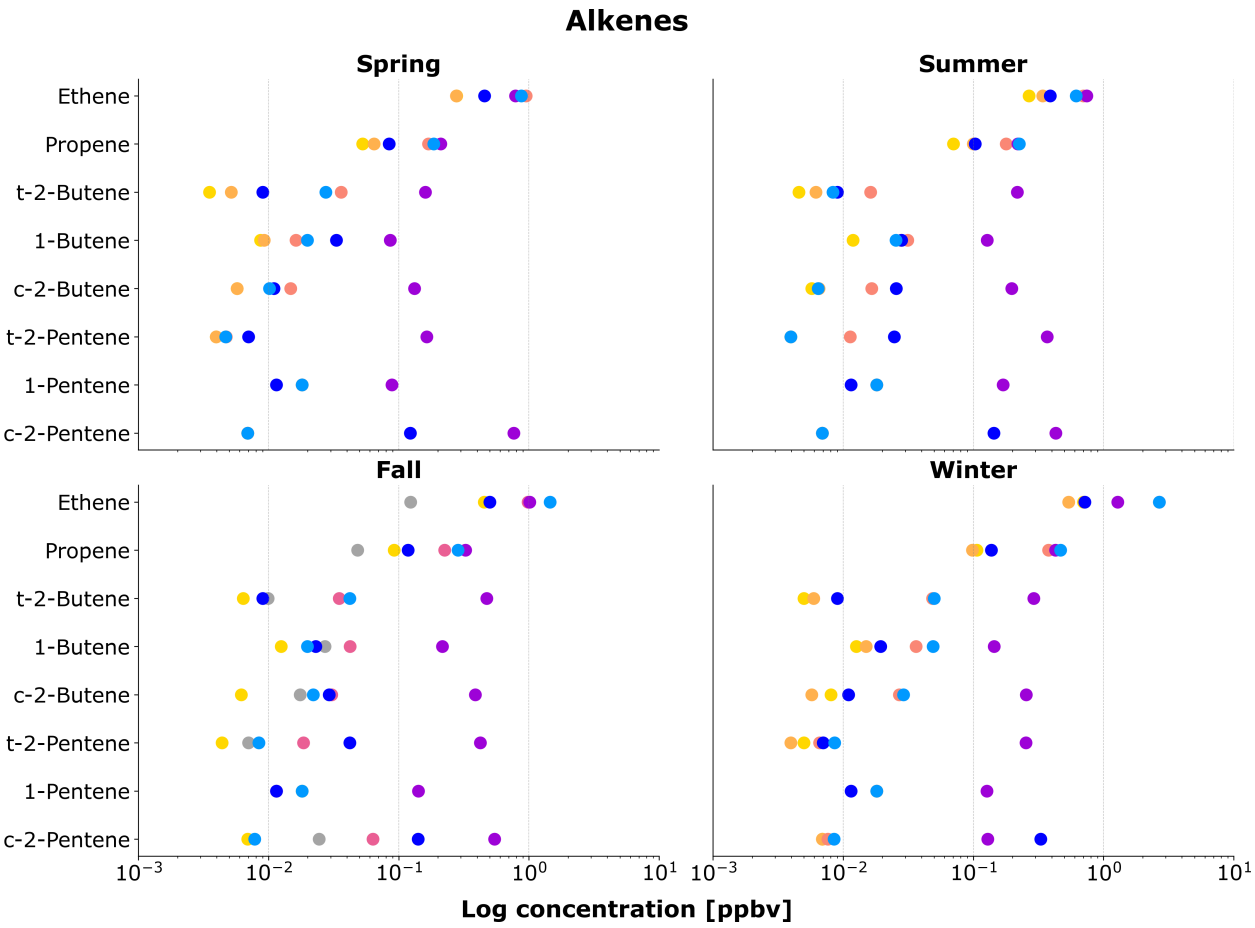

Figure B.3: Average log scale concentration [ppbv] of alkenes by season Northern Colorado. Species concentrations below the detection limit are replaced with 1/2 of their MDL value. The site colors and name abbreviations correspond to the map in Figure 2.1. The number of samples for each site and season is found on Figure B.1. Note, over 60% of the samples are below the MDL for: SPNA (fall *t*-2-butene, *c*-2-butene, *t*-2-pentene, *1*-pentene), FCW (spring *t*-2-butene, *1*-butene, *c*-2-butene, *t*-2-pentene, *1*-pentene, *c*-2-pentene; summer *t*-2-butene, *1*-butene, *c*-2-butene, *t*-2-pentene, *1*-pentene, *c*-2-pentene; fall *1*-butene, *t*-2-pentene, *1*-pentene, *c*-2-pentene; winter *1*-butene, *c*-2-butene, *c*-2-butene, *t*-2-pentene, *1*-pentene, *c*-2-pentene), FCN (spring *1*-butene, *c*-2-butene, *c*-2-butene, *t*-2-pentene, *1*-pentene, *c*-2-pentene; summer *c*-2-butene, *t*-2-pentene, *1*-pentene, *c*-2-pentene; winter *c*-2-butene, *t*-2-pentene, *1*-pentene, *c*-2-pentene), LES (spring *t*-2-pentene, *1*-pentene, *c*-2-pentene; summer *1*-pentene, *c*-2-pentene; winter *t*-2-pentene, *1*-pentene, *c*-2-pentene), FCNA (fall *1*-pentene), TES (spring *t*-2-butene, *c*-2-butene, *t*-2-pentene, *1*-pentene, *c*-2-pentene; summer *t*-2-butene, *c*-2-butene, *t*-2-pentene, *1*-pentene; fall *t*-2-butene, *1*-pentene; winter *t*-2-butene, *c*-2-butene, *t*-2-pentene, *1*-pentene), GRA (spring *c*-2-butene, *t*-2-pentene, *1*-pentene, *c*-2-pentene; summer *c*-2-butene, *t*-2-pentene, *1*-pentene, *c*-2-pentene; fall *t*-2-pentene, *1*-pentene, *c*-2-pentene; winter *1*-pentene, *c*-2-pentene).

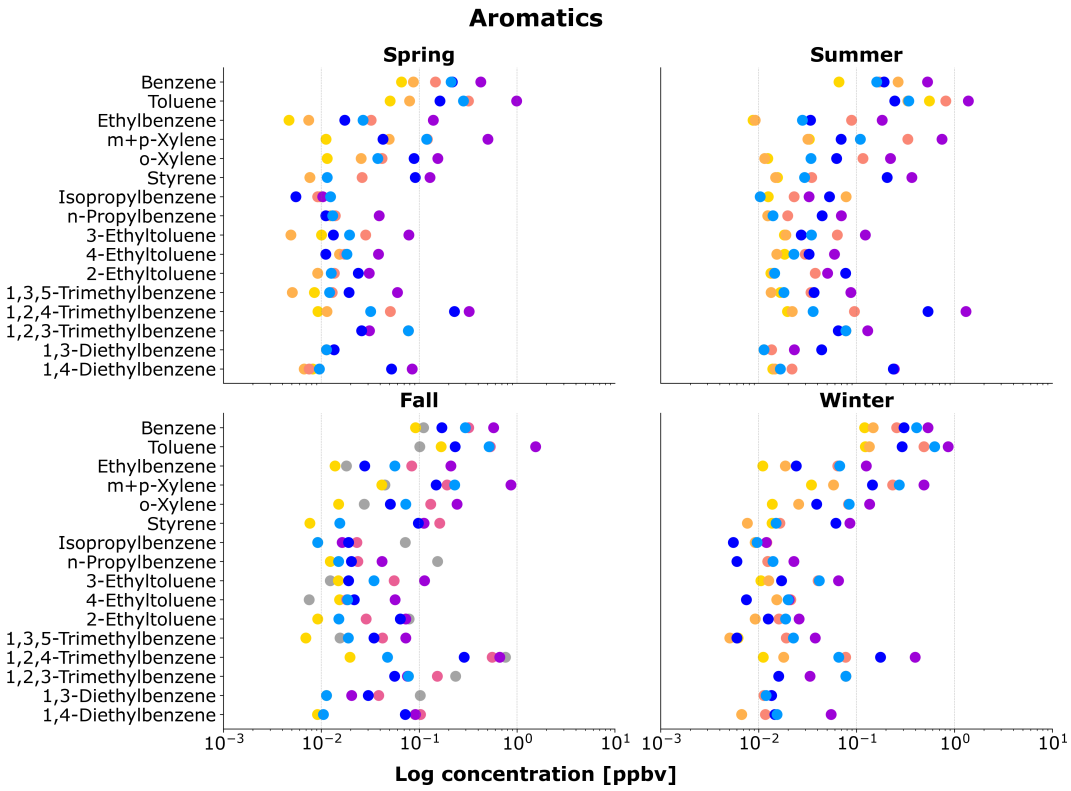

Figure B.4: Average log scale concentration [ppbv] of aromatics by season Northern Colorado. Species concentrations below the detection limit are replaced with 1/2 of their MDL value. The site colors and name abbreviations correspond to the map in Figure 2.1. The number of samples for each site and season is found on Figure B.1. Note, over 60% of the samples are below the MDL for: SPNA (fall ethylbenzene, *3*-ethyltoluene, *4*-ethyltoluene), FCW (spring ethylbenzene, *m+p*-xylene, *o*-xylene, styrene, isopropylbenzene, *n*-propylbenzene, *4*-ethyltoluene, *2*-ethyltoluene, *1*,*3*,*5*-trimethylbenzene, *1*,*2*,*3*-trimethylbenzene, *1*,*3*-diethylbenzene, *1*,*4*-diethylbenzene; summer ethylbenzene, *o*-xylene, isopropylbenzene, *n*-propylbenzene, *4*-ethyltoluene, *2*-ethyltoluene, *1*,*2*,*3*-trimethylbenzene, *1*,*3*-diethylbenzene; fall *o*-xylene, styrene, isopropylbenzene, *n*-propylbenzene, *4*-ethyltoluene, *2*-ethyltoluene, *1*,*3*,*5*-trimethylbenzene, *1*,*2*,*3*-trimethylbenzene, *1*,*3*-diethylbenzene, *1*,*4*-diethylbenzene; winter *o*-xylene, styrene, isopropylbenzene, *n*-propylbenzene, *4*-ethyltoluene, *2*-ethyltoluene, *1*,*3*,*5*-trimethylbenzene, *1*,*3*-diethylbenzene, *1*,*4*-diethylbenzene), FCN (spring ethylbenzene, *o*-xylene, styrene, isopropylbenzene, *n*-propylbenzene, *3*-ethyltoluene, *4*-ethyltoluene, *2*-ethyltoluene, *1*,*3*,*5*-trimethylbenzene, *1*,*2*,*3*-trimethylbenzene, *1*,*3*-diethylbenzene, *1*,*4*-diethylbenzene; summer *o*-xylene, *n*-propylbenzene, *4*-ethyltoluene, *2*-ethyltoluene, *1*,*2*,*3*-trimethylbenzene, *1*,*3*-diethylbenzene; winter styrene, isopropylbenzene, *n*-propylbenzene, *4*-ethyltoluene, *2*-ethyltoluene, *1*,*3*,*5*-trimethylbenzene, *1*,*2*,*3*-trimethylbenzene, *1*,*2*,*3*-trimethylbenzene, *1*,*3*-diethylbenzene, *1*,*4*-diethylbenzene), LES (spring isopropylbenzene, *n*-propylbenzene, *4*-ethyltoluene, *2*-ethyltoluene, *1*,*2*,*3*-trimethylbenzene, *1*,*3*-diethylbenzene, *1*,*4*-diethylbenzene; summer *1*,*2*,*3*-trimethylbenzene, *1*,*3*-diethylbenzene; winter isopropylbenzene, *n*-propylbenzene, *4*-ethyltoluene, *1*,*2*,*3*-trimethylbenzene, *1*,*3*-diethylbenzene), TGS (spring *1*,*3*-diethylbenzene; fall *1*,*3*-diethylbenzene; winter *1*,*3*-diethylbenzene), TES (spring ethylbenzene, isopropylbenzene, *n*-propylbenzene, *n*-propylbenzene, *3*-ethyltoluene, *4*-ethyltoluene, *1*,*3*,*5*-trimethylbenzene, *1*,*3*-diethylbenzene; summer isopropylbenzene, *n*-propylbenzene, *3*-ethyltoluene, *4*-ethyltoluene, *2*-ethyltoluene, *1*,*3*,*5*-trimethylbenzene, *1*,*2*,*3*-trimethylbenzene, *1*,*3*-diethylbenzene; fall isopropylbenzene, isopropylbenzene, *4*-ethyltoluene, *2*-ethyltoluene, *1*,*3*-diethylbenzene; winter isopropylbenzene, *n*-propylbenzene, *4*-ethyltoluene, *2*-ethyltoluene, *1*,*3*,*5*-trimethylbenzene, *1*,*2*,*3*-trimethylbenzene, *1*,*3*-diethylbenzene), GRA (spring styrene, isopropylbenzene, *2*-ethyltoluene; summer isopropylbenzene, *n*-propylbenzene, *4*-ethyltoluene, *4*-ethyltoluene, *1*,*2*,*3*-trimethylbenzene, *1*,*2*,*3*-trimethylbenzene, *1*,*3*-diethylbenzene, *1*,*3*-diethylbenzene, *1*,*4*-diethylbenzene; fall isopropylbenzene, *n*-propylbenzene, *4*-ethyltoluene, *2*-ethyltoluene, *1*,*2*,*3*-trimethylbenzene, *1*,*3*-diethylbenzene, *1*,*4*-diethylbenzene; winter styrene, isopropylbenzene, *n*-propylbenzene, *4*-ethyltoluene, *1*,*2*,*3*-trimethylbenzene, *1*,*3*-diethylbenzene).

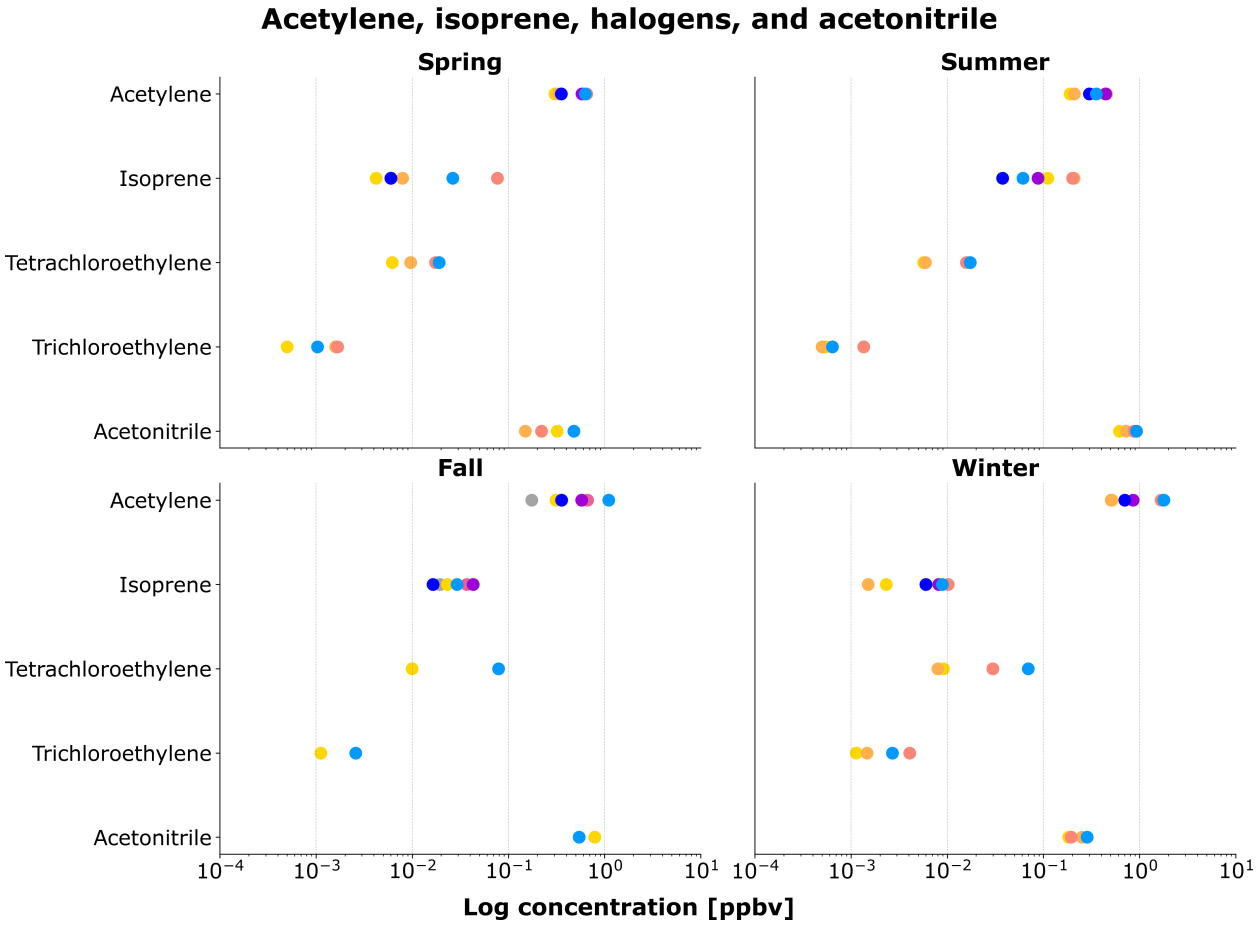

Figure B.5: Average log scale concentration [ppbv] of acetylene, isoprene, halogens, and acetonitrile by season Northern Colorado. Species concentrations below the detection limit are replaced with 1/2 of their MDL value. The site colors and name abbreviations correspond to the map in Figure 2.1. The samples collected in 2015-2016 were not analyzed for methane, tetrachloroethylene, trichloroethylene, or acetonitrile. The number of samples for each site and season is found on Figure B.1. Note, over 60% of the samples are below the MDL for: FCW (spring isoprene, trichloroethylene; summer trichloroethylene; fall trichloroethylene; winter isoprene, acetonitrile), FCN (spring isoprene, acetonitrile; summer trichloroethylene; winter isoprene), FCNA (fall isoprene), TGS (spring isoprene; winter isoprene), TES (spring isoprene; winter isoprene).

Table B.1: Seasonal mean and standard deviation concentration [ppbv] for 11 NMVOCs collected at various locations in Northern Colorado.

Species	FCW	FCN	LES	FCNA	SPNA	TGS	TES	GRA
Winter								
Ethane	7.3 ± 2.4	8.2 ± 1.4	16.8 ± 4.0	–	–	22.5 ± 11.4	26.8 ± 14.3	37.3 ± 12.4
Propane	3.7 ± 1.5	7.7 ± 1.1	7.8 ± 1.8	–	–	21.3 ± 8.9	21.3 ± 10.6	23.8 ± 8.0
i-Butane	0.5 ± 0.2	1.2 ± 0.1	1.2 ± 0.3	–	–	8.0 ± 2.7	3.5 ± 1.9	3.7 ± 1.3
n-Butane	1.4 ± 0.6	3.5 ± 0.4	2.9 ± 0.7	–	–	36.4 ± 9.3	10.3 ± 5.6	10.1 ± 3.8
i-Pentane	0.4 ± 0.1	1.0 ± 0.1	1.0 ± 0.3	–	–	11.2 ± 2.4	2.6 ± 1.5	3.0 ± 1.2
n-Pentane	0.4 ± 0.2	1.0 ± 0.1	0.9 ± 0.2	–	–	5.7 ± 2.0	2.7 ± 1.8	3.3 ± 1.3
n-Hexane	0.09 ± 0.04	0.38 ± 0.03	0.22 ± 0.07	–	–	1.06 ± 0.39	0.64 ± 0.40	0.87 ± 0.47
Benzene	0.12 ± 0.03	0.15 ± 0.03	0.26 ± 0.07	–	–	0.54 ± 0.13	0.30 ± 0.13	0.41 ± 0.14
Toluene	0.12 ± 0.08	0.14 ± 0.02	0.49 ± 0.24	–	–	0.86 ± 0.06	0.29 ± 0.13	0.63 ± 0.2
Acetylene	0.52 ± 0.11	0.50 ± 0.04	1.67 ± 0.47	–	–	0.85 ± 0.26	0.70 ± 0.32	1.79 ± 0.60
Spring								
Ethane	5.1 ± 1.6	5.5 ± 1.5	8.0 ± 2.8	–	–	9.8 ± 1.1	11.2 ± 2.2	16.0 ± 7.0
Propane	1.7 ± 0.5	4.5 ± 1.9	4.1 ± 0.8	–	–	10.5 ± 1.4	9.5 ± 1.7	9.8 ± 4.6
i-Butane	0.2 ± 0.1	0.7 ± 0.3	0.5 ± 0.2	–	–	4.3 ± 0.5	1.6 ± 2.6	1.6 ± 0.8
n-Butane	0.6 ± 0.2	2.0 ± 1.0	1.4 ± 0.4	–	–	18.2 ± 2.2	4.5 ± 0.8	4.3 ± 2.2
i-Pentane	0.2 ± 0.1	0.6 ± 0.3	0.6 ± 0.2	–	–	10.6 ± 3.5	1.2 ± 0.2	1.4 ± 0.7
n-Pentane	0.2 ± 0.1	0.6 ± 0.3	0.4 ± 0.1	–	–	4.4 ± 1.8	1.1 ± 0.1	1.5 ± 0.7
n-Hexane	0.03 ± 0.02	0.21 ± 0.04	0.11 ± 0.03	–	–	0.97 ± 0.34	0.26 ± 0.04	0.46 ± 0.27
Benzene	0.07 ± 0.02	0.09 ± 0.02	0.15 ± 0.04	–	–	0.43 ± 0.08	0.22 ± 0.10	0.21 ± 0.08
Toluene	0.05 ± 0.02	0.08 ± 0.04	0.32 ± 0.11	–	–	0.99 ± 0.24	0.16 ± 0.03	0.28 ± 0.13
Acetylene	0.30 ± 0.07	0.33 ± 0.06	0.65 ± 0.29	–	–	0.58 ± 0.22	0.35 ± 0.10	0.63 ± 0.29
Summer								
Ethane	2.8 ± 0.7	3.2 ± 1.2	6.0 ± 1.1	–	–	8.6 ± 1.4	10.5 ± 2.2	11.5 ± 3.0
Propane	1.3 ± 0.4	2.0 ± 0.5	3.4 ± 0.4	–	–	10.9 ± 2.5	9.5 ± 2.8	8.7 ± 4.3
i-Butane	0.2 ± 0.05	0.3 ± 0.1	0.5 ± 0.0	–	–	2.9 ± 0.6	1.6 ± 0.5	1.2 ± 0.4
n-Butane	0.4 ± 0.1	0.7 ± 0.2	1.3 ± 0.2	–	–	10.4 ± 2.0	4.7 ± 1.5	3.3 ± 1.0
i-Pentane	0.2 ± 0.04	0.3 ± 0.1	0.9 ± 0.2	–	–	15.5 ± 2.9	1.3 ± 0.4	1.2 ± 0.4
n-Pentane	0.2 ± 0.04	0.3 ± 0.1	0.6 ± 0.1	–	–	6.7 ± 1.1	1.3 ± 0.5	1.3 ± 0.4
n-Hexane	0.04 ± 0.01	0.06 ± 0.02	0.20 ± 0.05	–	–	1.27 ± 0.24	0.32 ± 0.10	0.33 ± 0.12
Benzene	0.07 ± 0.03	0.27 ± 0.17	0.17 ± 0.05	–	–	0.53 ± 0.13	0.19 ± 0.07	0.16 ± 0.05
Toluene	0.56 ± 1.24	0.33 ± 0.15	0.82 ± 0.43	–	–	1.38 ± 0.38	0.25 ± 0.08	0.34 ± 0.13
Acetylene	0.19 ± 0.05	0.21 ± 0.06	0.45 ± 0.09	–	–	0.44 ± 0.11	0.30 ± 0.14	0.35 ± 0.14
Fall								
Ethane	5.3 ± 3.2	–	–	13.1 ± 3.2	3.2 ± 0.9	10.8 ± 3.8	12.3 ± 4.9	25.3 ± 9.0
Propane	2.7 ± 2.2	–	–	10.1 ± 2.6	2.0 ± 0.7	12.2 ± 3.4	11.0 ± 5.0	15.9 ± 6.0
i-Butane	0.4 ± 0.4	–	–	2.1 ± 0.5	0.3 ± 0.1	7.4 ± 3.1	1.8 ± 0.9	2.7 ± 1.1
n-Butane	1.0 ± 1.0	–	–	5.5 ± 1.6	0.9 ± 0.3	34.6 ± 18.2	5.4 ± 2.6	7.3 ± 3.0
i-Pentane	0.4 ± 0.3	–	–	2.0 ± 0.7	0.3 ± 0.1	18.9 ± 3.2	1.5 ± 0.6	2.3 ± 0.9
n-Pentane	0.3 ± 0.4	–	–	1.7 ± 0.5	0.3 ± 0.1	8.3 ± 1.7	1.4 ± 0.8	2.4 ± 0.9
n-Hexane	0.11 ± 0.14	–	–	0.44 ± 0.11	0.07 ± 0.02	1.46 ± 0.33	0.36 ± 0.15	0.80 ± 0.34
Benzene	0.09 ± 0.03	–	–	0.32 ± 0.07	0.11 ± 0.07	0.58 ± 0.09	0.17 ± 0.05	0.30 ± 0.12
Toluene	0.17 ± 0.08	–	–	0.53 ± 0.10	0.10 ± 0.05	1.54 ± 0.41	0.23 ± 0.04	0.52 ± 0.18
Acetylene	0.31 ± 0.11	–	–	0.66 ± 0.37	0.18 ± 0.05	0.58 ± 0.15	0.36 ± 0.14	1.10 ± 0.73

B.2 Potential smoke impact from biomass burning

Leveraging three metrics for smoke detection, we briefly explore the potential influence of biomass burning smoke in the weekly-integrated canister samples. The whole air canister samples from the 2022-2025 sampling period (FCW, FCN, LES, and GRA) include acetonitrile measurements. As mentioned in Section 3.1, enhancement of acetonitrile can be utilized as a tracer for biomass burning emissions even in urban environments where there are other confounding emission sources (Huangfu et al., 2021). Additionally, we briefly examine potential smoke impact using the NOAA OSPO Hazard Mapping System (HMS) for real-time satellite analysis of smoke, fire, and dust as well as 1-hr averaged surface $PM_{2.5}$ concentration data from CDPHE monitors in Fort Collins (Site 9, Fort Collins - CSU - Edison) [40.571288°N, -105.079693°W] and Greeley (Site 6, Greeley - Hospital) [40.414877°N, -104.70693°W]. However, we note that this discussion is limited due to the small number of canister samples.

Figure B.6 illustrates the distribution of weekly-averaged concentrations of acetonitrile for each month at FCW and GRA. The outlier total NMVOC concentration highlighted in Figure 3.1 from the FCW canisters is the sample from 9/28/2023 to 10/5/2023. This sample contained 0.4 ppbv of acetonitrile. It had one day of light smoke identified by HMS and the week included 1-hr averaged $PM_{2.5}$ concentrations up to 14 $\mu g/m^3$. The i/n-pentane ratio was 1.11. The sample collected the week before had 1.75 ppbv of acetonitrile, one day of light smoke identified by HMS, and the week included 1-hr averaged $PM_{2.5}$ concentrations up to 16 $\mu g/m^3$. The enhancement of ethane, benzene, n-hexane, and isoprene is consistent with the most abundant VOCs identified in other studies (Chen et al., 2017; Permar et al., 2021). Further analysis could look at surface $PM_{2.5}$ concentration and other data from the EPA trailer in Chrisman Field as well as wind direction and other meteorological variables.

The outlier isoprene concentration highlighted in Figure 3.1 from GRA canisters is the sample from 4/4/2024 to 4/11/2024. This sample contained 2.83 ppbv of acetonitrile, which is the largest concentration collected in the GRA samples. HMS did not identify smoke plumes for this sample period and location. The sample included 1-hr averaged PM2.5 concentrations up to 12.5 $\mu g/m^3$

and the i/n-pentane ratio was 0.87. Previous studies indicate that air impacted by biomass burning may have low i/n-pentane ratios (Kumar et al., 2020; Rossabi and Detlev, 2018). We postulate that higher acetonitrile concentrations and variance in samples from GRA during the spring might be correlated with concurrent increases in agriculture or irrigation ditch burning activity in the surrounding area of Greeley.

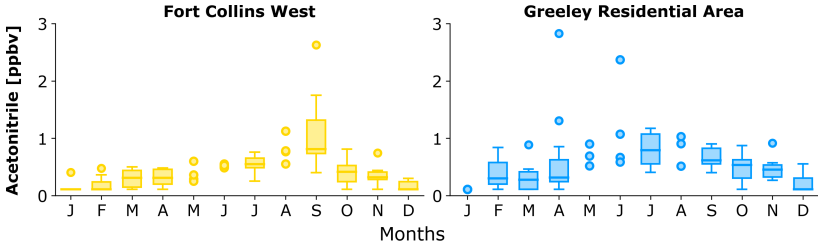

Figure B.6: Distribution of weekly-averaged concentrations [ppbv] of acetonitrile by month at two sites in Northern Colorado. Box and whisker plots show the median value (box middle), first quartile (box bottom), third quartile (box top), and range (whiskers for data within 1.5 times the interquartile range) including outliers (scatter points for data beyond 1.5 times the interquartile range) for months with n = 5 or greater samples. Individual data points are plotted for months with less than n = 5 samples. Measurements below species detection limits are replaced with 1/2 of their MDL value.

B.3 Estimated health quotients for ambient canister samples

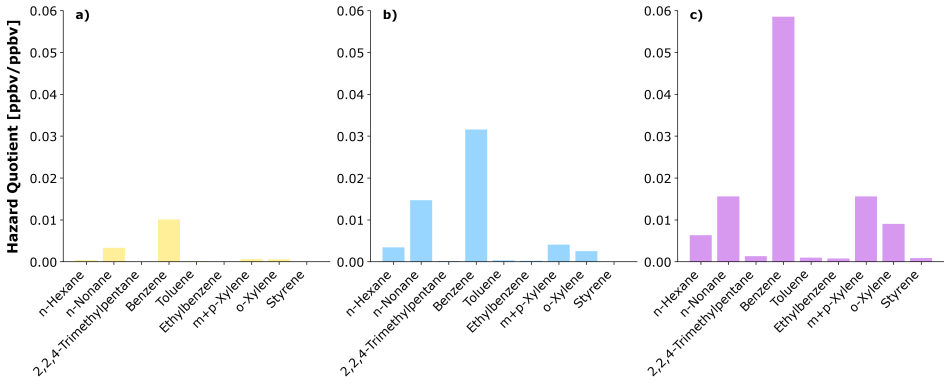

Figure B.7: Estimated health quotients (HQ) [ppbv/ppbv] for HAP compounds at (a) Fort Collins West (yellow), (b) Greeley Residential Area (blue), and (c) Timnath Gas Station (purple). The HQ is calculated as the annual-average weekly concentration divided by the appropriate noncarcinogenic chronic health guideline value for each compound. We use the chronic health guideline value outlined by the Colorado Department of Public Health and Environment (CDPHE, 2019). The HQ equation used for the calculation is from the Agency for Toxic Substances and Disease Registry (ATSDR, 2025).

B.4 Average *i*/*n*-pentane ratios for all sites by season

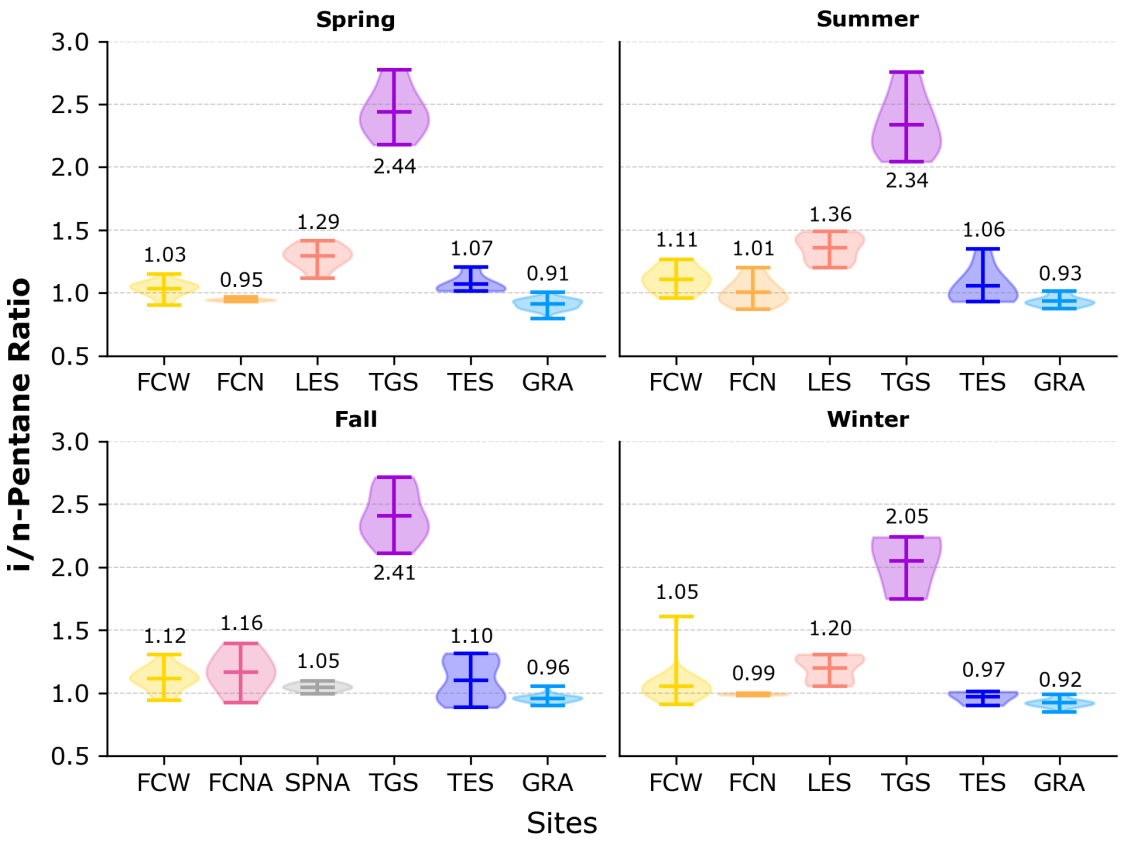

Figure B.8: Distribution of *i*/*n*-pentane [ppbv/ppbv] in Northern Colorado by season. Violin plots show the maximum, mean, and minimum values represented by the three colored lines. The mean ratios are printed above the violin plots. The site colors and name abbreviations correspond to the map in Figure 2.1. The number of samples for each site and season is found on Figure B.1.

B.5 PMF analysis source apportionment supporting materials

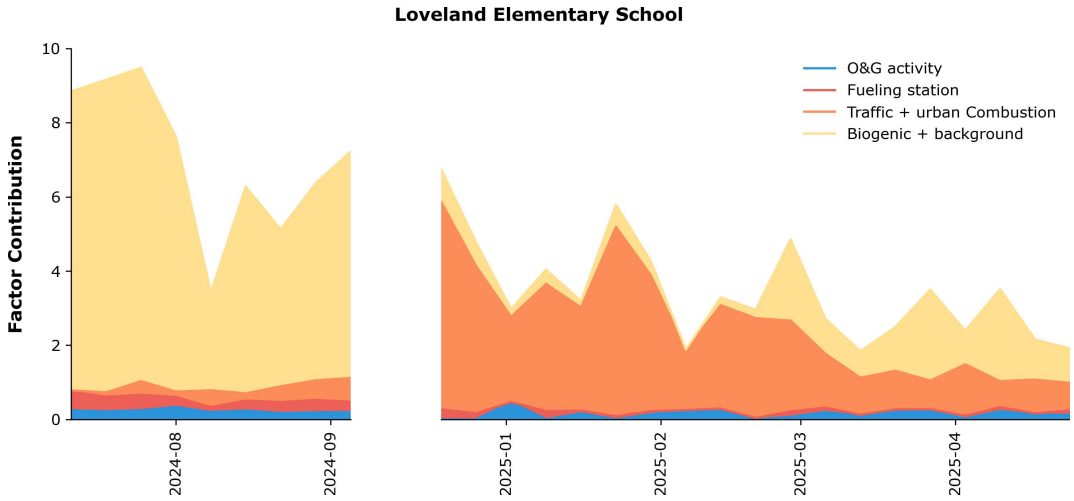

Figure B.9: Time series of four-factor PMF contributions at Loveland Elementary School. The factor source profiles are on Figure 3.5.

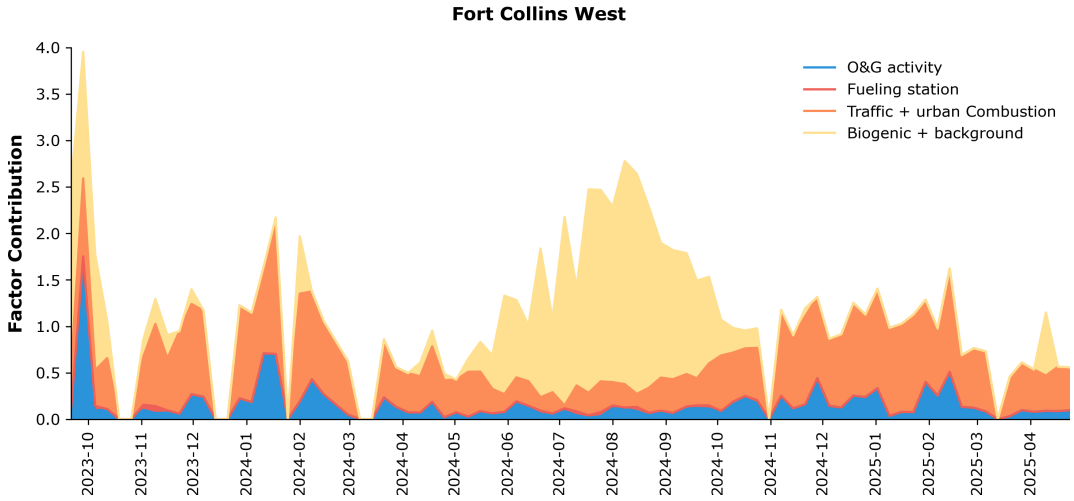

Figure B.10: Time series of four-factor PMF contributions at Fort Collins West. The factor source profiles are on Figure 3.5.

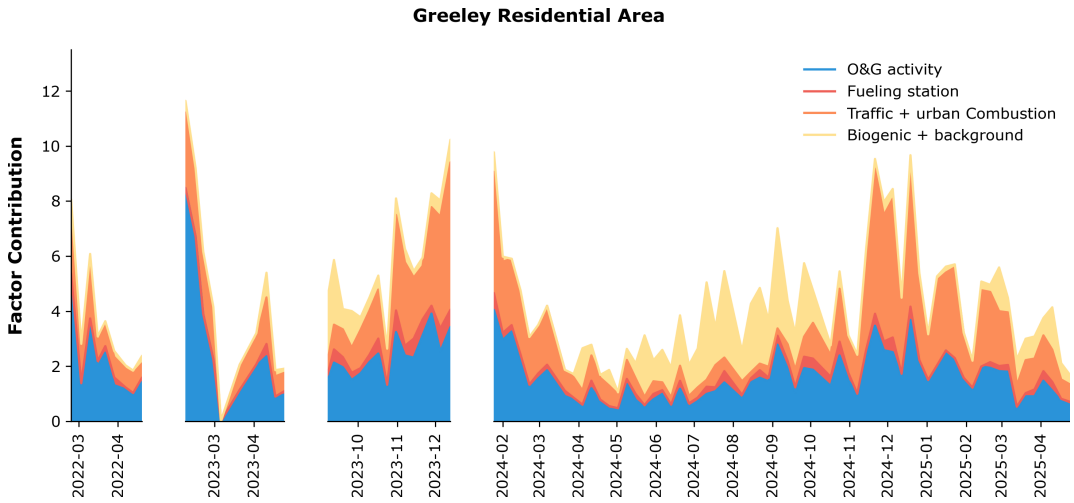

Figure B.11: Time series of four-factor PMF contributions at Greeley Residential Area. The factor source profiles are on Figure 3.5.

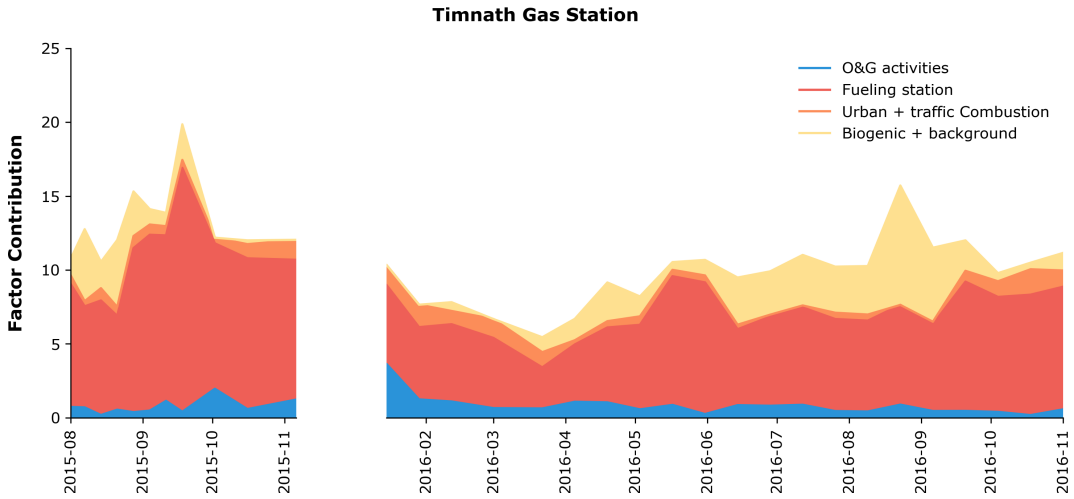

Figure B.12: Time series of four-factor PMF contributions at Timnath Gas Station. The factor source profiles are on Figure 3.5.

Table B.2: Average percentage contributions of sources from four-factor PMF analysis.

Species	FCW	LES	TGS	TES	GRA	SPNA
O&G Activity						
Ethane	28	10	58	89	62	59
Propane	45	19	46	94	77	73
i-Butane	51	23	23	92	79	76
n-Butane	55	24	19	92	80	76
i-Pentane	42	12	4	71	62	48
n-Pentane	52	20	11	86	76	66
n-Hexane	52	20	15	88	79	66
Benzene	19	6	12	72	49	35
Toluene	11	3	5	48	35	16
Acetylene	6	2	18	58	22	19
Total NMVOC	34	13	25	89	67	61
Urban + Traffic Combustion						
Ethane	68	81	35	8	36	32
Propane	52	72	13	4	22	19
i-Butane	48	69	5	3	18	16
n-Butane	45	64	4	3	16	14
i-Pentane	54	51	1	3	19	14
n-Pentane	44	54	2	3	15	12
n-Hexane	41	51	3	3	15	12
Benzene	67	64	11	10	42	28
Toluene	56	43	6	9	43	18
Acetylene	88	88	63	31	75	61
Total NMVOC	61	73	11	6	29	25
Fueling Station						
Ethane	0	0	0	0	0	0
Propane	0.1	2	38	1	1	2
i-Butane	0.3	8	72	4	3	8
n-Butane	0.4	11	78	6	4	10
i-Pentane	2	33	95	25	18	36
n-Pentane	1	18	87	10	8	17
n-Hexane	0.5	12	80	7	5	11
Benzene	0.2	4	69	6	3	6
Toluene	0.3	4	76	11	7	8
Acetylene	0	0.1	5	0.2	0.1	0.2
Total NMVOC	0.2	4	62	3	2	5
Biogenic + Background						
Ethane	4	9	7	3	1	9
Propane	3	8	3	1	1	6
i-Butane	0.2	0.4	0.1	0.1	0	0.3
n-Butane	0	0	0	0	0	0
i-Pentane	2	3	0.2	1	0.4	2
n-Pentane	3	8	1	1	1	5
n-Hexane	7	18	2	3	2	11
Benzene	15	27	8	12	5	31
Toluene	34	50	13	32	16	58
Acetylene	5	10	14	11	3	19
Total NMVOC	5	11	3	2	1	10

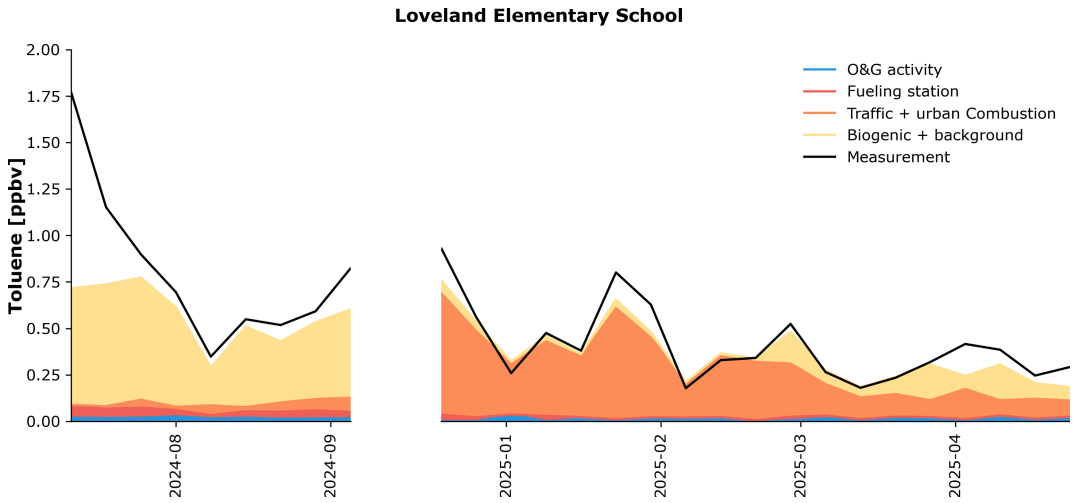

Figure B.13: Time series of reconstructed toluene concentrations [ppbv] at Loveland Elementary School from four-factor PMF analysis. The factor source profiles are on Figure 3.5 and the ambient toluene measurement from canister samples (black line) is included.

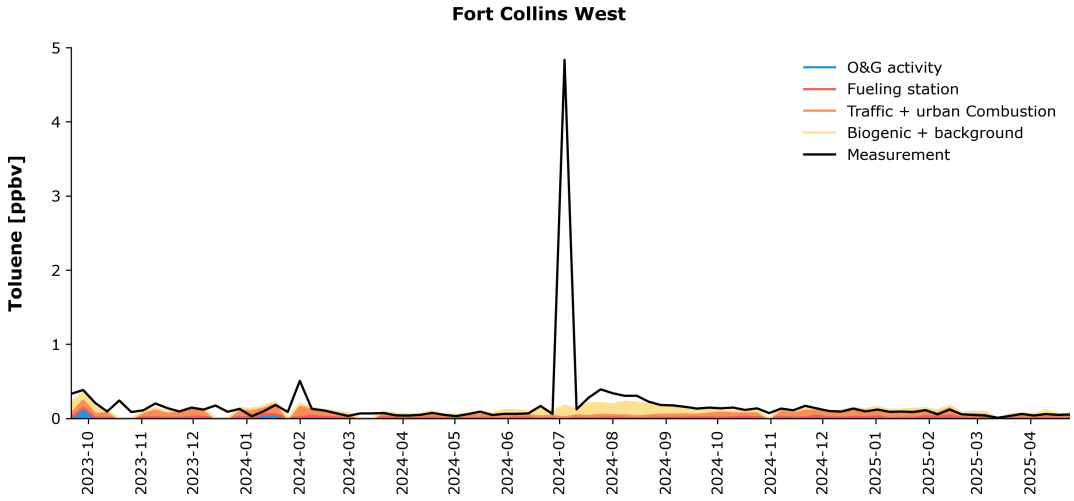

Figure B.14: Time series of reconstructed toluene concentrations [ppbv] at Fort Collins West from four-factor PMF analysis. The factor source profiles are on Figure 3.5 and the ambient toluene measurement from canister samples (black line) is included.

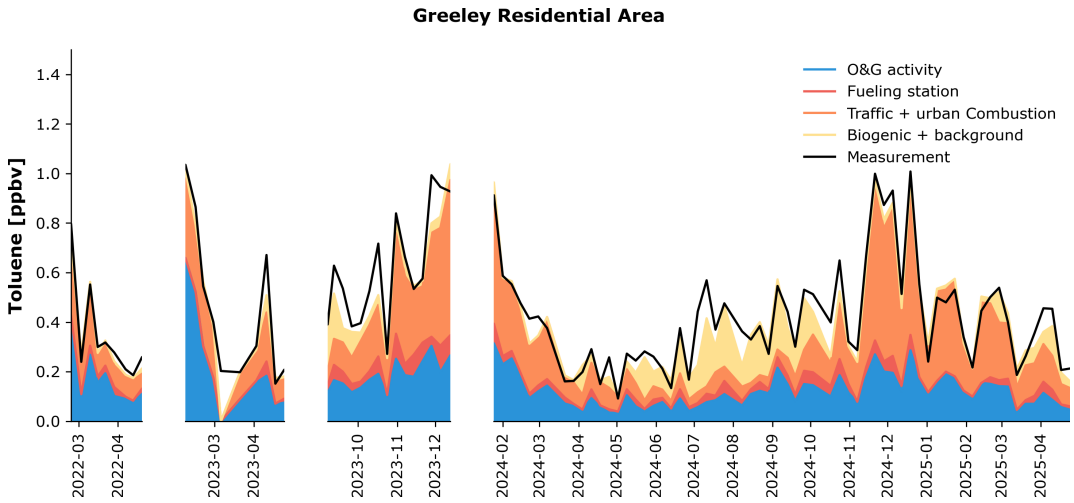

Figure B.15: Time series of reconstructed toluene concentrations [ppbv] at Greeley Residential Area from four-factor PMF analysis. The factor source profiles are on Figure 3.5 and the ambient toluene measurement from canister samples (black line) is included.

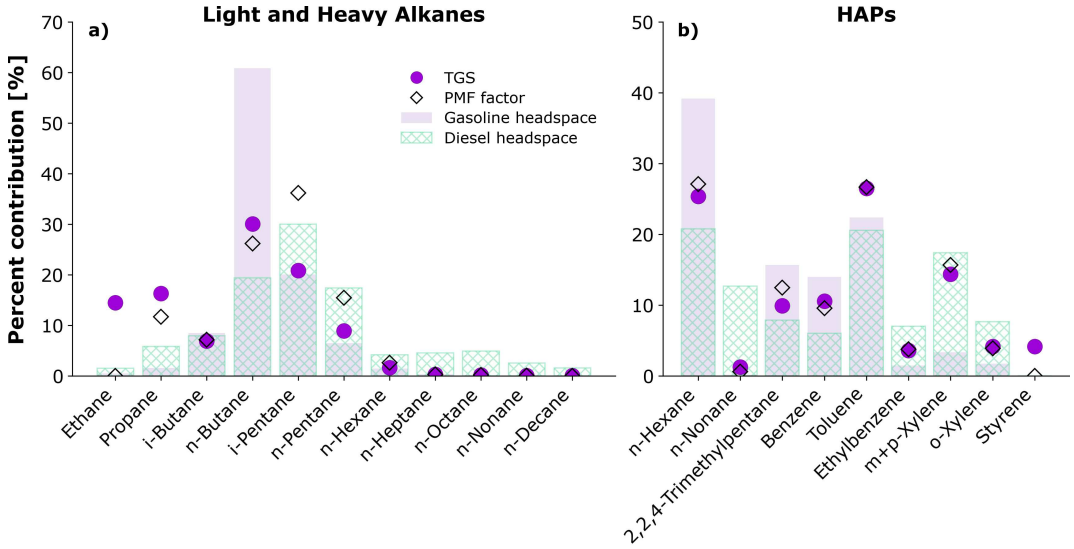

Figure B.16: Percent contributions [%] of average **(a)** light and heavy alkanes and **(b)** HAP compounds at three sites in Northern Colorado and in fuel headspace samples and four-factor PMF analysis. The colored circles represent the annual-average contributions for ambient concentrations from Timnath Gas Station (TGS; purple). The bar plot shows the average contributions of two gasoline (light purple) and diesel (light green) headspace samples. The modeled concentrations from four-factor PMF analysis (black diamonds) are also represented. Due to the influence of temporal trends, we exclude styrene from PMF analysis (Section A.4.3). We do not include tetrachloroethylene, trichloroethylene, and acetonitrile in the HAPs analysis as we did not measure them in the TGS samples.

Appendix C

Chapter 4

C.1 Galeton blowout in-plume canister sample

Table C.1: Concentrations of CH_4 [ppmv] and all 51 measured NMVOC [ppbv] from the in-plume canister sample from April 8, 2025 (Canister 1; Table 4.1).

Species	MDL
Methane	13.9
Ethane	2670
Propane	1420
i-Butane	239
n-Butane	693
i-Pentane	225
n-Pentane	371
n-Hexane	185
n-Heptane	152
n-Octane	107
n-Nonane	68.6
n-Decane	47.9
Cyclopentane	29.2
Cyclohexane	70.7
Methylcyclohexane	138
2,*3*,*4*-Trimethylpentane	1.35
2,*2*,*4*-Trimethylpentane	1.06
2,*3*-Dimethylpentane	41.9
2,*4*-Dimethylpentane	15.1
2-Methylhexane	16.0
3-Methylhexane	55.4
2-Methylheptane	54.9
3-Methylheptane	30.5
Ethene	0.09
Propene	0.03
t-2-Butene	0.002
1-Butene	0.001
c-2-Butene	0.03
t-2-Pentene	0

Table C.2: Concentrations of CH_4 [ppmv] and all 51 measured NMVOC [ppbv] from the in-plume canister sample from April 8, 2025 (Canister 1; Table 4.1) continued.

Species	MDL
1-Pentene	0.01
c-2-Pentene	0.002
Benzene	35.5
Toluene	90.9
Ethylbenzene	17.8
m+*p*-Xylene	98.1
o-Xylene	35.7
Styrene	0.02
Isopropylbenzene	2.6
n-Propylbenzene	6.0
3-Ethyltoluene	14.8
4-Ethyltoluene	6.0
2-Ethyltoluene	4.5
1,*3*,*5*-Trimethylbenzene	8.4
1,*2*,*4*-Trimethylbenzene	25.3
1,*2*,*3*-Trimethylbenzene	7.3
1,*3*-Diethylbenzene	1.0
1,*4*-Diethylbenzene	7.2
Acetylene	0.1
Isoprene	0.03
Tetrachloroethylene	0
Trichloroethylene	0
Acetonitrile	0

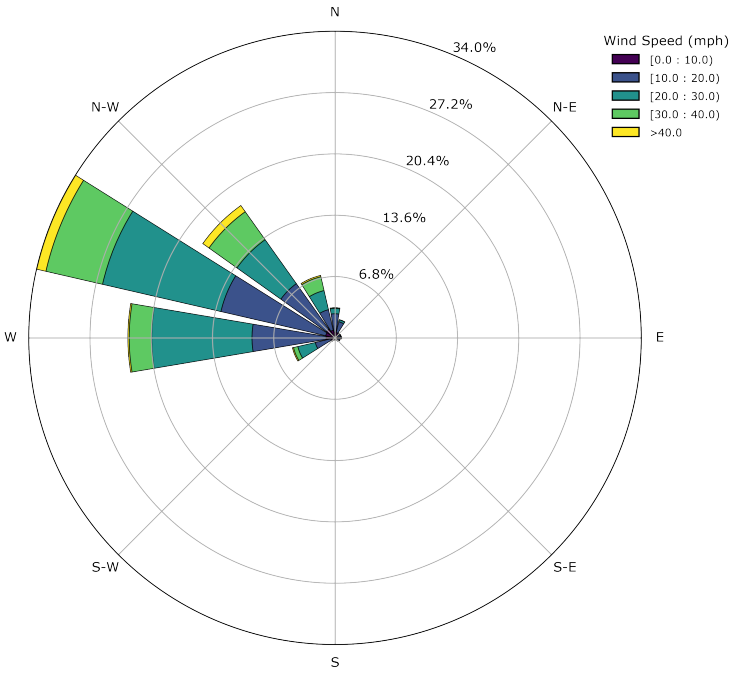

Figure C.1: Windrose showing wind speed and direction measured by the NIST mobile laboratory during the blowout in Galeton, CO on April 9, 2025.